# PhD Thesis

## Role of the metacaspase AtMC1 in stress-triggered protein aggregate formation in yeast and plants

LI LIANG  2021

UAB
Universitat Autònoma
de Barcelona

# ROLE OF THE METACASPASE AtMC1 IN STRESS-TRIGGERED PROTEIN AGGREGATE FORMATION IN YEAST AND PLANTS

**Liang Li**

Sota la direcció de: **Dra. Núria Sánchez Coll**

Tutoritzada per: **Dra. Mercè Llugany Ollé**

PER ACCEDIR AL GRAU DE DOCTOR DINS EL PROGRAMA DE DOCTORAT EN BIOLOGIA I BIOTECNOLOGIA VEGETAL DEL DEPARTAMENT DE BIOLOGIA ANIMAL, BIOLOGIA VEGETAL I ECOLOGIA
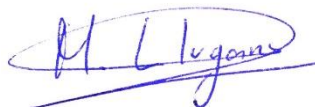
**Bellaterra, Març 2021**

**Núria Sánchez Coll**, directora de la present tesi i científic titular del Consejo Superior de Investigaciones Científicas (CSIC), i **Mercè Llugany Ollé**, turora de la present tesi i professora titular del Department de Biologia Animal, Biologia Vegetal i Ecologia a la Facultat de Biociències de la Universitat Autònoma de Barcelona, certifiquen:

Que la memória titulada "**Role of the metacaspase AtMC1 in stress-triggered protein aggregate formation in yeast and plants**", presentada per Liang Li amb la finalitat d'optar al grau de Doctor en Biologia I Biotecnologia Vegetal, ha estat realizada sota la seva direcció i, considerant-la acabada, autoritzen la seva presentació perqué sigui jutjada per la comissió correspondent.

I perqué consti als efectes oportuns, signa la present a Bellaterra, a de Març de 2021.

Dra. Núria Sánchez Coll
(Directora de la Tesi)

Dra. Mercè Llugany Ollé
(Tutora de la Tesi)

Liang Li
(Doctoranda)

# Acknowledgements

Liang Li

March 2021

# SUMMARY IN ENGLISH

Protein aggregation is a widespread phenomenon in cells that can be associated with pathological conditions. The formation of protein aggregates is induced by multiple types of stress, including thermal, chemical, nutrient deficiency and aging. However, the machinery that the formation and deposition of misfolded proteins into specific deposition sites is poorly understood in plants.

Metacaspases are critical regulatory factors that have been shown to participate in cell death and cell survival processes. For example, the *Saccharomyces cerevisiae* metacaspase ScMCA1 has been shown to be important for maintaining cellular proteostasis and limiting protein aggregation. Similarly, the *Arabidopsis thaliana* metacaspase AtMC1, acts both as a positive regulator of pathogen-triggered programmed cell death and also has a pro-survival homeostatic function in aging plants in parallel to a similar pro-survival function of autophagy.

In this thesis, we have used yeast model system to analyze the role of AtMC1 in protein aggregation. Our results show that the plant AtMC1 co-localized with aggregate markers into aggregate deposition sites in yeast during stress and aging. AtMC1 is required for efficient removal of terminally unfolded proteins in yeast and this role is evolutionarily conserved.

In addition, taking advantage of the extensive knowledge of protein quality control and protein aggregation in yeast, we have generated and characterized new markers of protein aggregation in plants. We have identified the Arabidopsis orthologues of yeast protein aggregate marker ScHSP104 and ScUBC9[TS], AtHSP101 and AtSCE1[TS]. Using these markers, we have characterized the function of AtMC1 in process of stress-triggered protein aggregation in plants. Our results show that the lack of AtMC1 leads to an increase in the

accumulation of proteins aggregates during heat stress and pathogen attack. We also found that AtMC1 co-localizes and co-immunoprecipitates with AtHSP101 *in planta*.

In summary, this work provides a deeper insight of AtMC1 function in protein quality control in plants. These data may contribute to the elucidation of the mechanisms controlling protein aggregation in plants that can help developing new strategies to fight against environmental stresses in the field.

# RESUM EN CATALÀ

L'agregació de proteïnes és un fenomen generalitzat a les cèl·lules que es pot associar a condicions patològiques. La formació d'agregats de proteïnes és induïda per múltiples tipus d'estrès, inclosos temperatura, químic, de nutrients i l'envelliment. No obstant això, la maquinària que permet la formació i deposició de proteïnes mal plegades en llocs específics de deposició és poc coneguda en les plantes.

Les metacaspases són factors reguladors crítics que han demostrat que participen en els processos de mort i supervivència cel·lular. Per exemple, s'ha demostrat que la metacaspasa de *Saccharomyces cerevisiae* ScMCA1 és important per mantenir la proteòstasi cel·lular i limitar l'agregació de proteïnes. De la mateixa manera, la metacaspasa d'*Arabidopsis thaliana* AtMC1, actua com a regulador positiu de la mort cel·lular programada desencadenada per patògens i també té una funció homeostàtica a favor de la supervivència en plantes envellides en paral·lel a una funció similar a la supervivència de l'autofàgia.

En aquesta tesi, hem utilitzat el llevat com a sistema model per analitzar el paper d'AtMC1 en l'agregació de proteïnes. Els nostres resultats mostren que l'AtMC1 es localitza conjuntament amb marcadors d'agregats en llocs de deposició d'agregats en llevats durant l'estrès i l'envelliment. Es requereix AtMC1 per a una eliminació eficient de proteïnes terminalment mal plegades en llevats i aquest paper és conservat evolutivament.

A més, aprofitant els amplis coneixements sobre control de qualitat de proteïnes i agregació de proteïnes en llevats, hem generat i caracteritzat nous marcadors d'agregació de proteïnes en plantes. Hem identificat els ortòlegs d'Arabidopsis del marcador d'agregats proteics en llevat ScHSP104 i ScUBC9TS, AtHSP101 i AtSCE1[TS], respectivament. Mitjançant aquests marcadors, hem caracteritzat la funció d'AtMC1 en el procés d'agregació de proteïnes desencadenada per estrès en plantes. Els nostres resultats mostren que la manca d'AtMC1 condueix a un augment de l'acumulació d'agregats de proteïnes durant l'estrès per calor i

l'atac de patògens. També hem trobat que l'AtMC1 co-localitza i co-immunoprecipita amb AtHSP101 in planta.

En resum, aquest treball proporciona una visió més profunda de la funció AtMC1 en el control de qualitat de proteïnes en plantes. Aquestes dades poden contribuir a l'aclariment dels mecanismes que controlen l'agregació de proteïnes en plantes que poden ajudar a desenvolupar noves estratègies per lluitar contra l'estrès ambiental al camp.

# INDEX

# INTRODUCTION

## 1.1 Regulated cell death

### 1.1.1 Importance of RCD in organismal and tissue physiology and pathology

Regulated cell death (RCD) is a fundamental biological process that tightly maintains the homeostasis in multicellular organisms, as part of core developmental processes or in response to the environment (Van Hautegem et al. 2015). For a long time, cell death was thought to be an inevitable and spurious consequence of cellular life. However, this concept has been revised during the last years based on the accumulated experimental evidence over the past decades that RCD is not unique to multicellular life forms (Ameisen 2002). Increasing evidence showing that multiple cell death pathways exist has instigated the concept that the consequences of tissue and organism-specific cell death are profoundly affected by the way a cell death takes place (Galluzzi et al. 2012, Green 2019).

RCD occurs in multicellular organisms as an integral part of development and morphogenesis, to control cell number, but it can also be activated as a defensive strategy to remove infected, mutated, or damaged cells (Vaux et al. 1999). Developmental RCD commonly involves the production of excess cells and removal of those that are unwanted. Frequently in plants, and occasionally in other organisms, cytoplasmic or structural components of the dead cell serve important functions. For instance, during xylem differentiation, RCD of the xylem tracheids and tracheary elements culminates in protoplasts clearance, producing interconnected hollow cell corpses with reinforced cell walls (Escamez et al. 2014). The root cap is involved in root growth, gravity sensing, and root system architecture (Kumpf et al. 2015). The periphery of the lateral root cap undergoes rapid turnover by eliminating cells at the root cap edge via RCD (Fendrych et al. 2014). Plant senescence controls nutrient remobilization during stress- or age-induced degeneration of tissues, organs, or entire organisms (Garapati et al. 2015). Cell death marks the final stage of plant senescence. To optimize nutrient recycling, cell death is tightly controlled and occurs once most nutrients have been recuperated.

Importantly, RCD can occur during plant immune responses to pathogen infection as part of a phenomenon traditionally known as the hypersensitive response (HR) (Goodman et al. 1994). The plant immune system is composed of two branches, wherein plasma membrane pattern-recognition receptors (PRRs) recognize conserved microbe-associated molecular patterns (MAMPS), whereas cytoplasmic NLRs (nucleotide-binding domain leucine-rich repeat (LRR)-containing gene family) recognize pathogen effectors (Jones et al. 2006). Limited, but very interesting similarities exist between animal and plant cell death at the morphological and molecular level (Pitsili et al. 2020).

In animals, several RCD types result in the activation of a family of aspartate-specific cysteine proteases (caspases). Mammalian caspases can be subdivided into three functional groups, including initiator caspases (caspase 2, 8, 9, and 10), executioner caspases (caspase 3, 6, and 7), and inflammatory caspases (caspase 1, 4, 5, 11, and 12) (Lamkanfi et al. 2002). Initiator caspases activate downstream executioner caspases carrying out the mass proteolysis that leads to apoptosis. Inflammatory caspases do not function in apoptosis but are rather involved in controlling inflammatory and host defence responses by cleaving key enzymes of infected cells for cell repair, by inducing a lytic cell death termed pyroptosis, and by engaging other mechanisms that contribute to restriction of pathogen replication (Lamkanfi 2011). With the exception of caspase 12, all inflammatory caspases participate in the activation of inflammasomes. Inflammasomes are intracellular protein complexes that detect and respond to MAMPs and endogenous damage-associated molecular patterns (DAMPs). Inflammasome complexes are thought to be assembled around members of the NOD-like receptor (NLR) or HIN-200 protein families. Recently, the first plant resistosome structure was reported, revealing significant structural similarities to inflammasome structures. The authors first resolved the cryo-electron microscopy structure of a full-length plant coiled-coil (CC)-NLR, the *Arabidopsis thaliana* HOPZ-ACTIVATED RESISTANCE1 (ZAR1), in resting and activation states. They found that the activated ZAR1 with its partner proteins form a wheel-like pentamer called resistosome that is thought

to be able to trigger cell death by perturbing plasma membrane integrity (Wang et al. 2019, Wang et al. 2019).

Animal apoptosis and plant RCD have many morphological similarities. Plasma membrane blebbing, cytoplasmic and nuclear shrinkage, chromatin condensation and fragmentation, and cytochrome c release have all been described in animal and plant cells undergoing developmental or stress-induced RCD (Balint-Kurti 2019, Dickman et al. 2013, Salguero-Linares et al. 2019). Ectopic expression of animal core regulators of apoptosis produces analogous RCD outcomes in plants (Chen et al. 2004, Dickman et al. 2001, Kabbage et al. 2010, Li et al. 2010). Furthermore, synthetic caspase substrates are processed by plant cells undergoing RCD, and caspase inhibitors can prevent RCD following pathogen recognition (Hatsugai et al. 2009, Rojo et al. 2004, Tran et al. 2014). Finally, several protease families that are unique to plants but are operationally or functionally analogous to caspases also function in RCD.

### 1.1.2 Proteases Involved in plant RCD

RCD in animals depends on caspase protease activity. However, the source of caspase-like activities in plants comes from radically different enzymes. Plant Vacuolar processing enzyme (VPE) is a cysteine proteinase originally identified as the proteinase responsible for the maturation and activation of vacuolar proteins in plants. VPE has been shown to exhibit similar enzymatic properties to animal caspase 1, which is a cysteine protease that mediates RCD in animals. In contrast to the cytosolic localization of caspases, VPE is localized in vacuoles. VPE promotes vacuolar disruption and initiates the proteolytic cascade leading to RCD in the plant stress response (Hatsugai et al. 2015). Plant cathepsin B was able to cleave the same caspase-3 synthetic substrate (DEVD) and was strongly inhibited by caspase-3 inhibitors and, to a lesser extent, by caspase-1 inhibitors (Cai et al. 2018). Cathepsin B downregulation reduced reactive oxygen species (ROS) accumulation and ER-stress-induced cell death. The plant 20S proteasome β subunit 1 (PBA1) was shown to have

caspase-3-like activity which has been shown to be required for RCD induced by *Pseudomonas syringae pv tomato* (Hatsugai, Iwasaki et al. 2009).

Interestingly, a family of proteases with a certain degree of structural similarity of caspases exist in plants, known as metacaspases (Uren et al. 2000). Similar to caspases, metacaspase family members can be subdivided into type I and type II metacaspases based on the presence (type I) or absence (type II) of an N-terminal prodomain (Fagundes et al. 2015). Every metacaspase consists of small (p10) and large (p20) catalytic subunit, each of which contains a catalytic dyad with cysteine and histidine residues. Unlike caspases, metacaspases have a strict requirement for cleavage after an arginine or lysine residue at the first position (P1) of the cleavage site. Caspases are activated upon dimerization which presumably enables basal catalytic activity, allowing autoprocessing of the zymogen. Metacaspases, on the other hand, do not dimerize, but most of them still undergo autoprocessing before activation. Autoprocessing activity of the vast majority of metacaspases is highly dependent on calcium and thus might be regulated by local changes in the concentration of $Ca^{2+}$ ions (Watanabe et al. 2011). The yeast metacaspase 1 YCA1/MCA, or according to the newly established nomenclature of metacaspases ScMCAIa, (Minina et al. 2020),exists as a monomer both in solution and as a crystals. Its crystal structure shows that it presents an an extra pair of antiparallel β-strands forming a continuous β-sheet with the six caspase-common β-strands, blocking potential dimerization (Wong et al. 2012).

In *Arabidopsis thaliana* (hereafter Arabidopsis) nine metacaspases have been identified (Type I: AtMCA1-3 and Type II: AtMCA4-9) and several of them have been shown to participate in cell death or stress responses. Arabidopsis type I metacaspase (AtMC1/AtMCAIa) is a positive regulator of immune cell death and co-immunoprecipitates with LESION SIMULATING DISEASE 1 (LSD1), whose absence triggers autoimmune phenotypes (Coll et al. 2010). AtMC1 function requires auto-catalytic processing and removal of the prodomain. In contrast, AtMC2, closely related to AtMC1 at the sequence level, acts antagonistically to AtMCA1, as a negative regulator of immune cell death.

AtMC2 function is independent of its putative catalytic residues. One of the most highly expressed type II metacaspase genes in Arabidopsis, metacaspase 4 (AtMC4), is a positive regulator of cell death induced by abiotic and biotic stressors, such as damage-induced immune response, some forms of fungal toxin-, bacterial pathogen- or herbicide-induced stress (Watanabe et al. 2011). The *atmc4* mutants are less sensitive to cell death induced by the mycotoxin fumonisin B1 (FB1), the herbicides methyl viologen (MV) and acifluorfen, and HR caused by avirulent *P. syringae* strains. The AtMC4 structure exhibits an inhibitory conformation in which a large linker domain blocks activation and substrate access (Zhu et al. 2020). The activation of AtMC4 and cleavage of its substrate involve multiple cleavages in the linker domain upon activation by $Ca^{2+}$. Upon damage, AtMC4 is activated by binding high levels of $Ca^{2+}$ and releases plant elicitor peptide 1 (Pep1) from its protein precursor PRECURSOR OF PEP1 (PROPEP1) by cleaving it behind a conserved arginine (Hander et al. 2019). AtMC8 is strongly up regulated by oxidative stresses caused by UVC, $H_2O_2$ or methyl viologen. Overexpressing AtMCA8 increased RCD whereas knocking it out reduced cell death triggered by UVC and $H_2O_2$ in protoplast (He et al. 2008). AtMC9 has a function on activities of papain-like cysteine proteases. In RCD preceding xylem formation, AtMC9 plays a role in clearance of the cell contents post mortem, that is after tonoplast rupture (Zhang et al. 2020).

### 1.1.3 Pro-survival role of metacaspases

In animals, some cell death proteases have been shown to have dual roles, also participating in pro-survival processes. Caspases play important roles in several different pathways, including, signaling, proliferation, differentiation, remodeling and neuronal plastictiy. Caspase-8 classically triggers the extrinsic apoptotic pathway, in response to the activation of cell surface Death Receptors (DRs) like FAS, TRAIL-R and TNF-R. Recent research implicating caspase-8 also plays a crucial pro-survival function by inhibiting an alternative form of RCD called necroptosis. Pathogen recognition by PRRs can trigger necroptosis. Pathogenic impairment of apoptosis by targeting caspase-8 leads to the release of

procaspase-8 block on necroptosis (Tummers et al. 2017). Caspase-3 has important roles in tissue differentiation, regeneration and neural development in ways that do not involve any apoptotic activity (Ishizaki et al. 1998, Solier et al. 2017, Yan et al. 2001). Caspase-2 represses transcription of the survivin gene, a general regulator of cell division and cytoprotection in tumors. This process involves caspase 2 proteolytic cleavage of the nuclear factor κB (NFκB) activator, RIP1. Lossing of RIP1 abolishes transcription of NFκB target genes, including survivin, resulting in deregulated mitotic transitions, enhanced apoptosis and suppression of tumorigenicity in vivo (Guha et al. 2010).

The paracaspase MALT1 is an arginine-specific cysteine protease. MALT1 binds to two proteins, caspase recruitment domain family member 11 (CARMA1) and BCL10 immune signaling adaptor (BCL10), to form CARD11–BCL-10–MALT1 (CBM) signalosomes, which activates nuclear factor-κB (NF-κB) signaling and other inflammatory pathways in activated lymphocytes (Ruland et al. 2019). MALT1 regulates NF-κB activation, cell adhesion, mRNA stability, and mTOR signaling through its proteolytic activity (Hamilton et al. 2014, Jeltsch et al. 2014, Uehata et al. 2013). MALT1-deficient mice are immunodeficient and impaired development of specific B-cell subsets, revealing that MALT1 plays an essential role in immunoreceptor-induced activation events (Klemm et al. 2006, Ruland et al. 2003).

Beyond their cell death functions, metacaspases have been also shown to participate in other cell-autonomous, beneficial, functions for survival and homeostasis. For example, the yeast metacaspase ScMCA1 appears to be required for proper cell cycle control, because cells lacking this metacaspase display an increased frequency of cell cycle arrest (Lee et al. 2008). ScMCA1 has also been shown to be involved in protein quality control (PQC), as revealed by its direct physical interaction with protein aggregates (Dick et al. 2013, Hill et al. 2014) and the impairment in the removal of such aggregates in *ΔScMCA1* cells (Hill, Hao et al. 2014, Shrestha et al. 2013). Increased expression of ScMCA1 alone improves the ability of cells to remove heat-induced aggregates, and counteracts the buildup of aggregated proteins

seen during replicative aging of mother cells (Hill, Hao et al. 2014), hence suggesting that ScMCA1 is a limiting factor in the cellular defense against protein damage. On the presence of the protein disaggregase HSP104, overproduction of MCA1 causes a robust extension of the replicative lifespan of cells (Hill, Hao et al. 2014). These results strongly advocate for ScMCA1 being involved also in pro-survival functions. ScMCA1 can still localize to protein aggregates in absence of HSP104. ScMCA1 prodomain contains a Q/N rich regon that has been suggested to be required for MCA1 localization to protein aggregates and to be important for PQC (Hill, Hao et al. 2014). In fact, Q/N rich proteins have been reported to bind and sequester Huntingtin aggregates , thereby limiting its toxicity (Park et al. 2013). ScMCA1 has also been shown to localize to PQC sites such as the juxtanuclear quality control compartment (JUNQ) and to the peripheral insoluble protein deposit (IPOD) (Shrestha et al. 2013) (described in more detail in section 1.2.4).

In other organisms, such as the fungus *Aspergillus fumigatus*, metacaspases CasA and CasB facilitate growth under conditions of endoplasmic reticulum stress. Metacaspase activity in *A. fumigatus* contributes to the apoptotic-like loss of membrane phospholipid asymmetry at stationary phase, and suggest that CasA and CasB have functions that support growth under conditions of endoplasmic reticulum stress (Richie et al. 2007). In the protozoan parasite *Trypanosoma cruzi*, metacaspases have been suggested to be involved in an apoptosis-like phenomenon. The regulation of metacaspase-3 activity is important for cell cycle completion inside the mammalian host. On the other hand, inducible overexpression of metacaspase-5 lacking its C-terminal domain caused an apoptotic-like response. These results suggest that the two *T. cruzi* metacaspases could play an important role in the life cycle (Laverriere et al. 2012). In the protozoan parasite *Leishmania mexicana*, a *MCA* gene-deletion mutant amastigotes replicated significantly faster than wild-type amastigotes in macrophages and in mice, but not as axenic culture in vitro (Castanys-Muñoz et al. 2012). The *MCA* gene of *Leishmania major* (LmjMCA) is essential for the correct segregation of the nucleus and kinetoplast, functions that could be independent of programmed cell death, and that the

amount of LmjMCA is crucial. The absence of MCAs from mammals makes the enzyme a potential drug target against protozoan parasites (Ambit et al. 2008).

**Table 1. Non-death roles of metacaspases**

| Name | Organism | Function | Reference |
|---|---|---|---|
| MCA2, MCA3 and MCA5 | *Trypanosoma brucei* | Viability of the bloodstream form of the parasite | (Helms et al. 2006) |
| LmjMCA | *Leishmania major* | Stage progression regulation during cellular division | (Ambit et al. 2008) |
| ScMCA1 | *Saccharomyces cerevisiae* | Maintains proteostasis and limits protein aggregation | (Lee et al. 2008, Shrestha et al. 2019) |
| CasA and CasB | *Aspergillus fumigatus* | Contributes to the apoptotic-like loss of membrane phospholipid asymmetry at stationary phase | (Richie, Miley et al. 2007) |
| TcMCA3, TcMCA5 | *Trypanosoma cruzi* | Play an important role in the life cycle | (Laverriere, Cazzulo et al. 2012) |
| AtMC1 | *Arabidopsis thaliana* | Negatively regulates senescence in older tissues | (Coll et al. 2014) |
| PhMC1 | *petunia* | Negative regulator of senescence in petals | (Chapin et al. 2017) |

Our lab previously showed  AtMC1 has a pro-survival role in aging plants that acts in parallel to a similar pro-survival function of autophagy (Coll, Smidler et al. 2014). Similar to autophagy mutants, *atmc1* mutant plants accumulated more protein aggregates, pointing towards a homeostatic function of the protein that acts in parallel to autophagy.
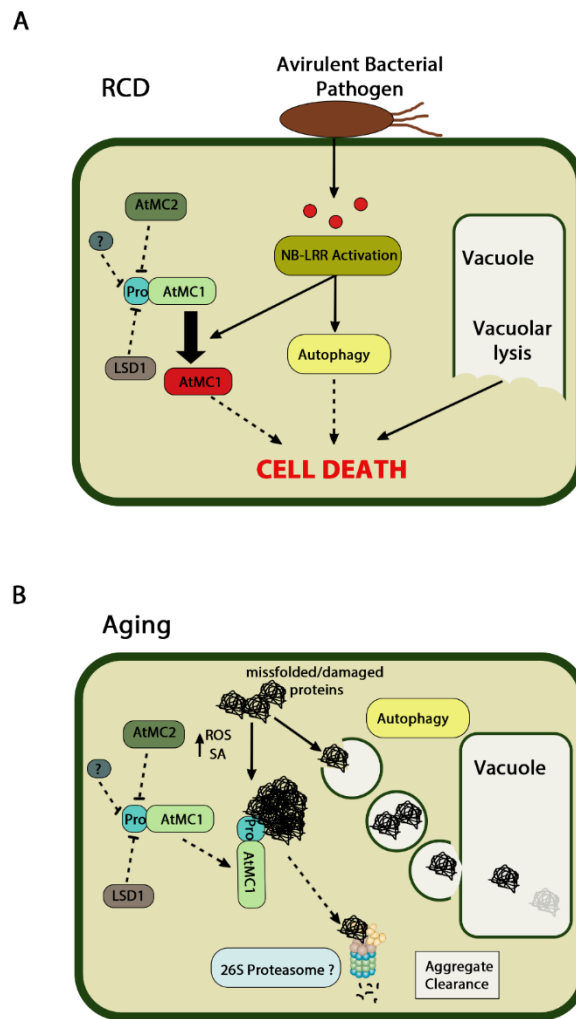
**Figure 1. Proposed model integrating the dual pro-death/pro-survival functions of AtMC1 and autophagy at different developmental stages.** (A) Pro-death functions of autophagy and AtMC1 in HR control in young plants. (B) Pro-survival role of autophagy and AtMC1 in aging cells. Adapted from (Coll, Smidler et al. 2014).

Autophagy, a conserved degradation pathway, is responsible for elimination and recycling of damaged or aggregated proteins and organelles. The unwanted materials are firstly sequestered by a double-membraned structure, the autophagosome, that then fuses with lysosome and ultimately are degraded and recycled. Autophagy degradation system produces free amino acids, di- and tri- peptides as well as larger peptides that are released into the cytosol for de novo synthesizing molecules or to provide energy for cellular renovation and homeostasis. Autophagy plays an essential quality control function in the cell by promoting protein turnover and selectively disposing of dysfunctional or damaged

organelles(Ravikumar et al. 2010). In animals, this homeostatic function includes degradation of aberrant aggregates formed by neurodegenerative-associated proteins to protect against a wide range of disease such as Parkinson's, Alzheimer's and Huntington's disease.

## 1.2 Proteostasis

Proteostasis or protein homeostasis is the process that regulates proteins both inside and outside the cell in order to preserve proteome integrity and thereby to promote viability at both the cellular and organism levels. Proteostasis requires precise control of protein synthesis, protein folding, conformational maintenance, and finally to protein degradation by autophagy and the proteasome (Klaips et al. 2018). As such, a complex and adaptive proteostasis network coordinates these processes with the macromolecular elements including transcription factors, folding enzymes, molecular chaperones and degradation components. The capacity to maintain proteostasis varies between cell types (Labbadia et al. 2015), and is thought to decline with aging and also exposure to environmental stress (Powers et al. 2009). Although this capacity is finite at any point in time, it can be spatially and temporally altered by varying the amount and/or activity of individual components. This intricate balance is required in the use of energy and resources to maintain the functional integrity of the proteome. Otherwise, an imbalance in proteostasis causes widespread acute and chronic perturbations of physiological states and disease.

### 1.2.1 Protein folding and aggregation

A single cell can express thousands of proteins at any given time, which are initially synthesized in the ribosome; most of these biomolecules become functional by folding into a unique three-dimensional structure. Thus, the process by which proteins achieve a functional form, termed "protein folding", is extremely important for maintaining living systems. In vivo, protein folding begins to occur even during a nascent chain is still

associated with the ribosome, and there is evidence that some proteins do fold at least partially in such a co-translational manner (Hardesty et al. 2001). The major part of the protein folding process is known to take place in the cytoplasm after the nascent polypeptide is released from the ribosome or in specific compartments such as the endoplasmic reticulum (ER) following translocation through membranes (Dobson 2003). As incompletely folded chains expose hydrophobic acid residues and regions of unstructured polypeptide molecule that are largely buried in the native state, such species are prone to aggregate. Proteins of more than 100 amino acids in length fold via intermediate states with incompletely buried hydrophobic residues (Brockwell et al. 2007, Dinner et al. 2000). The generation of these intermediates increases the risk of aggregation, particularly in the crowded environment of the cell, as it increases non-specific interactions (Ellis et al. 2006). The folded three-dimensional structures of most proteins need to be partially unfolded and remodeled in order to form or disperse functional protein complexes, leaving them at risk of misfolding and aggregation. Unfolded or misfolded proteins aggregate and are toxic to cells; they must be degraded to avoid the accumulation of these protein aggregates inside the cell. To maintaining protein homeostasis, the cell invests in intricate quality control mechanisms comprising of various chaperone proteins that act to oversee the folding/refolding of proteins as well as degradation machineries that facilitate the removal of unwanted misfolded conformers and aggregated material (Bukau et al. 1998, Goldberg 2003, Hartl 1996, Rubinsztein 2006).

Protein misfolding increases and the generation of protein oligomers or larger aggregates can cause by various factors such as high temperature, low pH, oxidative stress, abnormal presence of metal ions, mutations, transcriptional, translational or posttranslational errors, and aging (Abramov et al. 2020, Chamachi et al. 2017, Higuchi-Sanabria et al. 2018, Tamás et al. 2018). It is therefore not surprising that failure to fold correctly, or to remain correctly folded, will give rise to the malfunctioning of living systems and therefore to disease. Indeed, it is becoming increasingly evident that a wide range of human diseases is associated with

aberrations in the folding process. Some of these diseases (e.g. cystic fibrosis) result from the simple fact that if proteins do not fold correctly they will not be able to exercise their proper functions. In other cases, misfolded proteins escape all the protective mechanisms and form intractable aggregates within cells. An increasing number of pathologies, including Alzheimer's and Parkinson's diseases, the spongiform encephalopathies and late-onset diabetes, are known to be directly associated with the deposition of such aggregates in tissues.

## 1.2.2 Chaperone proteins

Molecular chaperones are a set of proteins that interact with, stabilize or help another protein to fold into its functional conformation, without contributing conformational information or being part of the final structure (Hartl et al. 2011). Some chaperones are called heat shock proteins (HSPs) due to their upregulation upon stresses such as increased temperature, although some members are constitutively expressed and play important roles under non-stress conditions (Feder et al. 1999). HSPs are divided into subfamilies based on their molecular weights (e.g. HSP100, HSP90, HSP70, HSP60, HSP40, and small HSPs). In addition, chaperones have also been classified functionally into three fundamental classes as holdases, foldases and disaggregases. Holdases stabilize non-native protein conformations, and assist folding to the native state, preventing their aggregation in an ATP-dependent manner. They are responsible for the delivery of these client proteins to foldases when conditions return to normal. Foldases have one or more ATP-binding domains and directly help client proteins to fold utilizing the energy from ATP hydrolysis (Slepenkov et al. 2002). Disaggregases are also ATP-dependent proteins that disentangle the client aggregated proteins and transfer them to a holdase and/or foldase for refolding (Bösl et al. 2006). These chaperones form cooperative pathways and networks to ensure proper protein folding and maintain a healthy proteome.

The HSP70 family of molecular chaperones is one of the most versatile chaperone proteins that assists various folding processes such as folding and assembling of newly translated

proteins, refolding of misfolded or aggregated proteins. The HSP70 chaperones are monomeric and contain two different domains called the N-terminal ATPase domain and C terminal substrate-binding domain. The HSP70 C-terminal domain binds short hydrophobic peptide sequences of about seven residues that are exposed by nascent and nonnative protein substrates (Clerico et al. 2015, Rüdiger et al. 1997). The affinity of the C-terminal domain for protein substrate is allosterically regulated by ATP binding and hydrolysis in the N-terminal ATPase domain. This process may cooperate with ATP-independent small HSPs which function as holdases, and are denominated co-chaperones. De novo folding is modulated by the combined action of HSP70s with different co-chaperones and other molecular chaperones including HSP40s and chaperonins. Among the co-chaperones of HSP70s, HSP40s are a class of essential and universal partners in almost all aspects of proteostasis. The HSP40 cochaperones possess a J domain, which interacts with the nucleotide-binding domain of HSP70, which stimulates the ATPases activity of HSP70. The HSP70/HSP40 machinery exhibit herterogeneity in structure, localization, and function, thus it is one of the most important chaperone system across all kingdoms of life.

HSP104 is a hexameric AAA+ protein disaggregase found in yeast that can rapidly transduce energy from cycles of ATP binding and hydrolysis to resolve disordered protein aggregates, preamyloid oligomers, amyloids, and prions. It has been reported that HSP104 enhances yeast survival ~10,000-fold after a variety of environmental stresses which induce protein misfolding and subsequent aggregation (Sanchez et al. 1992). The orthologues of HSP104 in plant (HSP101) and bacteria (ClpB) have similar functions (Parselt et al. 1991, Queitsch et al. 2000). HSP104 synergize with HSP70/HSP40 machinery complex to rapidly resolve denatured protein aggregates and refold proteins to native structure and function (Cashikar et al. 2005, Glover et al. 1998, Shorter et al. 2019, Weibezahn et al. 2004). HSP70/HSP40 machinery complex can assist present aggregated substrates to HSP104, and likely help substrate refolding after release from the aggregate (Tessarz et al. 2008). This rapid

renaturation of damaged proteins obviates the large energetic cost of protein degradation and de novo synthesis.

HSP104 is composed of an N-terminal domain (NTD), two nucleotide-binding AAA+ domains (NBD1 and NBD2), a distinctive coiled-coil middle domain (MD) inserted within the NBD1, and a short C-terminal domain (CTD) (Hoskins et al. 2009). Like many other AAA+ ATPase, HSP104 activity is dependent on the formation of hexamers and requires ADP or ATP binding to NBD2 (Parsell et al. 1994, Schirmer et al. 2001). Based on structural analysis have revealed that the HSP104 NTD is crucial for cooperativity and plasticity of HSP104/ClpB (Sweeny et al. 2015). NTD of HSP104 enables cooperative substrate translocation, which is critical for prion dissolution and potentiated disaggregase activity. The HSP104 NTD can also interact with the HSP70/HSP40 machinery, which is important for the survival under heat stress, since the lack of NTD HSP104 has been shown to be defective in HSP70 and HSP40 interaction and dissolution of prions (Lee et al. 2017, Sweeny, Jackrel et al. 2015). The NBD1 and NBD2 are highly structurally conserved, including regions involved in ATP binding and hydrolysis, as well as pore loops that couple conformational changes of the AAA+ protein due to ATP hydrolysis to substrate remodeling .In addition to the conserved AAA+ motifs, NBD2 was discovered to contain a nuclear localization signal (NLS) (Tkach et al. 2008). The ATPase activity of HSP104 NBD1 and NBD2 as the key ATP-consuming processes enabling aggregate dissolution (Sathyanarayanan et al. 2020). HSP104 MD dictates the activity of the disaggregase. MD plays an important role in the NBD1-NBD2 communication and hexamer stabilization (Cashikar et al. 2002). The tightly association of MD with NBD1 in a horizontal confirmation leads to low activity, while the tilted MD has low affinity with NBD1 thus results in higher disaggregation rate. Thus, the disaggregase activity of HSP104 in vivo is efficiently and tightly controlled via the activated and repressed states of MD. The CTD last four residues are a conserved DDLD motif that allows binding to the chaperone Cpr7, but is dispensable for HSP104-mediated thermotolerance. The elimination of the whole CTD

results in HSP104 unable to assemble and becomes aggregation prone at high temperature, highlighting a novel structural role for this region (Mackay et al. 2008).

### 1.2.3 Protein degradation

In addition to chaperone systems folding and re-folding of nonnative proteins, protein degradation systems can recognize and eliminate misfolded or damaged proteins that may otherwise disrupt proteostasis. Among various protein degradation systems, the ubiquitin proteasome system and autophagy are two major pathways that contribute to clearance of misfolded and proteotoxic proteins. The degradation systems ensure proper protein function, reducing proteotoxicity stress and protein aggregation.

### 1.2.3.1 The ubiquitin proteasome system (UPS)

Ubiquitin (Ub) is a highly conserved 76-residue protein (~8.5 kDa) which is present in all eukaryotes, including yeast, plants, and human. As one of the most studied protein posttranslational modifiers, ubiquitin is covalently attached to an $\varepsilon$-amino group of the lysine residues of the substrate protein, in a reaction termed ubiquitination. Ubiquitination is carried out through a conserved three-step enzymatic cascade by the E1 activating enzyme, the E2 conjugation enzyme, and E3 protein ligase, leading to the formation of an iso-peptide bond between the C terminus of ubiquitin and the lysine on the target protein (Hershko et al. 1998, Pickart 2001). Reversely, the attached ubiquitin can be removed by deubiquitinating enzymes (DUBs).

Ubiquitin has six lysine residues exposed on its surface: Lys6, Lys11, Lys27, Lys29, Lys33, Lys48, and Lys63. Any of its seven lysine residues can be ubiquitinated, as well as its N-terminus (Met1), leading to eight types of homotypic polyubiquitin chains and an almost infinite variety of heterotypic or branched polyubiquitin chains (Komander et al. 2012). Based on the current studies, all the possible linkages types have been detected in cells through proteomics studies (Wagner et al. 2011, Xu et al. 2009). These diverse ubiquitin

chains are thought to be the distinct signals recognized by specific ubiquitin receptors, participating a wide variety of cellular processes. Among all the different types of ubiquitin chains, Lys-48 linked chains, the most predominant linkage type in cells (Xu, Duong et al. 2009), are found to be associated with protein degradation for many years (Hershko and Ciechanover 1998, Swatek et al. 2016). Recent studies have also shown that ubiquitin linkages other than Lys48, except Lys-63 type, are also related to protein degradation based on the proteomics study (Finley 2009, Xu, Duong et al. 2009).

The ubiquitin labeled proteins are recognized by the 26S proteasome for degradation. The ubiquitin-proteasome system (UPS) is a major intracellular protein degradation system (Schwartz et al. 2009). The 26S proteasome is a large, multi-subunit, ATP-dependent protease that unfolds and degrades polyubiquitinated proteins (Voges et al. 1999). In the UPS, AAA protein p97 is a central component which is thought to act as a molecular chaperone, guiding protein substrate to the 26S proteasome (Kloppsteck et al. 2012). The unfolded protein is then fed into the 26S proteasome and broken down into short peptides (Fu et al. 2001, Yang et al. 2004). The UPS system plays a prominent regulatory role in all aspects of growth and development in plants.

### 1.2.3.2 Autophagy

Autophagy, a conserved lysosomal degradation pathway, is responsible for elimination and recycling of damaged or aggregated proteins and organelles. The unwanted materials are firstly sequestered by a double-membraned structure, the autophagosome, that then fuses with the lysosome/vacuole and ultimately are degraded and recycled. The autophagy degradation system produces free amino acids, di- and tri- peptides as well as larger peptides that are released into the cytosol to de novo synthesize molecules or to become energy for cellular regeneration and homeostasis. Most likely, autophagy evolved both as a non-selective bulk degradation pathway for intracellular components, and as a quality control mechanism to facilitate selective removal of toxic or surplus structures (Johansen et al. 2011).

This homeostatic function includes degradation of aberrant aggregates formed by neurodegenerative-associated proteins to protect against a wide range of disease such as Parkinson's, Alzheimer's and Huntington's disease.

Autophagy is based on the action of a system of proteins and protein complexes. The key components of autophagy consist of many autophagy-related (*ATG*) genes that were originally characterized in yeast, and have been found in almost all other organisms including plants and humans. Autophagy begins with the formation of phagophore, a crescent-shaped double membrane that expands and fuses to form a double-membrane vesicle, the autophagosome (Tooze et al. 2010). In mammals, the most upstream autophagy factors are ATG9 vesicles and the ULK1 complex, which contains ATG101, ATG13, focal adhesion kinase (FAK) family-interacting protein of 200 kD (FIP200) and ULK1/2. The ULK1 complex and ATG9 vesicles translocate independently to the autophagosome formation site on or close to the endoplasmic reticulum (ER) (Axe et al. 2008, Itakura et al. 2012, Karanasios et al. 2016). The ULK1 complex plays an important role in nucleating the isolation membrane (Lane et al. 2017). ATG9 vesicles likely compose a part of the autophagosome membrane (Noda 2017). Then, the upstream factors recruit the class III phosphoinositide 3-kinase PI3K complex (consisting of ATG14, Beclin 1, VPS15, and VPS34) to generate phosphatidylinositol 3-phosphate (PI3P). ATG2A/B and PI3P binding WIPI2 and two ER transmembrane proteins, VMP1 and TMEM41B, are required for expansion of phagophore (An et al. 2019, Dooley et al. 2014, Maeda et al. 2019). In yeast, the Atg1 complex is composed of Atg1, Atg13, Atg17, Atg29, and Atg31, and Atg18 is a WIPI2 homolog (Mizushima et al. 2011). The elongation of membranes is regulated by the ATG5-ATG12 conjugation system and the microtubule associated protein-1 light chain-3 (LC3-ATG8) conjugation system. ATG5-ATG12 forms a complex with ATG16L, which facilitates autophagosome elongation. LC3II-positive autophagosomes are trafficked along microtubules to lysosomes for degradation. Autophagosome-lysosome fusion appears to be mediated by the SNARE proteins VAMP8 and Vti1B (Furuta et al. 2010).
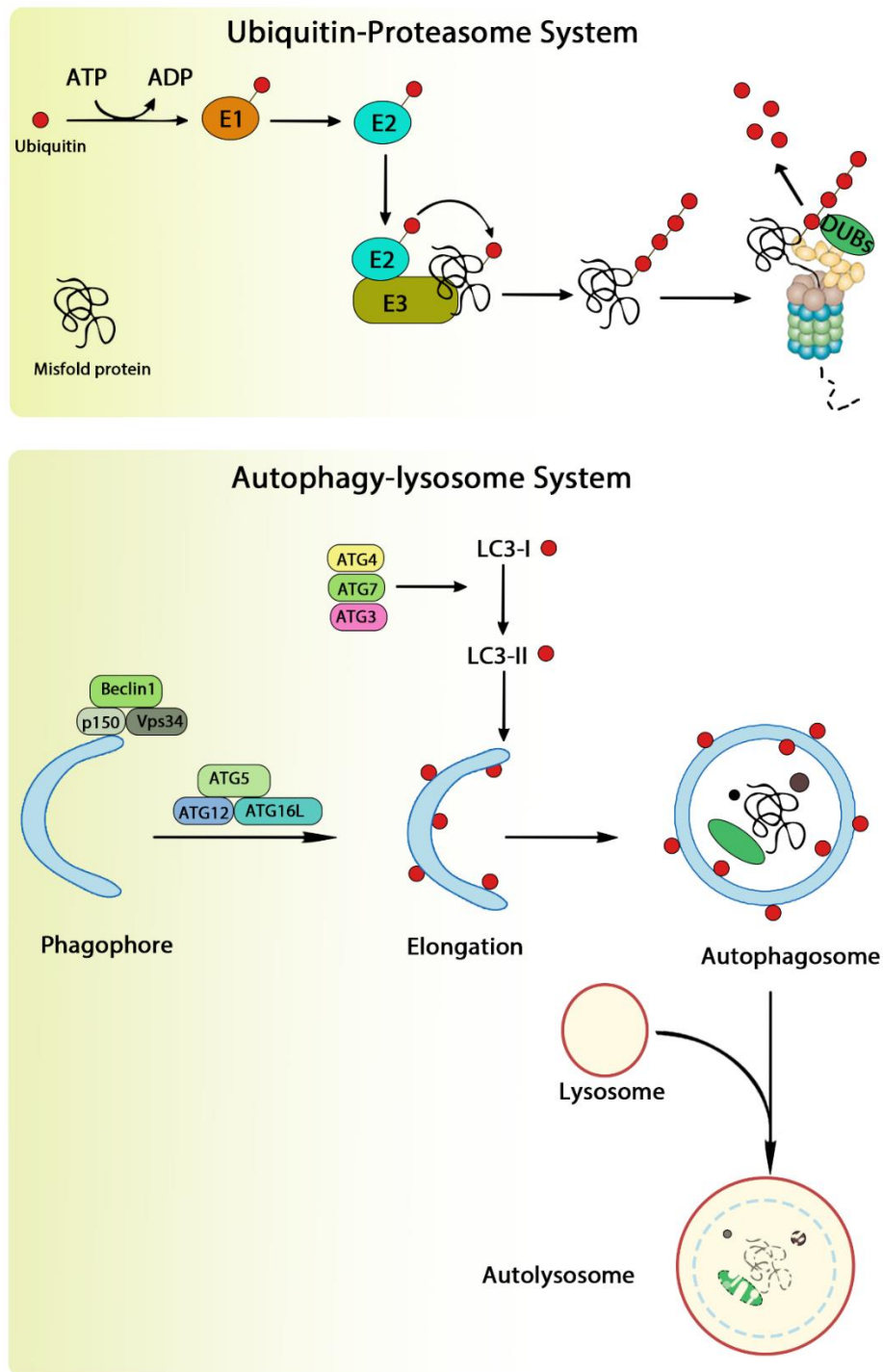
**Figure 2. Overview and comparison of UPS and autophagy.** Upper: The Ubiquitin-Proteasome System. The proteasome degradation of misfolded proteins occurs through an enzymatic cascade of ubiquitination. Initially through ubiquitin is attached to a cysteine residue of an activating enzyme, E1, in an ATP-dependent manner. The active ubiquitin is then associated with a cysteine residue of a ubiquitin conjugating enzyme, E2. Finally, specificity of ubiquitin transfer is ensured by E3 ubiquitin ligase family of proteins that bind to misfolded proteins. Ubiquitinated misfolded proteins are de-ubiquitinated and unfolded before degradation in the inside of the barrel-shaped proteasome. Lower: Autophagy is able to degrade large and heterogeneous cytosolic material, including aggregated proteins, organelles, bacteria. Initiation of the

autophagy process is mediated by the ULK1 complex in response to Initiation of the autophagy process is mediated by the ULK1 complex in response to various cellular signals. Formation of the phagophore also requires class III phosphoinositide 3-kinase (PI3K) complex, which is composed of VPS34 (vacuolar protein sorting 34) PI3K, ATG14L, VPS15, and Beclin 1. The ATG5-ATG12-ATG16 complex and LC3II promote the elongation of the phagophore and are required for the formation of the autophagosome. Eventually, the autophagosome fuses with a lysosome, which delivers hydrolytic enzymes for the degradation of the engulfed intracellular material.

## 1.2.4 Cellular aggregate deposition sites

Protein aggregation has multiple and even opposing consequences for cell physiology. On the one hand, aggregation is associated with aging, pathophysiological states, and toxicity of cells. On the other hand, directing aggregated proteins to specific compartments can counteract cell toxicity and facilitate subsequent quality control activities (Arrasate et al. 2004, Cohen et al. 2006). The deposition of protein aggregates exhibits marked spatial organization. Spatially distinct, specific aggregate deposition sites are differentially occupied by misfolded protein species (Sontag et al. 2014, Tyedmers et al. 2010).

Insoluble inclusion bodies frequently form in bacteria and also in eukaryotic cells that overexpress heterologous proteins (Ventura et al. 2006). Usually, one or two inclusions form at the cell poles but also in mid- or quarter-cell positions, which are future sites for septation (Kirstein et al. 2008, Lindner et al. 2008, Winkler et al. 2010). In *Escherichia coli*, such aggregates are typically localized to the old cell pole, was shown to slow down their growth in a dosage-dependent manner, thereby giving rise to the pattern of aging and rejuvenation in growing microcolonies (Lindner, Madden et al. 2008, Winkler et al. 2010).

A specialized form of inclusion bodies in the cytoplasm of mammalian cells is termed the aggresome (Johnston et al. 1998). Aggresomes localize to an indentation of the nuclear envelope at the microtubule-organizing centre (MTOC) and often surround the centriole. The exterior of aggresomes is sheeted by a cage-like shell formed by the intermediate filament vimentin. Their overall structure and size vary and depends on cell type and the aggregating substrate. Aggresome formation is initiated by the formation of smaller

aggregates in the periphery, which then move in a dynein-based manner along the microtubule cytoskeleton to the final perinuclear site at the MTOC.

Protein aggregates deposition sites is often studied in eukaryotic cell *Saccharomyces cerevisiae*. In yeast, the main deposition sites can by classified as the Cytosolic Quality Control Compartment (CytoQ) (Miller et al. 2015), the IntraNuclear Quality Control Compartment (INQ) (Gallina et al. 2015) and the JUxtaNuclear Quality Control Compartment (JUNQ) (Kaganovich et al. 2008). The JUNQ displays a perinuclear localization in an indentation of the nuclear envelope, the INQ is an intranuclear site. It is currently under debate whether they represent identical or independent structures. JUNQ transiently accumulates misfolded proteins that are ubiquitylated and are presumably substrates for proteasomal degradation. Substrates at the JUNQ are still mobile and exchange rapidly with the surrounding cytoplasm. IPOD harbors terminally aggregated, insoluble proteins, including carbonylation-sensitive proteins and amyloidogenic proteins such as Htt103Q or the yeast prions (Tyedmers et al. 2010). The chaperone HSP104 is often found in an arrangement around the periphery of the IPOD (Kaganovich, Kopito et al. 2008, O'Driscoll et al. 2015). HSP104 bound aggregates to a perivacuolar inclusion site reminiscent of the IPOD (Hill et al. 2016). SUMO ubiquitin-conjugating enzyme 9 variant (UBC9$^{TS}$) that misfolds above 30 °C, was degraded by the ubiquitin–proteasome pathway. UBC9$^{TS}$ accumulated in structures resembling the juxtanuclear inclusion formed (JUNQ), closely followed by cytosolic puncta. Recovery of the denatured UBC9$^{TS}$ accumulated in the JUNQ but not in the IPOD after return to the permissive temperature (Kaganovich, Kopito et al. 2008). HSP104 and UBC9$^{TS}$ are used as marker for different aggregates deposition sites in yeast.

## 1.3 Plant proteostasis PQC in plant

Plants, like animals, are vulnerable to the contrasting and fluctuating environmental conditions, including a wide range of pathogens. Unlike animals, plants do not flee to avoid

adverse conditions that jeopardize their survival. They have developed responses to defend themselves against the aggression of pathogens and adapted to the physical variations of their environment. Plants are able to induce defense responses when pathogens are perceived. Although they do not produce antibodies, they have evolved receptor proteins that recognize pathogens at the cell surface and within the cytoplasm and fight infections cell-autonomously.

Cells have evolved different PQC strategies based on the localization of the misfolded proteins. For example, endoplasmic reticulum (ER)-localized misfolded proteins are degraded by the ER-associated protein degradation (ERAD) pathway (Vembar et al. 2008). In this pathway, misfolded proteins first undergo retro-translocation to the cytoplasm, followed by the covalent attachment of poly-ubiquitin chains for proteasome degradation. Polyubiquitination requires a series of enzymes: ubiquitin activating enzyme (E1); ubiquitin conjugating enzyme (E2); and ubiquitin ligase (E3). As ubiquitin ligases mediate substrate recognition, they are the "signature components" of the different PQC degradation pathways. Unlike the cytoplasm, the nucleus does not face to the misfolding of damaged proteins in the folding of nascent proteins. That is because nuclear proteins are synthesized in the cytoplasm and are imported into the nucleus through the nuclear pore. Thus, nuclear PQC mainly focuses on misfolded proteins that emerge during or after nuclear import. The nucleus engages in limited translation events and may have to manage a low level of translational products. Furthermore, failures in cytoplasmic PQC can reduce the amount of correctly folded nuclear proteins, which can subsequently burden nuclear PQC pathways by decreasing the levels of functional nuclear proteins.

### 1.3.1 ER protein quality control in plant

It is well known that the proper function of a protein strictly depends on its native conformation, but protein folding is a fundamentally error-prone process. The endoplasmic reticulum (ER) is the cellular port of entry for secretory and membrane proteins to enter the

secretory pathway and is a folding compartment for proteins to attain their native conformations through interactions with molecular chaperones, sugar-binding lectins, and folding enzymes (Gidalevitz et al. 2013). Misfolded proteins not only lead to functional deficiency but also induce dominant-negative and cellular toxicity effects, and it is thus essential that the ER should possess several highly stringent protein quality control mechanisms to closely monitor the folding process, allowing export of only correctly folded proteins to their final destinations but retaining incompletely/mis-folded proteins for additional rounds of chaperone-assisted folding. A high efficient ER-mediated protein quality control (ERQC) system can also differentiate terminally misfolded proteins from folding intermediates and/or reparable misfolded proteins, stopping the futile folding cycles of the former proteins and eliminating them via a multistep degradation process widely known as ER-associated degradation (ERAD) that involves ubiquitination, retro-translocation, and cytosolic proteasome (Smith et al. 2011).

Once proteins fail to reach its native conformation within a certain time, proteins are directed to degradation pathways. In most cases the aberrant proteins are dislocated to the cytosol for proteasomal degradation. Alternatively, misfolded proteins can be eliminated via a proteasome-independent cytosolic pathway or targeted for degradation to the lytic vacuole or lysosome (Cui et al. 2012). Vacuolar delivery may be required during severe ER stress, when proteins aggregate in the ER. Under such conditions, the ER-associated degradation capacity is likely to be insufficient to restore protein homeostasis, leading to the induction of autophagy and delivery of cargo to the vacuole for degradation. In Arabidopsis, it was shown that ER stress-inducing agents trigger autophagy by activating the unfolded protein response in an INOSITOL-REQUIRING ENZYME 1b (IRE1b)-dependent manner (Liu et al. 2012). Importantly, the response depended on the accumulation of unfolded proteins, as chaperones overexpression reduced autophagy activation in the presence of ER stress-inducing agents (Yang et al. 2016). Autophagy was also triggered by the overexpression of constitutively misfolded proteins. ER quality-control autophagy has also been described in

mammals as a mechanism to remove non-aggregated misfolded proteins that are resistant to ER-associated degradation (Liu, Burgos et al. 2012). When ER-associated degradation was specifically blocked, a normal ER- ER-associated degradation is a conserved associated degradation substrate was directed toward the ER quality-control autophagy pathway, suggesting a compensation mechanism.

### 1.3.2 Nuclear protein quality control in plant

The nuclear protein quality control mainly focuses on the integrity of the nuclear genome and the quality of mRNA prior to export from the nucleus. The protein aspect of nuclear quality control also plays an important role in proteostasis because an escalating failure to remove or repair misfolded nuclear proteins can lead to a deterioration in the integrity of the nuclear genome and the quality of the mRNA produced. Over the last decade, studies of misfolded nuclear proteins have revealed some of the folding and degradative PQC systems that function in the nucleus and these appear to operate on similar overarching principles as PQC systems in the cytoplasm with chaperones, small heat-shock proteins, and ubiquitin ligases generally managing misfolded nuclear proteins.

One distinct aspect of the nucleus is that it contains a high concentration of DNA, which is organized into chromatin. Due to the negative charge of DNA, many structural chromatin proteins have a considerable positive charge, such as histones. In addition, the nuclear proteome is enriched for proteins that possess low complexity, intrinsically disordered regions (Meng et al. 2016), suggesting these proteins have a broad capacity for conformational flexibility. Furthermore, chromatin is dynamic and there is ongoing remodeling that involves continuous assembly and disassembly of DNA-RNA-protein complexes (Längst et al. 2015). These factors are potentially a considerable source for protein misfolding and aggregation specific to the nucleus.

The majority of nuclear proteins are degraded by the nuclear proteasomes, but a recent study has reported that some nuclear proteins are first exported to the cytoplast and degraded by

cytoplasmic proteasomes (Chen et al. 2014). The ubiquitin ligase involved in nuclear PQC that is nuclear-localized and specific targeting misfolded nuclear proteins for ubiquitination and proteasome degradation.

### 1.3.3 Autophagy in plant

Plant autophagy plays an important role in delaying senescence, nutrient recycling, and stress responses. Autophagy is a process in which cytosol and organelles are sequestered within double-membrane vesicles that deliver the contents to the lysosome/vacuole for degradation and recycling of the resulting macromolecules (Klionsky 2005). During autophagy, an isolation membrane forms, elongates and sequesters cytoplasmic constituents including organelles. The edges of the membrane then fuse to form a double-membrane vesicle termed autophagosome, which can fuse with the lysosomes or vacuoles to deliver the content for degradation (Levine et al. 2005).

Over the past twenty years, more than 30 *ATG* genes have been identified in Arabidopsis  (Kwon et al. 2008). Similar *ATG* genes from other plants including tobacco, rice and maize have also been reported and functionally analyzed (Chung et al. 2009, Liu et al. 2005, Shin et al. 2009, Su et al. 2006). These studies have shown that autophagy plays an important role in nutrient recycling and utilization in plants. Under nitrogen- or carbon-limiting conditions, both the formation of the autophagosome and expression of some of the *ATG* genes are induced (Thompson et al. 2005, Xiong et al. 2005). Furthermore, Arabidopsis mutants defective in autophagy are hypersensitive to nitrogen- or carbon-limiting conditions. Apparently, during nutrient deprivation, cells rely on autophagy for degradation of cellular structures or macromolecules for free nutrients and energy in order to survive nutrient starvation. Other studies have revealed that autophagy is also involved in the regulation of plant senescence (Doelling et al. 2002, Hanaoka et al. 2002, Ishida et al. 2008). Plant senescence can be considered a process of nutrient redistribution. In the parts of plants undergoing senescence such as old leaves, autophagy participates in

the degradation of cellular structures and molecules including chloroplasts and chloroplast proteins for efficient nutrient relocalization and utilization by young tissues and developing fruits and seeds.

Autophagy is involved in plant response to biotic stresses. Emerging evidence indicates that autophagy is a key regulator of plant innate immunity and contributes with both pro-death and pro-survival functions to antimicrobial defences, depending on the pathogenic lifestyle (Hofius et al. 2017). Autophagy is initiated in response to recognition of pathogen-associated molecular patterns (PAMPs) by certain pattern recognition receptors (PRRs) including toll-like (TLR) and nucleotide-binding, leucine-rich repeat proteins (NLR) receptors. One of the most effective mechanisms in plant immune responses against biotrophic pathogens is immunity-related RCD (also known as hypersensitive responses or HR). In *Tobacco mosaic virus* (TMV)-inoculated *Nicotinana benthamiana* (hereafter *N. benthamiana*) expressing the N resistance gene, virus-induced silencing of *ATG6* and *ATG7* genes resulted in expansion of N-mediated HR to uninfected tissue in inoculated leaves and uninfected distant leaves (Liu, Schiff et al. 2005). Likewise, antisense suppression of Arabidopsis *ATG6* limited HR RCD triggered by the *RPM1* R gene in response to the avirulent *P. syringae* pv. tomato *DC3000* expressing the *AvrRpm1* effector (Patel et al. 2008). These studies indicate that autophagy negatively regulates HR RCD in plant immune responses to biotrophic pathogens. Arabidopsis WRKY33, a transcription factor important for plant resistance to necrotrophic pathogens (Zheng et al. 2006), interacts with an autophagy protein, ATG18a, in the nucleus, suggesting possible involvement of autophagy in plant responses to necrotrophic pathogens (Lai et al. 2011). Indeed, autophagy is induced by infection of the necrotrophic fungal pathogen *Botrytis cinerea* and Arabidopsis autophagy mutants exhibited enhanced susceptibility to the necrotrophic pathogens *B. cinerea* and *Alternaria brassicicola* (Lai, Wang et al. 2011, Lenz et al. 2011). Thus, autophagy plays an important role in plant resistance to necrotrophic fungal pathogens.

Autophagy is also induced in plants during abiotic stresses including oxidative, high salt and osmotic stress conditions (Liu et al. 2009, Slavikova et al. 2008). In addition, transgenic RNAi-*AtATG18a* lines defective in autophagy are hypersensitive to ROS, salt and drought conditions (Liu, Xiong et al. 2009). Likewise, rice mutant for *OsATG10b* was hypersensitive to methyl viologen (MV)-induced oxidative stress (Shin et al. 2009). Thus, autophagy is involved in in plant responses to a variety of abiotic stresses.

# OBJECTIVES

The main goals of this thesis are described below:

**Characterization of the AtMC1 protein quality control function in yeast cells.**

1. To analyze the subcellar localization of AtMC1 in yeast during heat stress and aging.

2. To analyze the function of AtMC1 in degradation of misfolded proteins in yeast.

**Characterization of the AtMC1 protein quality control function in plants.**

3. To identify yeast protein aggregate marker orthologues in plant.

4. To analyze the AtHSP101-containing protein aggregate dynamics in plant during heat stress and pathogen attack.

5. To analyze the AtSCE1$^{TS}$ -containing protein aggregate dynamics in plant during heat stress and pathogen attack.

6. To analyze the interaction between AtMC1 and AtHSP101 in plants.

# RESULTS

## 3.1 Arabidopsis AtMC1 localizes in ScHSP104 and ScUB9$^{TS}$-containing foci during heat stress and aging in yeast

The budding yeast *Saccharomyces cerevisiae* expresses a single type I metacaspase ScMCA1, which participates both in programmed cell death (PCD) and in protein quality control (PQC) (Hill et al. 2015, Lee, Puente et al. 2008). ScMCA1, also known as ScMCAIa (Minina, Staal et al. 2020), is recruited into the cytosolic protein aggregates or CytoQs were misfolded proteins initially accumulate, and promotes aggregate clearance (Lee et al. 2010). In addition, over-expression of *ScMCA1* extends the life span of yeast mother cells in a heat shock protein ScHSP104 disaggregase-and proteasome-dependent manner(Hill, Hao et al. 2014).

Previous work in the lab showed that the Arabidopsis metacaspase AtMC1, also known as AtMCAIa (Minina, Staal et al. 2020), is a positive regulator of HR (Coll, Vercammen et al. 2010). In addition, AtMC1 also plays a pro-survival homeostatic function in aging plants in parallel to autophagy(Coll, Smidler et al. 2014). Full-length AtMC1 localizes to insoluble protein aggregates and this accumulation increases with aging. In agreement with that, *atmc1* mutant plants showed a higher protein aggregate content compared to wild-type plants. We hypothesized that this novel pro-survival role of AtMC1 may be functionally related to aggregate clearance similar to has been shown for the single budding yeast metacaspase ScMCA1 (Hill, Hao et al. 2014, Lee, Brunette et al. 2010).

The yeast *Saccharomyces cerevisiae* is easy to grow in the laboratory, has been used as a model system for studying eukaryotic cellular processes and genetically tractable. Scientists have established yeast as a formidable research tool to explore protein misfolding and cellular protein quality control (Di Gregorio et al. 2018). Many of these findings in yeast models have been confirmed in studies using other model organisms (e.g. worms, flies and mice) and even human (Becker et al. 2017, Dahiya et al. 2020, Neef et al. 2010, Tenreiro et al. 2017). Yeast models have been established and delivered novel insights into how different misfolded proteins disturb cellular functions and thus cause toxicity and diseases. In addition,

yeast has only one metacaspase and does not have any apparent homologs. Together, these advantages make yeast an attractive model system to study AtMC1 functions in aggregate clearance.

To test whether AtMC1 can associate with protein protein quality compartments and protein aggregates in yeast, we generated yeast lines that expressed *AtMC1* fused to *mCherry* or *GFP* together with different protein quality control compartment markers, such as ScHSP104, ScUBC9$^{TS}$ and SIK1. *ScHSP104-GFP-HIS3* was co-transformed with the *AtMC1-mCherry* into yeast BY4741 cells for co-localization experiments. ScUBC9 (SUMO-conjugating enzyme) mutant ScUBC9$^{TS}$, harbouring a missense mutation (Y68L) with a temperature-sensitive (TS) phenotype (Betting et al. 1996). The stable ScUBC9$^{TS}$ is fully functional at 28 °C but denatures above 33 °C. ScUBC9$^{TS}$ localizes diffusely in the nucleus and the cytosol under normal conditions. However, when cells are shifted to 37 °C, the ScUBC9$^{TS}$ forms cytosolic protein aggregates (Kaganovich, Kopito et al. 2008). ScUBC9$^{TS}$ fused to mCherry (ScUBC9$^{TS}$-mCherry) and driven by the galactose-regulated promoter was created as a protein aggregate reporter. RFP-tagged SIK1, was used as a nucleolar marker (Huh et al., 2003). *ScUBC9$^{TS}$-mCherry* and *SIK1-RFP* were separately co-transformed with *AtMC1-GFP* into *Scmca1Δ* yeast strain for co-localization experiments.

We analyzed localization of AtMC1-mCherry and different CytoQ compartment markers comparing basal, non-stressed conditions with conditions known to result in the formation of protein aggregates and the activation of protein quality control mechanisms, such as heat and aging (Saarikangas et al. 2015, Vabulas et al. 2010). Under basal conditions, AtMC1-mCherry localization was diffuse throughout the cell (Figure 4A). However, heat stress (38 °C for 30 min) promoted the formation of protein aggregates and AtMC1-mCherry converged into discrete foci. In these foci, we observed co-localization of AtMC1-mCherry with ScHSP104-GFP (Figure 4B).

We also studied whether AtMC1 co-localized with the protein aggregate marker ScUBC9$^{TS}$. In this case, AtMC1 was labeled with GFP, while ScUBC9$^{TS}$ was labeled with mCherry. After heat stress, AtMC1-GFP and ScUBC9$^{TS}$-mCherry foci were observed in the protein aggregates. These foci are highly merged (86%), indicating the co-localization of AtMC1-GFP and ScUBC9$^{TS}$-mCherry (Figure 4B).

In order to ascertain whether AtMC1 foci were exclusively cytoplasmatic or if they were at least partly localized to the nucleus we co-expressed the nuclear marker *SIK1-RFP* with *AtMC1–GFP* under tet-off promoter. We observed that AtMC1 is mostly localized in the cytoplasm, with only 3% cells exhibiting nuclear signal (Figure 4B). This is different from what was found in yeast ScMCA1, which co-localized into nuclear with SIK1 (Hill, Hao et al. 2014).

To address the subcellular localization of AtMC1 in the aging cell, we isolated old cells using the biotin- streptavidin system (Smeal et al. 1996). We grew cells for 10 generations and analyzed microscopically the replicative age-associated protein aggregates. We observed formation and co-localization of AtMC1-mCherry with ScHSP104-GFP foci in aged stationary-phase cultures (Figure 4C), a second physiological stress capable of promoting protein aggregation.

From these data, we conclude that AtMC1 is actively expressed in response to heat stress and aging. It co-localizes with cytosolic protein aggregates. These co-localization data is similar to what was previously found in the yeast ScMCA1(Hill, Hao et al. 2014), which may indicate that there is certain functional conservation between Arabidopsis AtMC1 and yeast ScMCA1 in terms of cytosolic protein aggregate targeting or clearance.

**Figure 4. Co-localization study of AtMC1 and compartment markers ScHSP104, ScUBC9[TS] and SIK1 upon heat stress and aging.** (A) A plasmid harboring AtMC1-mCherry was transformed into *Scmca1Δ* BY4741 cells. Representative images of cells expressing endogenous ScHSP104 tagged with GFP and AtMC1 tagged with mCherry at non-stressed conditions are shown. The C-terminal tagging does not hamper ScHSP104 disaggregation activity (Specht et al., 2011). AtMC1-mCherry and ScHSP104-GFP diffuse throughout the cells. (B) Cells were imaged after heat stress (37 °C for 30 minutes). Co-localization of AtMC1-mCherry and ScHSP-104 discrete foci are shown. where a single locus of the respective gene is tagged with the fluorescent marker indicated. Plasmids harboring *AtMC1-GFP* and *ScUBC9[TS]-mCherry* or *Sik1-RFP* were transformed into *Scmca1Δ* BY4741 cells. AtMC1-GFP, ScUBC9[TS]-mCherry and Sik1-RFP form discrete foci indicated by the tagged fluorescent markers. AtMC1-GFP co-localizes with ScUBC9[TS]-mCherry foci but not to Sik1-RFP after heat stress. (C) Cells were imaged after 12 generations. Representative images show the co-localization of AtMC1-mCherry and ScHSP104-GFP in aged cells.

Next, we examined whether protease activity or the catalytic cysteine of AtMC1 is important for its localization to protein aggregates. To test this hypothesis, we used the catalytic dead

version of the protein AtMC1$_{CACA}$(Coll, Vercammen et al. 2010). This version contains amino acid point substitutions in cysteine 99 and 220, which result in an inactive version of the protease. AtMC1$_{CACA}$ was fused to a mCherry fluorescent tag and its localization during heat stress was analyzed. Under basal conditions, AtMC1$_{CACA}$ localization was diffuse throughout yeast cells, similar to the wild-type version of AtMC1. After heat stress, we observed formation and co-localization of AtMC1$_{CACA}$-mCherry with ScHSP104-GFP foci (Figure 5A).

Similar to the wild-type version of AtMC1, the catalytic dead version co-localized with ScHSP104 and ScUBC9$^{TS}$ separately during heat stress (Figure 5B). These results indicate that the protease catalyitic activity of AtMC1 is not required for localization of the protein into ScHSP104 or ScUBC9$^{TS}$-containing aggregates. In order to ascertain whether AtMC1 foci were exclusively cytoplasmatic or if they were at least partly localized to the nucleus we co-expressed nuclear marker SIK1-RFP with AtMC1$_{CACA}$-GFP. We observed that AtMC1$_{CACA}$ is mostly localized in the cytoplasm, with 5% cells exhibiting nuclear signal (Figure 5C). Together, these data suggest that AtMC1 localization to protein aggregates does not require its catalytic activity.
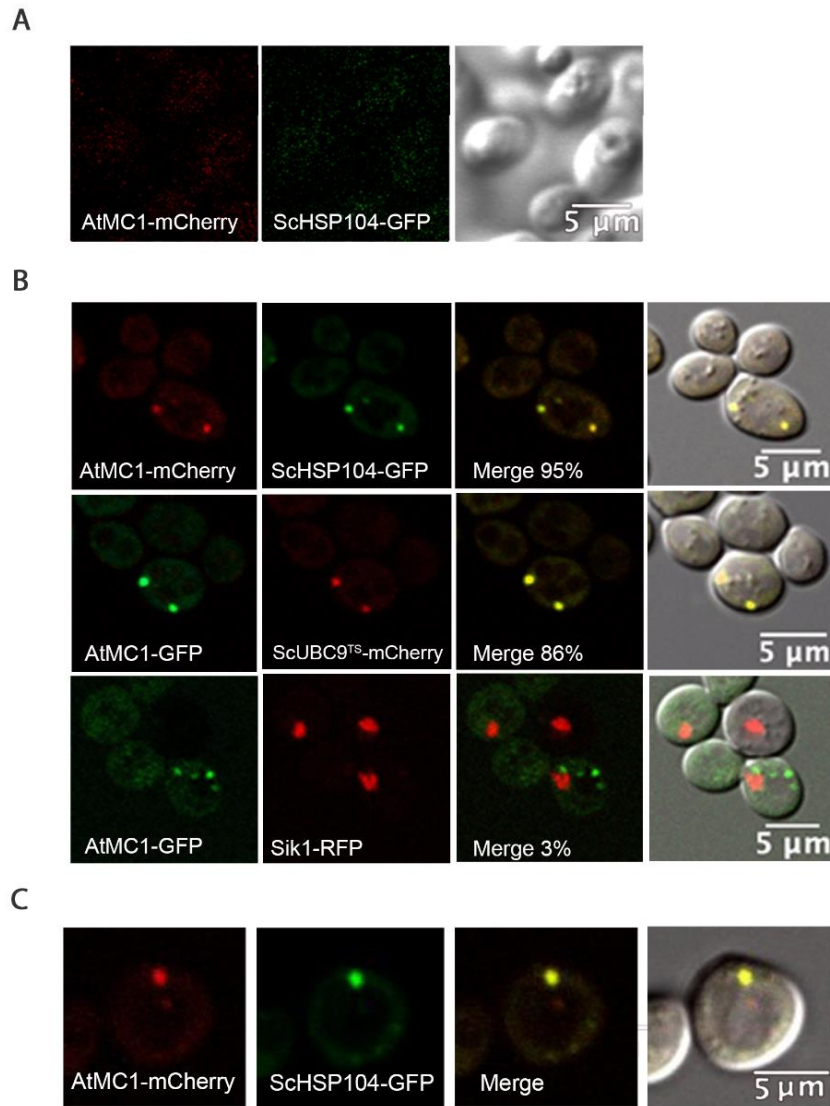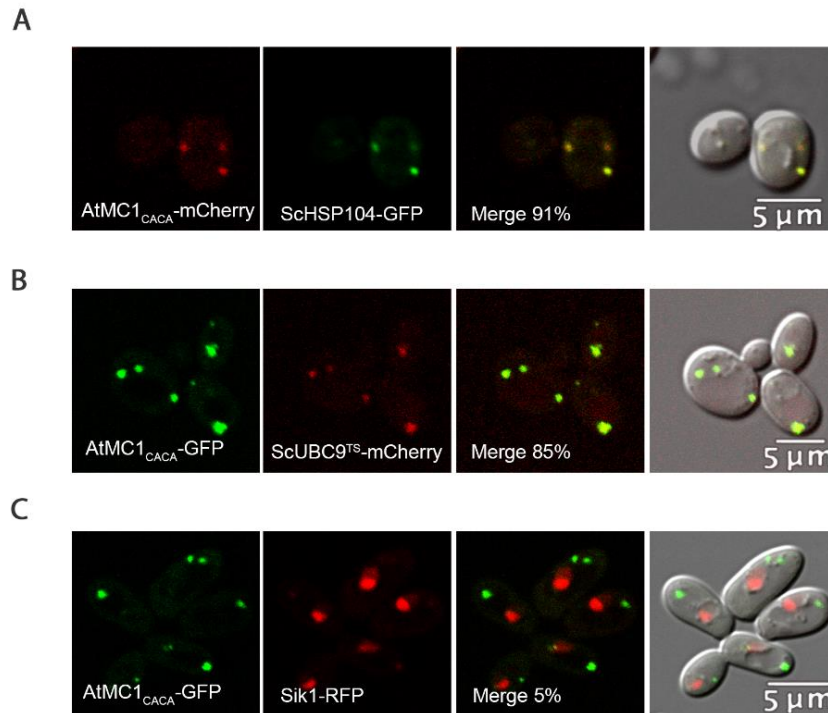
**Figure 5. Co-localization study of AtMC1$_{CACA}$ and compartment markers ScHSP104, ScUBC9$^{TS}$ and SIK1 upon heat stress.** (A) The plasmid harboring AtMC1$_{CACA}$-mCherry was transformed into *Scmca1Δ* BY4741 cells. Representative images of cells expressing endogenous ScHSP104 tagged with GFP and AtMC1 tagged with mCherry are shown. (B) The plasmids harboring AtMC1$_{CACA}$-GFP and ScUBC9$^{TS}$-mCherry were transformed into *Scmca1Δ* BY4741 cells at the same time. Representative images show that AtMC1$_{CACA}$-GFP co-localizes with ScUBC9$^{TS}$-mCherry foci during heat stress. (C) The plasmids harboring AtMC1$_{CACA}$-GFP and SIK1-RFP were transformed into *Scmca1Δ* BY4741 cells at the same time. Representative images show that AtMC1$_{CACA}$-GFP does not co-localize with SIK1-RFP during heat stress. Cells in (A)(B)(C) were imaged after heat stress (37 °C for 30 minutes).

## 3.2 AtMC1 participates in the degradation of misfolded proteins in yeast

Considering the localization of AtMC1 into protein aggregates, we wanted to determine whether it had a role in clearance of misfolded proteins in yeast. It has been reported that the yeast metacaspase *ScMCA1Δ* deletion mutant strain affected misfolded protein degradation activity (Hill, Hao et al. 2014). In order to study the role of AtMC1 in elimination of misfolded proteins, we used a cytoplasmically localized substrate ΔssCL*myc (Figure 6A). The degradation ΔssCL*myc by the proteasome does not require any of the cytoplasmic helper components of the ERAD pathway (Eisele et al. 2008, Medicherla et al. 2004). In these experiments, the plasmid harbouring the constitutively expressing misfolded protein ΔssCL*myc was transformed into a yeast strain defective in the *LEU2* gene. In wild- type

strains the ΔssCL*myc protein including the Leu2 moiety is rapidly eliminated by the proteasome. These strains are unable to complement the leucine auxotrophy and therefore cannot grow (Figure 6A). In contrast, strains defective in *Scmca1* are able to grow due to stabilization of the Leu2 containing-substrate and by this complementing the *LEU2* deficiency.

We generated *Scmca1Δ*-AtMC1 yeast strain, using the $P_{GPD}$-*AtMC1-HA* fusion gene integrated into the deleted *Scmca1Δ* genomic site of the *Scmca1Δ* strain. Expression of the AtMC1-HA fusion protein was confirmed by immunoblot using anti-HA antibody (Figure 6B).

As expected, *Scmca1Δ* mutant strain exhibited strong growth when compared to wild type on medium lacking leucine, indicating stabilization of the substrate due to defects in protein degradation (Figure 6C) and confirming previous results (Hill, Hao et al. 2014). Interestingly, we found that yeast *Scmca1Δ* mutant complemented with a wild-type copy of AtMC1 reduced growth on medium lacking leucine, indicating that AtMC1 participates in ΔssCL*myc degradation. We next measured the levels of ΔssCL*myc in these strains. Western blot analysis showed that ΔssCL*myc was strongly stabilized in *Scmca1Δ* cells, whereas its levels were sharply reduced in wild-type yeast and in the AtMC1 *Scmca1Δ* complemented cells (Figures 6D and E). These results further reinforce the idea that AtMC1 is required for efficient removal of terminally unfolded proteins. Together, these data demonstrate that, similar to ScMCA1, AtMC1 is required for efficient removal of terminally unfolded proteins in yeast and that this role is evolutionarily conserved.
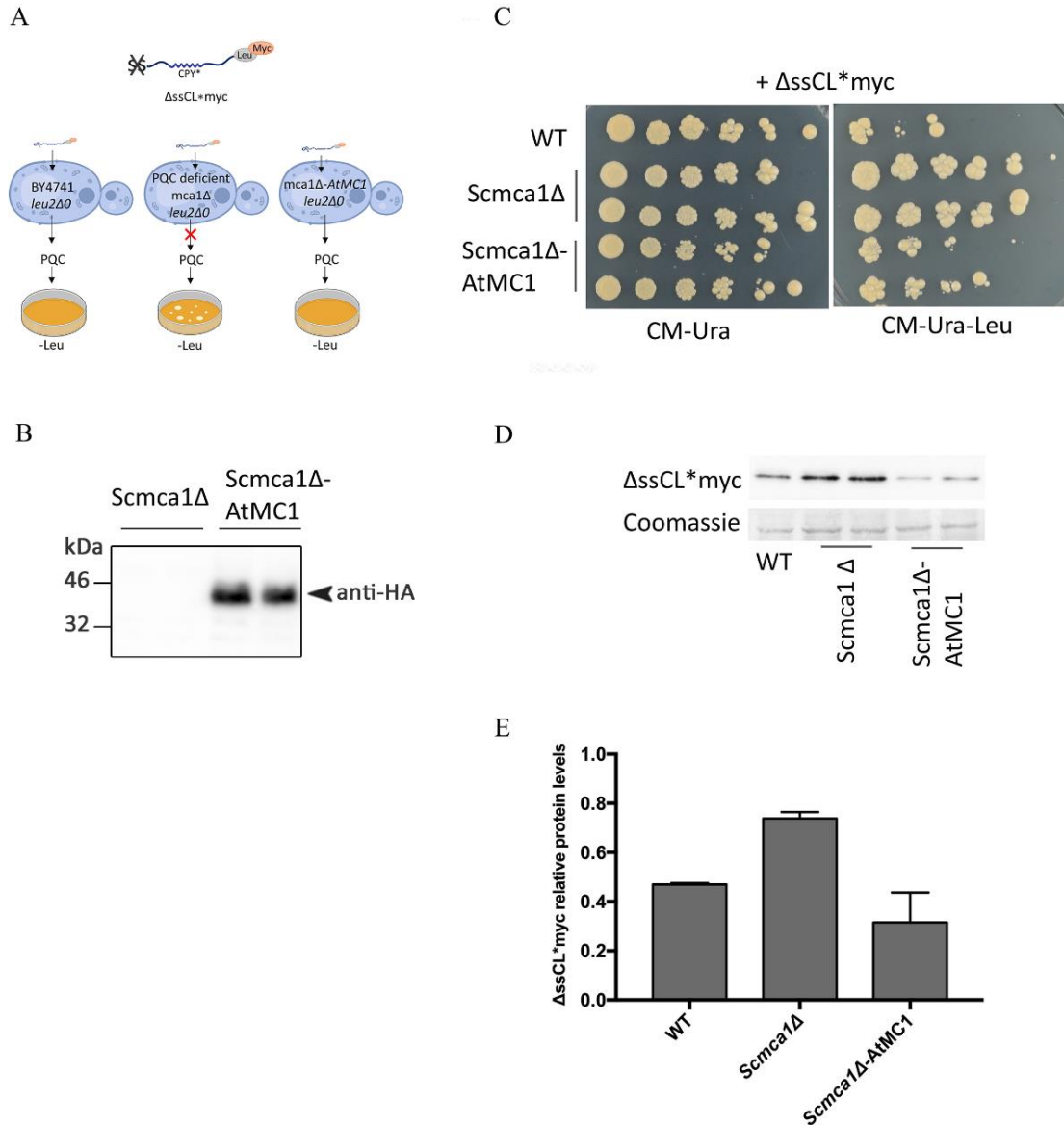
**Figure 6. AtMC1 participates in clearance of the terminally misfolded ΔssCL\*myc protein in yeast.** (A) Schematic drawing of the chimeric protein ΔssCL\*myc, consisting of cytoplasmically misfolded CPY\* C-terminally fused to Leu2 and a myc tag. (B) Western blot analysis of *Scmca1Δ*-AtMC1 yeast strain. *Scmca1Δ* and *Scmca1Δ*-AtMC1 yeast strains total protein were extracted and 25 µg of total protein were analysed by SDS-PAGE and anti-HA immunoblot. Black arrow indicates AtMC1-HA (41 kDa). (C) Serial dilutions of wild type (WT), *Scmca1Δ* mutant and AtMC1 complement cells *Scmca1Δ*-AtMC1 expressing ΔssCL\*myc (ΔssCL\* fused to Leu2) were spotted on indicated media and incubated for 3 days at 30 °C. Enhanced growth on plates lacking leucine indicates stabilization of ΔssCL\*myc, whereas reduced growth indicates increased degradation. N = 3. (D) Western blot analysis of ΔssCL\*myc levels of the indicated strains with anti-myc antibody. The coomassie stained gel represents the total amount of loaded proteins. (E) Western blot quantifications using ImageJ and GraphPad Prism 7.0.

Given the promising results that we obtained in yeast, next we addressed the question of whether AtMC1 role in misfolded protein aggregate clearance was conserved in plants. In

contrast to yeast, plant protein aggregate markers are poorly studied. Therefore, we had to develop the tools to study the phenomenon in planta. The plant orthologues of *ScHSP104* and *ScUBC9* are *AtHSP101* and *AtSCE1*, respectively. Therefore, we analyzed these genes and generated transgenic plants in the appropriate backgrounds to determine whether these proteins could also serve as aggregate markers in plants.

## 3.3 Identification and analysis of the ScHSP104-like gene sequence

Yeast ScHSP104 belongs to a large family of highly conserved proteins known as the HSP100 or Clp protein family (Squires and Squires, 1992). Members of the HSPl00/Clp family are found in both prokaryotes and eukaryotes, where they are present in the cytosolic nuclear compartment and in organelles. Some members are induced by heat; others are not. The HSPl00/Clp proteins share two large blocks of sequence homology (ca. 200 amino acids) centred around two ATP binding consensus elements. The ATP binding domains are flanked by less conserved N-terminal, spacer, and tail domains (Gottesman et al., 1990; Squires and Squires, 1992).

*AtHSP101*, the Arabidopsis ortholog of yeast *ScHSP104*, encodes a molecular chaperone belonging to the ClpB/HSP100 family of AAA+ proteins. AtHSP101 contains two highly conserved ATP binding domains and more variable N-terminal, spacer, and C-terminal. AtHSP101 protein is 43% identical to the yeast ScHSP104 protein. AtHSP101 is able to provide thermotolerance to yeast cells that are missing their own ScHSP104 (Schirmer et al. 1994). Hence, the Arabidopsis AtHSP101 protein is both a structural and functional homolog of yeast ScHSP104. The ClpB/HSP100 family of AAA+ chaperones assemble into homohexamers capable of disaggregating misfolded proteins. AtHSP101, which is known as a cytosolic heat shock protein, is also involved in refolding proteins which form aggregates under heat stress (Bhandawat et al. 2020, McLoughlin et al. 2019).

**Figure 7. Phylogenetic tree and sequence alignment of AtHSP101 and ScHSP104.** (A) Phylogenetic tree of ScHSP104 and AtHSP101 with its homologous proteins in Arabidopsis based on the amino acid sequences. The tree is drawn to scale, with branch lengths in the same units as those of the evolutionary distances used to infer the phylogenetic tree. Evolutionary analyses were conducted in MEGA X (Kumar et al. 2018). (B)Alignment of amino acid sequences of AtHSP101 with yeast ScHSPl04. Alignment was performed with T-COFFEE using default parameters (Clustal W). Domains form N- to C-terminal: N-terminal domain is marked in blue, NBD1domain is marked in yellow, M-domain, NBD2 is marked in green and C-terminal domain is marked in purple.

## 3.3 Identification and analysis of the ScUBC9-like gene sequence

In Arabidopsis, the ortholog of yeast ScUBC9 is SUMO CONJUGATING ENZYME 1 (AtSCE1), the only SUMO-conjugating enzyme in Arabidopsis (Xiong et al. 2013). The amino acid sequence of AtSCE1 showed a high degree of conservation with ScUBC9 protein in the yeast by BLAST analysis using TAIR database. Amino acid sequence in AtSCE1 is 53% homologous to ScUBC9. Like ScUBC9, AtSCE1 has a conserved UBCC (Ub-Conjugating enzyme Catalytic) domain that spans most of the protein and includes a positionally conserved cysteine that forms the thiol ester linkage with the peptide modifier (Kurepa et al. 2003). Phylogenetic analysis reflected that AtSCE1 has high degree of homology with orthologs from diverse organisms indicating that plant AtSCE1 proteins may have evolved from a common ancestor (Figure 8A).

The Y68L mutant of ScUBC9 has a temperature-sensitive phenotype, which causes that the ScUBC9$^{TS}$ variant forms cytosolic protein aggregates at 37 °C (Kaganovich, Kopito et al. 2008). Thus, the Y68L mutant of ScUBC9 can be used as a marker for protein aggregates. Based on the highly conserved sequence and structure, including the Y69/Y68 amino acid (Figures 8B and C), between AtSCE1 and ScUBC9, we thus used the AtSCE1 Y69L mutant (AtSCE1$^{TS}$) as a marker to study protein aggregate dynamics in Arabidopsis.
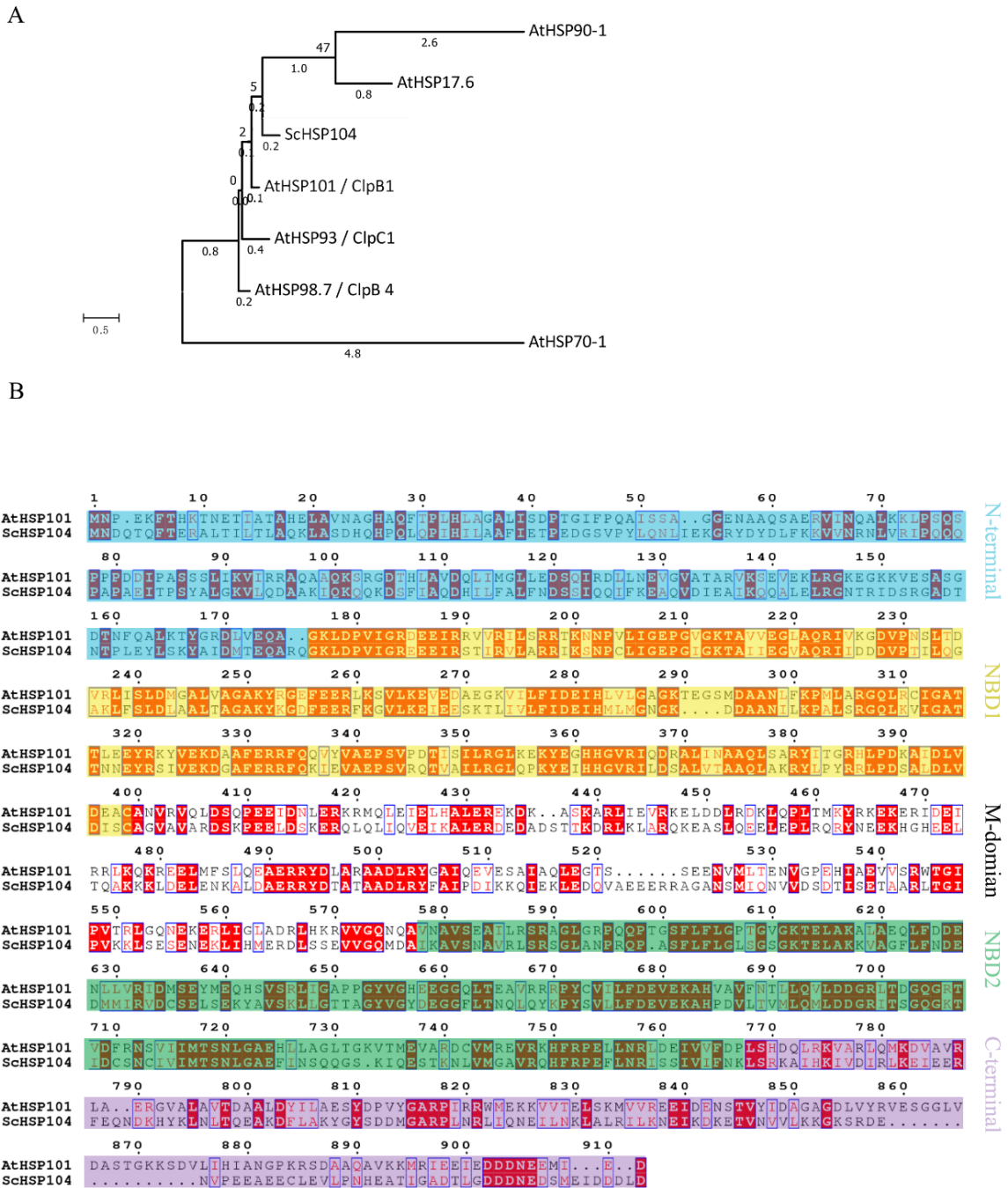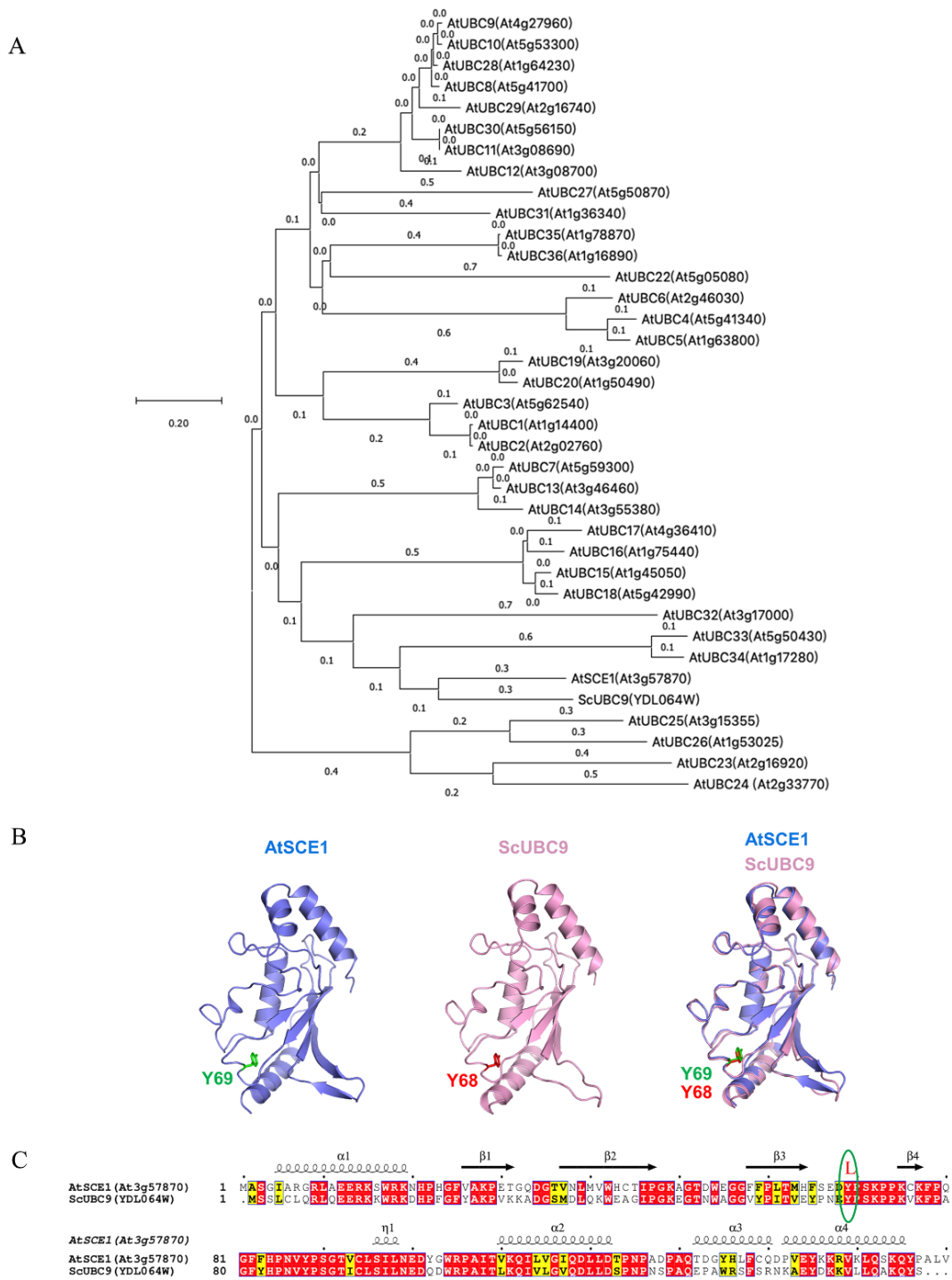
**Figure 8. Phylogenetic tree and sequence alignment of AtSCE1 and ScUBC9.** (A) Phylogenetic tree of ScUBC9 and AtSCE1 with its homologous proteins in Arabidopsis based on the amino acid sequences. The species names are indicated. The tree is drawn to scale, with branch lengths in the same units as those of the evolutionary distances used to infer the phylogenetic tree. Evolutionary analyses were conducted in MEGA X. (B) Structures of AtSCE1 (blue, PDB code: 6GV3) and ScUBC9 (pink, PDB code: 3ONG) are shown and their structures are superimposed with root-mean-square deviation of 0.58Å. The amino acid Y69 (green) in AtSCE1 and Y68 (red) in ScUBC9 in structures are highly conserved. ScUBC9 Y68L mutant (ScUBC9[TS]) and AtSCE1 Y69L mutant (AtSCE1[TS]) were used for the formation of

cytosolic protein aggregates in this study. (C) Protein sequence alignment of AtSCE1 and ScUBC9. The green circle indicates Y69 in AtSCE1 and Y68 in ScUBC9. Sequences are aligned online with Clustal Omega and formatted using ESPript.

## 3.4 AtMC1 and AtHSP101 co-localize in the cytosol of Arabidopsis protoplasts

Our next goal was to investigate the cellular localization of AtHSP101 in plant cells and whether it co-localized with AtMC1. First, we analyzed localization of AtHSP101 fused to GFP under the control of its native promoter (*P$_{AtHSP101}$::AtHSP101-GFP)* in Arabidopsis leaf protoplasts. For this, we extracted leaf protoplasts of transgenic plants stably expressing *P$_{AtHSP101}$::AtHSP101-GFP* in *atmc1* background and observed its localization using confocal laser scanning microscopy. Images obtained after 16 hours of protoplast culture clearly showed that the AtHSP101-GFP signal was observed in numerous speckles throughout of the cytoplasm (Figure 9A).

To assess whether AtHSP101 and AtMC1 co-localized in Arabidopsis, we transfected leaf protoplasts of *P$_{AtHSP101}$::AtHSP101-GFP* transgenic plants with a *35S::AtMC1-RFP* construct following Schapire et al. (2016). RFP and GFP signal were examined 16 hours after transfection under the confocal microscope. As shown in Figure 9B both AtMC1 and AtHSP101 formed speckles, with two sizes distinguishable: large and small. AtMC1 speckles largely overlapped with AtHSP101-GFP speckles. Two types of speckles could be observed both in overlapped AtMC1-RFP speckles and these big speckles always overlapped (Figure 9C), then AtHSP101-GFP formed much more small speckles than the AtMC1-RFP formed. Co-localization of AtMC1-RFP and AtHSP101-GFP in leaf protoplasts may support physical interaction between both proteins within speckles.
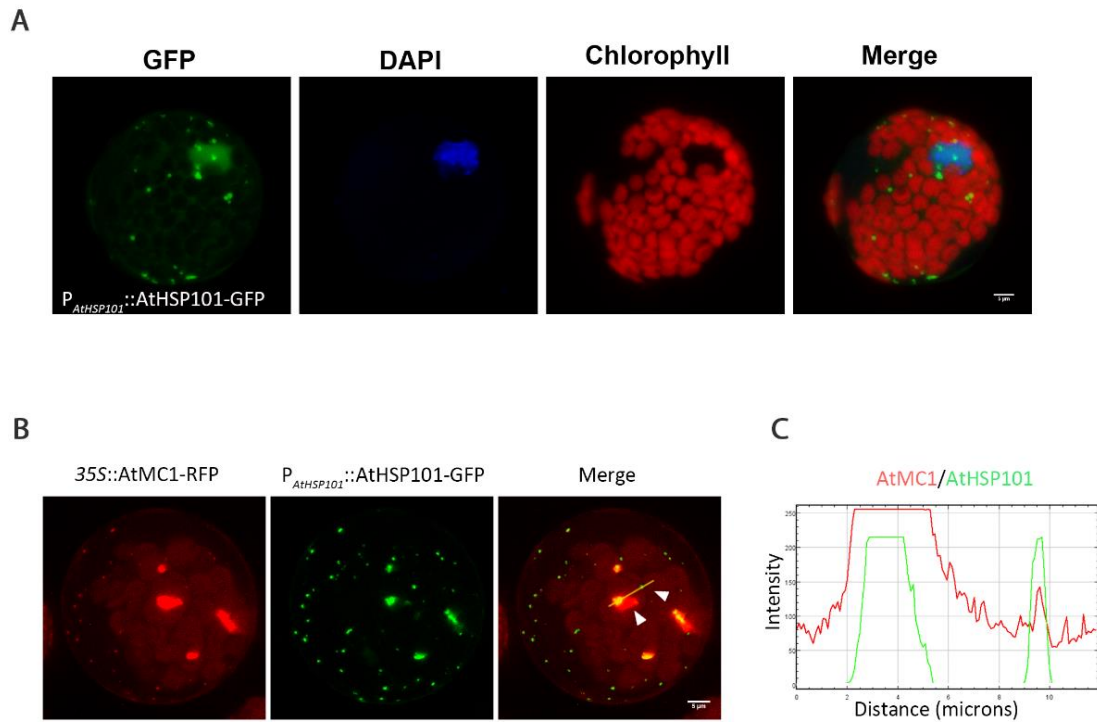
**Figure 9. Subcellular localization and co-localization of AtHSP101 and AtMC1.** (A) Confocal microscopic analyses of GFP signals from Arabidopsis leaf protoplasts of transgenic plants stably expressing *$P_{AtHSP101}$::AtHSP101-GFP* in *atmc1* background. Images of the GFP signal (green), nucleus stained with DAPI (blue), chlorophyll fluorescence (red), and merged (combined fluorescence from GFP, chlorophyll and DAPI). Scale bars, 5 µm. (B) Confocal images of Arabidopsis protoplast 16 h after PEG-mediated transient expression of the indicated constructs. Images of GFP signal (green), RFP signal (red) and merge (green plus red) from the same cell were shown. The white arrowheads indicate co-localization of AtHSP101-GFP and AtMC1-RFP in the small and big speckles. in Scale bars, 5 µm. (C) The line profile plots indicate the fluorescence intensity distribution of green and red channels through the yellow line in the merged panel B. The fluorescence intensity was calculated using ImageJ software.

## 3.5 AtHSP101 co-immunoprecipitates with AtMC1 in plants

To test whether AtMC1 co-immunoprecipitates with AtHSP101 in plant cells we used transient co-expression of the proteins in *N. benthamiana* using *Agrobacterium tumefaciens*-mediated transformation. *$P_{AtHSP101}$::AtHSP101-GFP* ($OD_{600}$=0.5) (~128 kDa), and *35S::GFP* ($OD_{600}$=0.05) (~27 kDa), were each transiently co-expressed with HA-fused AtMC1 under the control of a dexamethasone promoter (*Dex::AtMC1-HA*, ~40 kDa) ($OD_{600}$=0.2). As negative controls, *35S::GFP* and *Dex::AtMC1-HA* were used. All constructs were co-expressed together with the anti-silencing vector p19 (Voinnet et al. 2003)

(OD$_{600}$=0.1). Two days after *N. benthamiana* leaf infiltration, heat stress was applied to the whole plant (1 h at 38 °C) and the day after leaves were collected for protein extraction.

Total protein was extracted and quantified (inputs). Equal amounts of each extract were subjected to immunoprecipitation using magnetic beads coupled with anti-GFP antibody. Proteins bound to the magnetic beads were eluted after several washes as described in detail in the material and methods section (bound fraction). Input and bound samples were subjected to western blot analysis using anti-HA and anti-GFP antibodies. As shown in Figure 10A, AtMC1 co-immunoprecipitated with AtHSP101-GFP but not with the GFP control.

The pro-domain of AtMC1 has been shown to act as a negative regulator of the protein, as its removal results in a constitutively active form of the protein (Coll et al. 2010,). To test whether the pro-domain was required for the co-immunoprecipitation with AtHSP101, we co-expressed the prodomain-less version of AtMC1 (*Dex::AtMC1-ΔN-HA*) with *P$_{AtHSP101}$*::AtHSP101-GFP. AtMC1-ΔN co-immunoprecipitated with AtHSP101-GFP but not with the GFP control, indicating that the pro-domain of AtMC1 is not required for interaction with AtHSP101 (Figure 10B).

We also tested the requirement of an intact AtMC1 catalytic site for the co-immunoprecipitation with AtHSP101. We co-expressed the catalytic dead version of the protein AtMC1CA (*Dex::AtMC1$_{CACA}$-HA*) with *P$_{AtHSP101}$*::AtHSP101-GFP. AtMC1CA still co-immunoprecipitated with AtHSP101-GFP but not with the GFP control, albeit to a lesser extent than the wild type AtMC1version (Figure 10C).
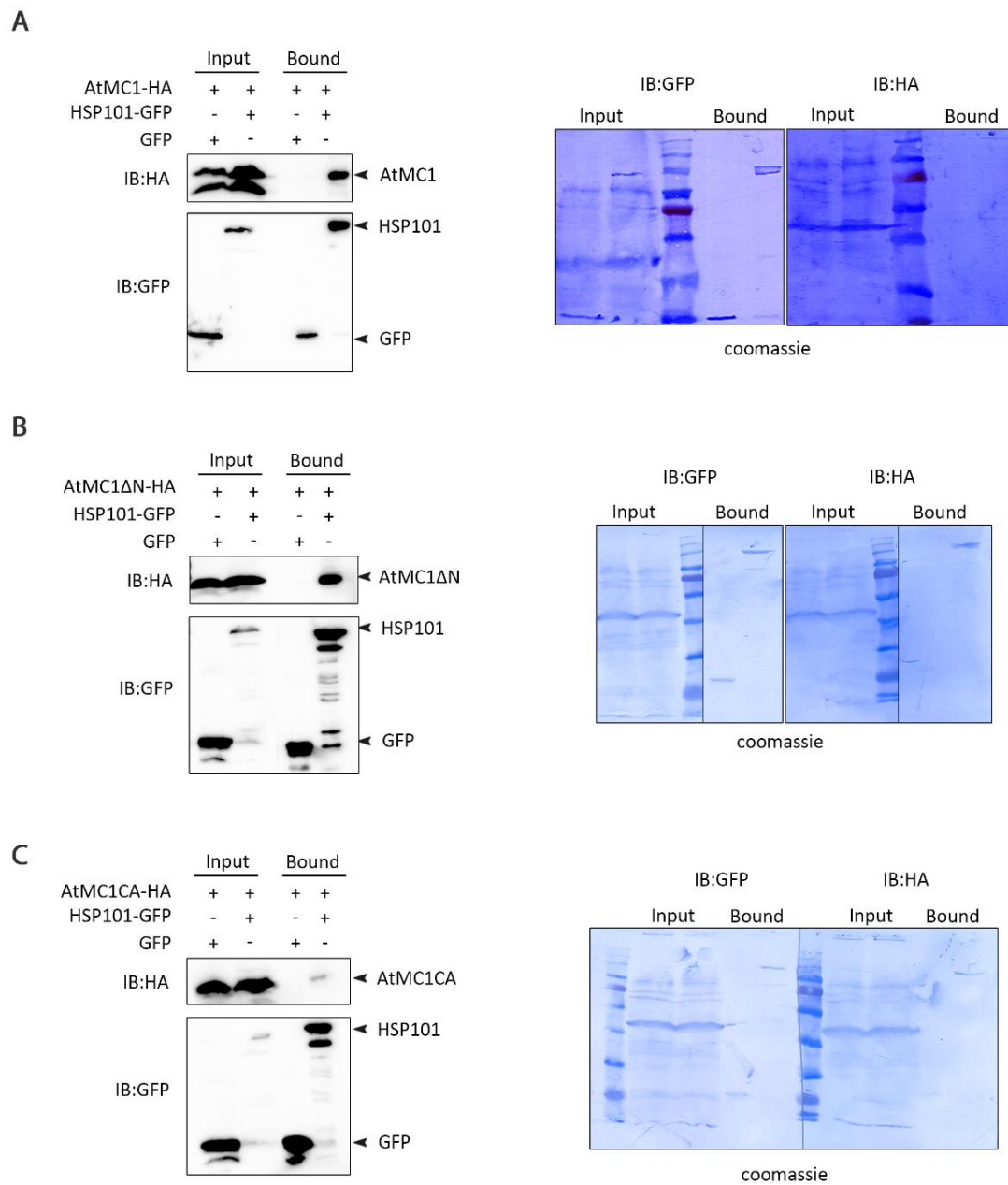
**Figure 10. AtMC1-AtHSP101 co-immunoprecipitation occurs independently of AtMC1 prodomain but an intact catalytic core is partly required.** Different AtMC1-HA forms (CA, catalytic dead; ΔN, prodomain-less) were transiently expressed in *N. benthamiana* leaves alone or in combination with AtHSP101-GFP. Total proteins were extracted (input), incubated with magnetic beads coupled to green fluorescent protein (GFP) and, after stringent washes, proteins bound to the beads were eluted (bound). Input and bound fractions were either Coomassie-stained or probed against anti-GFP to detect AtHSP101 or against anti-HA to detect AtMC1 (A), AtMC1-ΔN (B) or AtMC1-CA (C).

## 3.6 AtHSP101 Forms Dynamic Foci during Heat Stress and Recovery

Our yeast data together with the *in planta* data showing that AtMC1 and AtHSP101 co-localize and co-immunoprecipitate, led us to speculate that these two proteins may function together in aggregate clearance. Similar to the yeast metacaspase ScMCA1, Arabidopsis AtMC1 might be recruited to protein aggregate foci together with the disaggregase AtHSP101 to facilitate aggregates degradation by the proteasome. To analyze whether AtMC1 was required for protein aggregate clearance involving AtHSP101, we generated transgenic lines stably expressing $P_{AtHSP101}::AtHSP101-GFP$ on a *atmc1* mutant background. In our analysis, we also included transgenic lines expressing $P_{AtHSP101}::AtHSP101-GFP$ on an autophagy mutant background (*atg18a*) and the *atmc1 atg18a* double mutant background. As a control, we used $P_{AtHSP101}::AtHSP101-GFP$ transgenic plants on a wild-type background. In the past, we showed that the AtMC1 localizes to insoluble protein aggregates that increase with age. Furthermore, *atmc1atg18a* double mutant accumulated a further extent age-dependent insoluble aggregates than the single *atmc1* mutant (Coll, Smidler et al. 2014). Plant lacking *atg18a* are defective in autophagosome formation, *atmc1* mutant displayed normal autophagosome formation, which indicates that AtMC1 acts in a parallel pathway to autophagy in relation to insoluble aggregate clearance. AtMC1-mediated aggregate clearance and autophagy could constitute two complementary processes controlling cellular homeostasis during stress responses and aging by virtue of their ability to eliminate accumulated cellular debris.

AtHSP101-GFP is present at very low levels in non-stressed Arabidopsis seedlings but highly accumulates upon heat stress (Hong et al. 2001). To study the dynamics of AtHSP101 protein during heat stress recovery, we used a protocol in which seedlings grown at 22 °C are treated with an hour heat shock at 38 °C, followed by recovery at 22 °C. The representative images were taken from the epidermal layer (40 Z-stacks with stack size of 0.36 µm) after 0, 2, 4, 8, 24, 48, 72 and 120 hours post recovery (hps). In Col-0 background we observed dynamic aggregate foci formation in the thermo-recovery period. Under basal

conditions AtHSP101 exhibited very low expression (Figure 11A). However, heat stress caused proteotoxic stress and led to dramatic increase of misfolded aggregate proteins. This triggered synthesis of molecular chaperones such as AtHSP101. AtHSP101-GFP accretion gradually increased till 24 hps, then gradually dissipated to basal levels at 120 hps (Figure 11A). AtHSP101-GFP foci were distributed in both the nucleus and the cytoplasm, but is mainly in the cytoplasm in 2, 4 and 8 hps. The number of nuclear AtHSP101-GFP foci was more than cytoplasm in 48, 72 and 120 hps though there was an obvious gradual decrease because of the PQC kick off in nucleus (Figures 11A and B).

As expected, AtHSP101-GFP expression was strongly enhanced after heat stress, and became concentrated in discrete cytoplasmic foci and nuclear foci (Figure 11A). At 2 hours post-stress (hps), the foci in the cytoplasm were very large, having an average diameter of 2.5 µm and a maximum diameter of 10 µm. The nuclear foci were smaller than the cytoplasmic foci, having an average diameter of 0.9 µm and mostly with only one focus per nucleus observed. At 4 hps, the AtHSP101-GFP foci coalesced into small foci during the recovery phase but the nuclear foci increased in size over time. The cytoplasmic foci become mostly diffuse at 48 hps. At 24 hps, the AtHSP101-GFP foci coalesced into small foci during the recovery phase but the nuclear foci increased in size over time. The cytoplasmic foci become mostly diffuse at 48 hps. However, the nuclear foci are persisted even after 72hr of recovery. Together, these data show that AtHSP101 is rapidly recruited to dynamic cytoplasmic foci after heat stress and persists in the nucleus of the cell, which could imply that the cytoplast more quickly disaggregate/refold their protein complement and/or is better protected against protein misfolding/aggregate.

Next, we investigated the role of AtMC1, autophagy or the combination of both in AtHSP101 heat foci dynamics. Plants lacking *atmc1*, *atg18a* or both (*atmc1 atg18a* mutants) showed altered AtHSP101 dynamics. *atmc1*, *atg18a* and *atmc1 atg18a* mutants started accumulating AtHSP101 aggregates 2 hps. However, they had more aggregates that were larger in size. These aggregates remained longer in the cytoplasm when compared to wild-

type. At 48 hps there no aggregates were observed in a wild-type background, whereas in *atmc1, atg18a* and *atmc1 atg18a* mutants a considerable number of aggregates were observed. At 72 hps very conspicuous aggregates were observed in the nucleus of *atmc1*, *atg18a* and *atmc1 atg18a* mutants, potentially indicating defects in protein aggregate clearance. When comparing the defects in single *atmc1* or *atg18a* mutants to the double *atmc1 atg18a* mutants, the effects were more marked in the latter, which indicates an additive phenotype or independent participation of the two pathways in the process. In conclusion, our data indicates that AtMC1- and autophagy-mediated processes participate in clearance of heat stress-induced AtHSP101 aggregates, as defects of this pathways result in delayed dismissal of these nucleo-cytoplasmic aggregates.

A
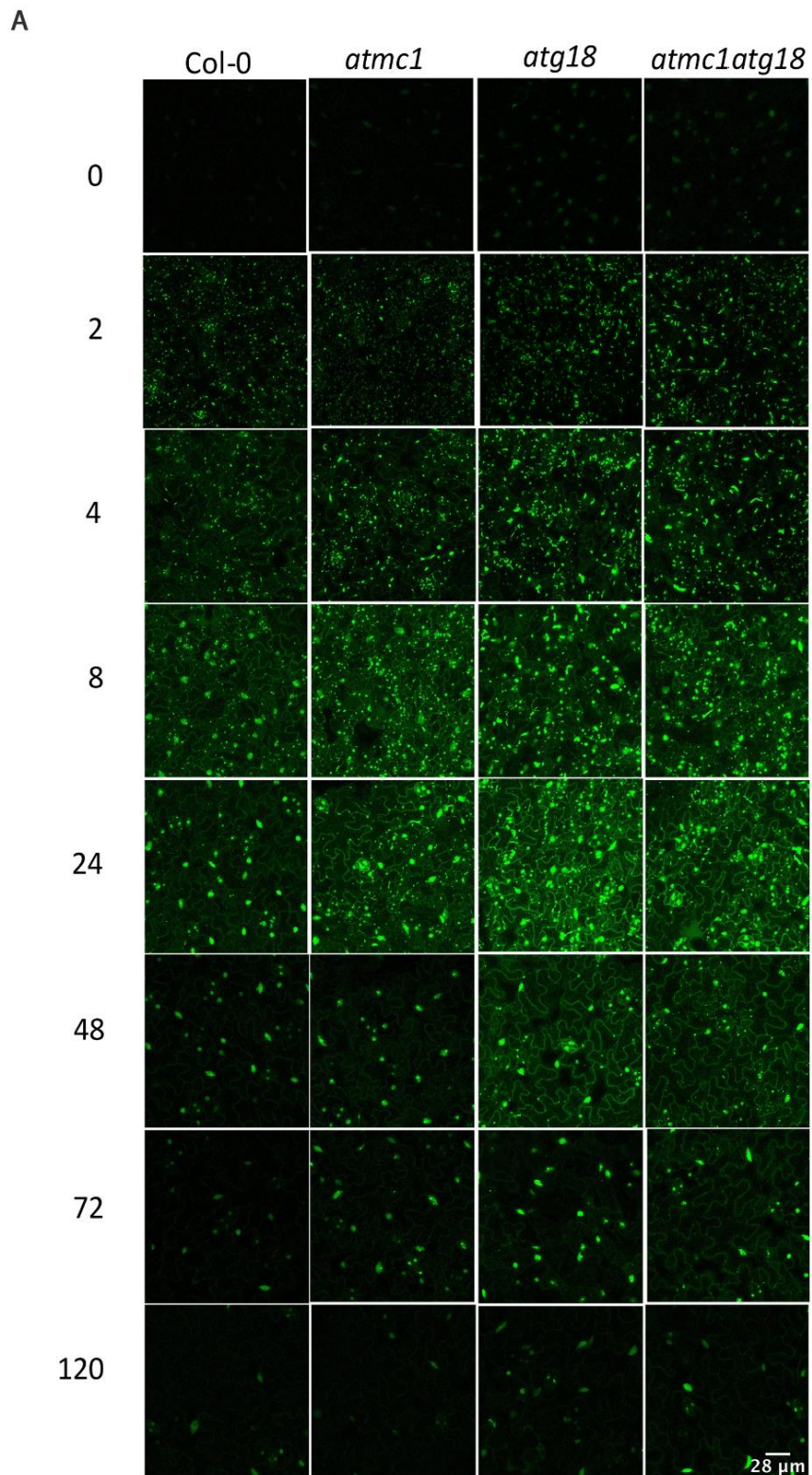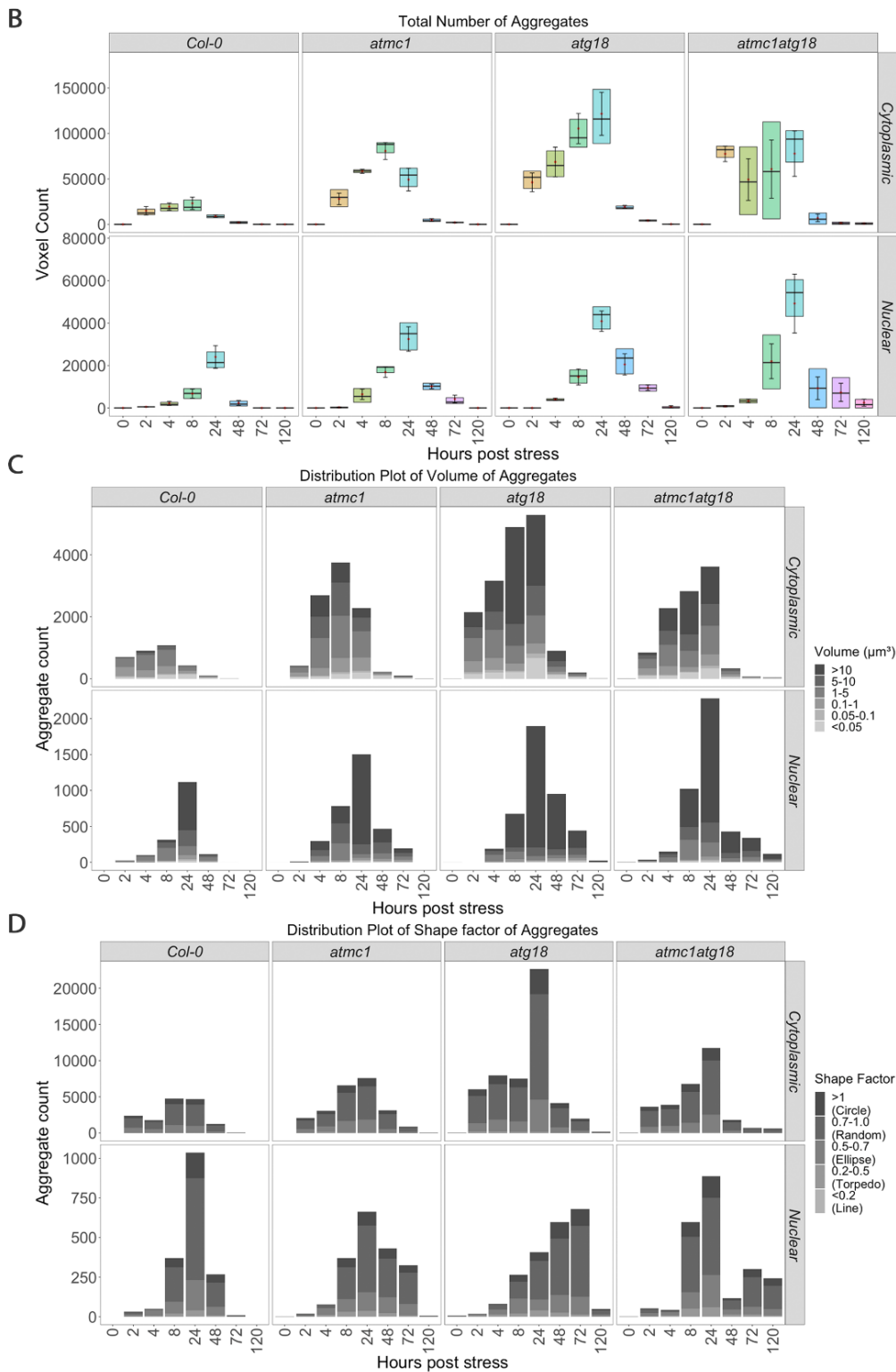
**Figure 11. AtHSP101-GFP dynamics during heat stress recovery are altered in *atmc1* and autophagy mutants**. 14-day-old AtHSP101-GFP seedlings grown on solid medium at 22 °C in long days (16-h light/8-h dark) were heat acclimated at 38 °C for 1 h and allowed to recover at 22 °C for different periods of time at which images were taken using a confocal microscope. (A) The representative images were taken from the epidermal layer (40 Z-stacks with stack size of 0.36 µm) after 0, 2, 4, 8, 24, 48, 72 and 120 hours post recovery (hps). Scale bars = 28µm. (B) Total number of AtHSP101 foci

measured after heat stress in leaf cells. Each bar represents the measurement of AtHSP101foci from multiple confocal microscope photos. The central line locates the median value, + indicates the average value, the box encompasses the upper and lower quartiles, and the error bars show the maxima and minima of the number distributions. (C) The volume of AtHSP101 foci measured after heat stress in leaf cells. (D) The shape of AtHSP101 foci measured after heat stress in leaf cells.

## 3.7 AtHSP101 are mostly destined for autophagy-mediated degradation rather than 26s proteasomal degradation

To test how AtHSP101 aggregates were cleared, we investigated AtHSP101 foci dynamics after treatment with proteasome and autophagy inhibitors. MG132 blocks proteasomal degradation whereas Concanamycin A (ConA) causes accumulation of proteins degraded by autophagy in the vacuole. Six-day-old Wt, *atmc1*, *atg18*, or *atmc1 atg18* seedlings stably carrying the *P_{AtHSP101}::AtHSP101-GFP* transgene were pre-treated with 1 h heat stress at 38 °C, then incubated in liquid medium containing either 50 μM MG132 or DMSO as a solvent control. Seedlings were kept for 16 h in dark and then observed by microscopy. Leica confocal images are shown in Figure 12A. Treatment with the proteasomal inhibitor MG132 did not result in significant differences in AtHSP101 foci levels compared with DMSO-treated controls.

ConA, a V-ATPase inhibitor, is frequently used to stabilize vacuole proteins (Yoshimoto et al. 2004). Six-day-old Wt, *atmc1*, *atg18*, or *atmc1 atg18* seedlings stably carrying the *P_{AtHSP101}::AtHSP101-GFP* transgene were pre-treated with 1 h heat stress at 38 °C, then incubated in liquid medium containing either 1 μM ConA or DMSO as a solvent control. The seedlings were kept for 16 h in dark and then observed by microscopy. Leica confocal images are shown in Figure 12B. In wild-type leaves treated with ConA, there were many AtHSP101-GFP-containing foci in vacuoles, suggesting that they may be carried by autophagic bodies. In contrast, vacuoles in *atg18* and *atmc1 atg18* were small and did not contain spherical structures (Figure 12B). Remarkably, autophagy inhibitor ConA significantly blocked the removal of AtHSP101 protein foci at the 16 h of the recovery phase in Col-0 and *atmc1* mutants. In these backgrounds, numerous foci can be observed inside

the vacuoles and video images show that the foci are highly mobile, following the typical brownian movement of proteins in the vacuole. In contrast, in the *atg18a* and *atmc1 atg18a* mutant backgrounds, impaired in the autophagosome formation, no differences were observed after ConA treatment compared to the control. These results indicate that AtHSP101 foci are cleared via autophagy, rather than the proteasome.

A
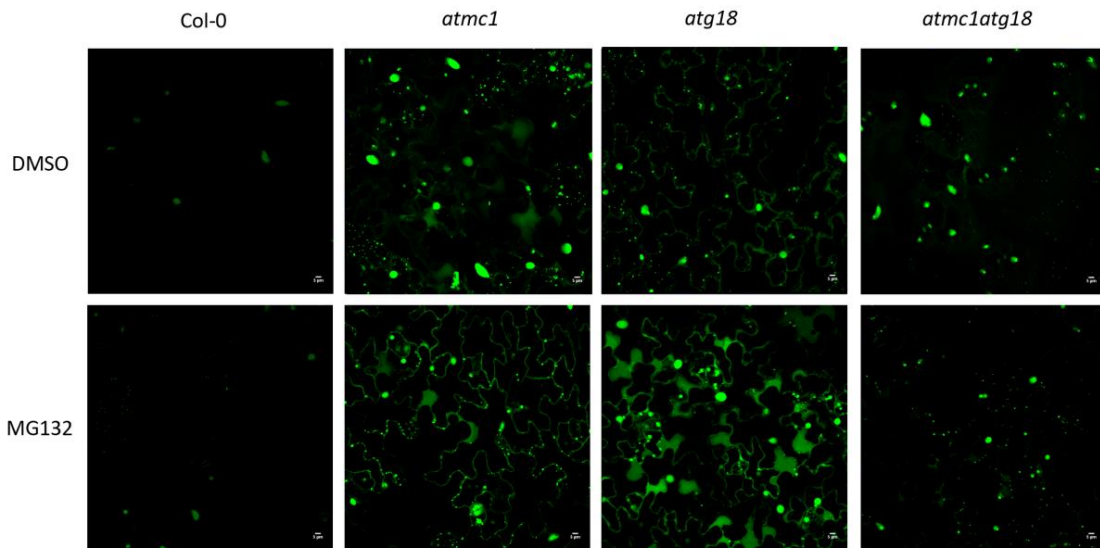


B
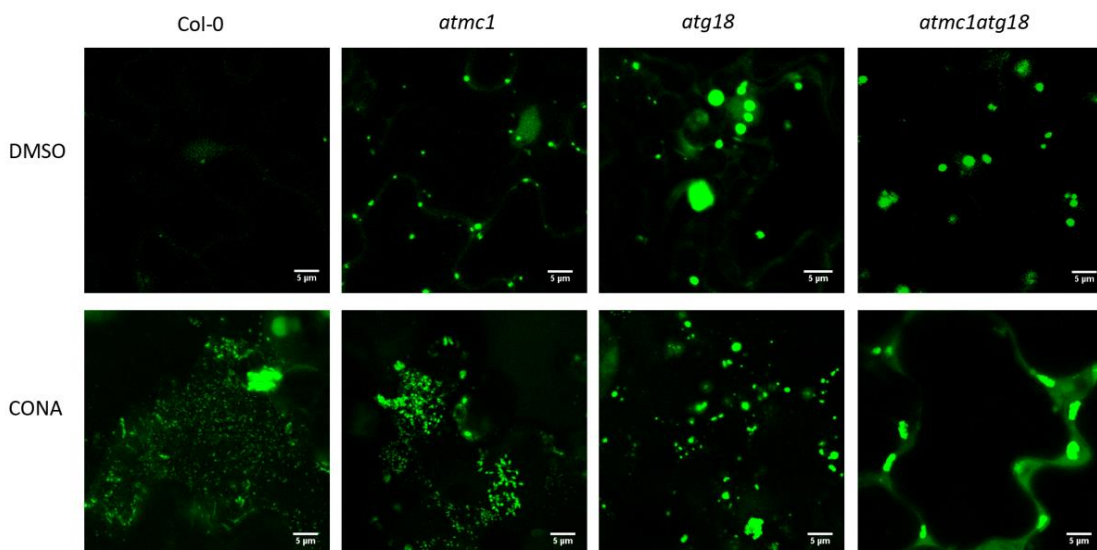
**Figure 12. Autophagy, but not the proteasome, participate in the clearance of AtHSP101-GFP-containing foci formed during the recovery phase after a heat stress treatment.** Fluorescence images of leaf epidermal cells of transgenic Arabidopsis cell stably expressing AtHSP101-GFP heated at 38 °C for 1 h followed by MG132 treatment or ConA treatment or DMSO treatment as control (see Methods). (A). MG132-treated cells not accumulated small GFP-labeled foci in the central vacuole.   (B). ConA-treated cells accumulated small GFP-labeled bodies in the central vacuole in the Col-0 and *atmc1*mutant background plant, while autophagy mutant *atg18* and *atmc1atg18* are not observed.

## 3.8 AtHSP101 Forms Dynamic Foci upon Pathogen attack

Based on our initial observation that AtHSP101 forms dynamic foci after heat stress treatment, we wondered whether AtHSP101 foci formation and clearance was exclusively a response to heat stress or it also occurred after pathogen attack. We infected 2-week-old transgenic Arabidopsis seedlings expressing AtHSP101-GFP with *P. syringae* pathovar tomato strain (*Pto* DC3000 expressing the type III effector *avrRpm1 Pto* DC3000(*avrRpm1*)). Recognition of AvrRpm1 triggers hypersensitive response programmed cell death mediated by the intracellular NLR receptor RPM1. Compared with the non-infected control, AtHSP101-GFP foci are more abundant upon infection. Additionally, the *atmc1, atg18a* and *atmc1 atg18a* mutants showed higher AtHSP101 foci content than wild-type Col-0 plants upon infection (Figure 13). This indicates protein aggregates also form as part of the defense response against pathogens, and that AtMC1 and autophagy participate in clearance of these aggregates.
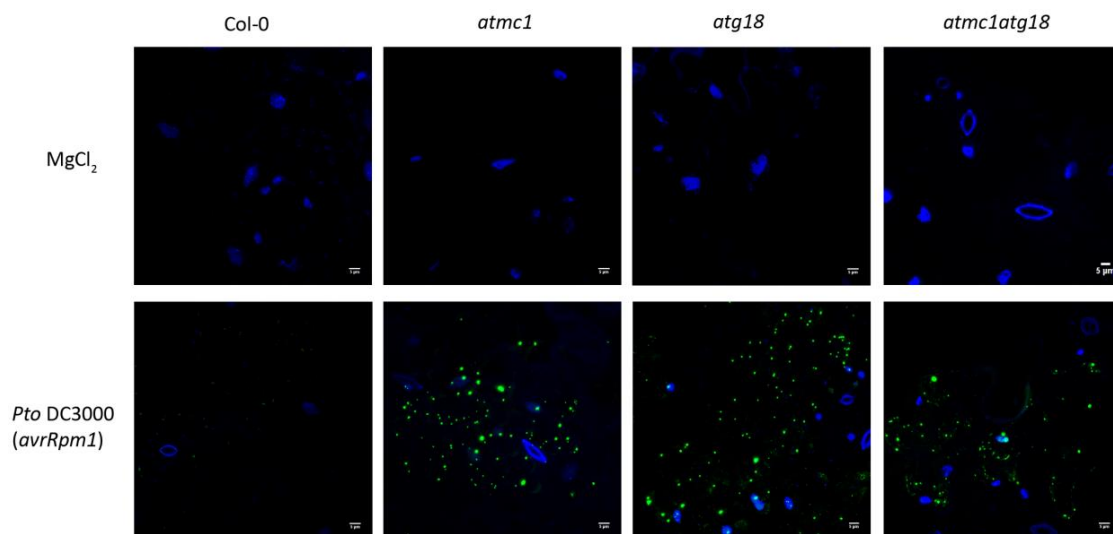
**Figure 13. AtHSP101-GFP Containing foci are found upon *P. syringae* infection.** 14-day-old AtHSP101-GFP seedlings of the indicated phenotypes were vacuum infiltrated with 500,000 colony-forming units (CFU)/ml of Pto DC3000(avrRpm1) or MgCl2. After 6 h, leaves were stained with the DAPI and imaged.

## 3.9 AtSCE1$^{TS}$ Forms Dynamic Foci during Heat Stress

The Arabidopsis AtSCE1$^{TS}$ (AtSCE1$^{TS}$ is the mutation of the 69 tyrosine residues to leucine) was transiently expressed in *N. benthamiana* leaves as a fusion with cyan fluorescent protein (CFP). AtSCE1$^{TS}$-CFP localized in the cytoplasm and diffused into the nucleus. AtSCE1$^{TS}$-CFP accumulated into small fluorescent foci after heating for 1h at 42 °C. We could not observe foci formation at lower heat stress temperatures. The AtSCE1$^{TS}$-CFP fluorescent foci were relatively more uniform in size than AtHSP101-GFP foci, having an average diameter of 1.78 ± 0.44μm a maximum diameter of 2.14 μm. By monitoring fluorescence recovery after photobleaching that AtSCE1$^{TS}$-CFP foci were relatively immobile, while AtHSP101-GFP foci were not. The AtSCE1$^{TS}$-CFP fluorescent foci pattern was clearly distinguishable from the pattern observed in AtHSP101. To determine AtSCE1$^{TS}$ localization in its native Arabidopsis system, we created stable transgenic plants expressing AtSCE1$^{TS}$ fused to CFP under the control of the cauliflower mosaic virus 35S promoter. Transgenic lines were analysed by confocal laser scanning microscopy, and CFP fluorescence was observed in the cytoplasm and nucleus. To investigate the AtSCE1$^{TS}$ localization after heat stress, the 2-week-old transgenic Arabidopsis seedlings were placed under heat stress (42 °C for 1h). AtSCE1$^{TS}$-CFP fluorescence is observed to form small foci in the cytoplasm and nucleus. These foci in the cytoplasm and nucleus show a similar size have an average diameter of 1μm.
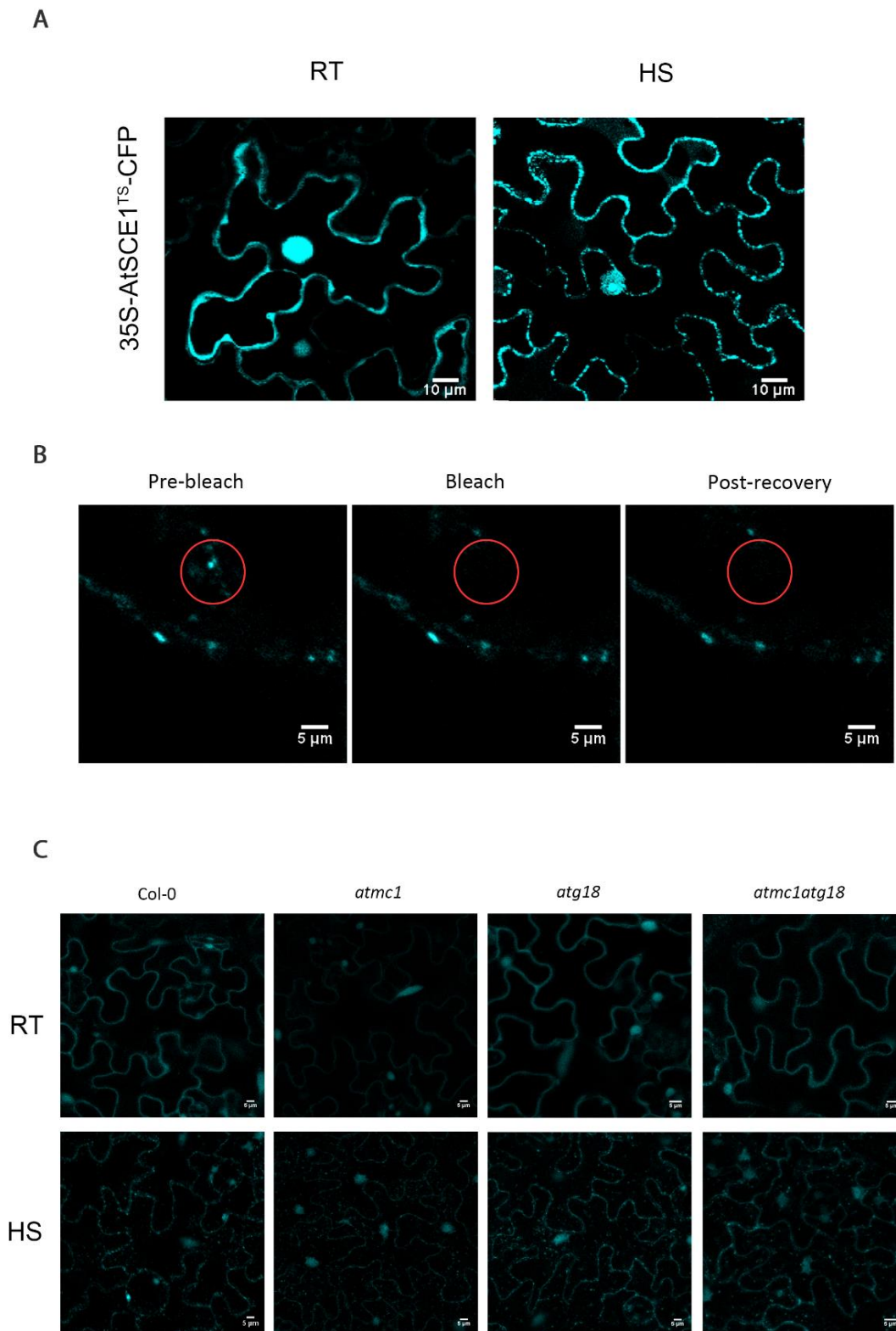
**Figure 14. Heat stress induces the formation of AtSCE1 $^{TS}$ -CFP-containing foci.** (A). The *35S::AtSCE1$^{TS}$-CFP* transiently expressed in *N. benthamiana* leaves as a fusion with cyan fluorescent protein (CFP). AtSCE1$^{TS}$ -CFP localises to the cytoplasm and diffuses into the nucleus under normal condition. AtSCE1$^{TS}$-CFP foci accumulated after heating for 1h at 42 °C. (B). Determination of FLIP of AtSCE1$^{TS}$-CFP that is expressed in *N. benthamiana* leaves. The circle indicates

the area that is photobleached. The post-recovery image was taken 3 min after photobleaching. (C). 14-day-old *35S::AtSCE1^{TS}-CFP* seedlings of the indicated phenotypes were heated at 42 °C for 1 h. RT, room temperature; HS, heat stress.

## 3.11 AtSCE1^{TS} subcellular localization upon pathogen attack

Based on the results that AtHSP101 forms dynamic foci after *P. syringae* infection, we wondered whether AtSCE1^{TS} was also localized into protein aggregate foci after pathogen attack. Two-week-old AtSCE1^{TS}-CFP transgenic Arabidopsis seedlings were infected with *Pto* DC3000 (*avrRpm1*) and their subcellular localization was tested under confocal laser scanning microscopy. However, we could not observe AtSCE1^{TS}-CFP aggregate foci formed after infection. The distribution of AtSCE1^{TS}-CFP signals was diffused throughout the cytoplasm and nuclear similar to the non-infected control. Together, our data indicate that AtSCE1^{TS} aggregate formation is limited to heat stress, but does not occur in response to pathogen attack.
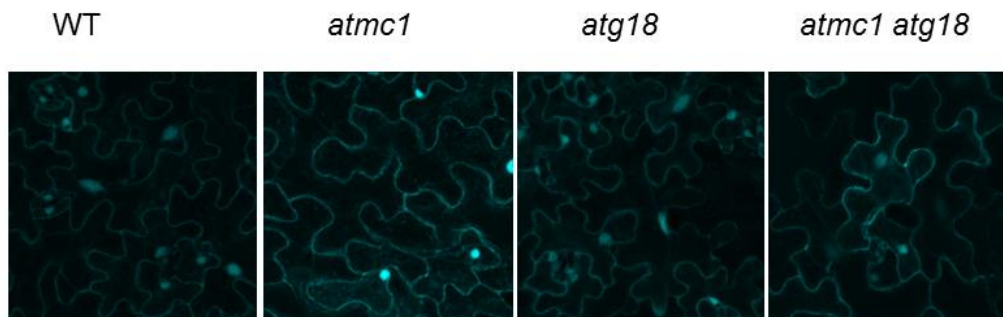


**Figure 15. AtSCE1^{TS}-CFP Containing foci are not formed upon pathogen attack.** (A). 14-day-old *35S ::AtSCE1^{TS}-CFP* seedlings of the indicated phenotypes were vacuum infiltrated with 500 000 colony-forming units (CFU)/ml of *Pto* DC3000(*avrRpm1*) or MgCl2. After 12 h, leaves were imaged.

## 3.12 AtMC1 negatively regulate dark-induced senescence

Research in our lab showed that AtMC1 is a negative regulator of natural senescence in Arabidopsis (Coll, Smidler et al. 2014). Light plays an essential role in senescence regulation and darkening of leaves leads to rapid senescence, especially when only a part of the plant is affected. Leaf senescence is a developmentally programmed event, which

involves a number of physiological, biochemical, and molecular changes, including a decline in photosynthetic efficiency, decreases in chlorophyll and protein contents, and increases in membrane ion leakage and expression of senescence-associated genes (*SAGs*) (Sarwat et al. 2013). The chloroplast is the organelle which shows the earliest sign of senescence symptoms (Soudry et al. 2005). In order to determine the possible roles of AtMC1 in regulating senescence, we compared the response of atmc1 mutants with wild-type and a complemented line (*atmc1 P$_{AtMC1}$::AtMC1-HA*) to dark-induced senescence (Weaver et al. 2001). For this, we covered the seventh individual fully expanded leaves with aluminium foil and whole plants were grown under long-day condition for 5 days. In *atmc1* mutant plants, the senescence phenotype progressed faster than in Col-0 plants (Figure 16A). The transgenic *AtMC1* complemented lines showed only partial complementation of the *atmc1* mutant senescence phenotype. To better analyze the observed senescence phenotype, we also examined the chlorophyll content in the Col-0, *atmc1* mutant and AtMC1 complemented plants after the dark-induced senescence treatment. A significant reduction (40%) in both chlorophyll a and b contents was observed in leaves of *atmc1* mutant plants compared with Col-0 plants. Concomitantly, the chlorophyll content of AtMC1 complemented plants showed a slight reduction. To this end, Quantitative PCR analysis was used to determine the transcript abundance of a common senescence marker *AtSAG12*. In response to 5 days of dark, the transcript abundance of *AtSAG12* increased in wild-type, *atmc1* mutant and AtMC1-complemented plants. Expression of *AtSAG12* was significantly higher in *atmc1* mutant than in Col-0 and AtMC1 plants.
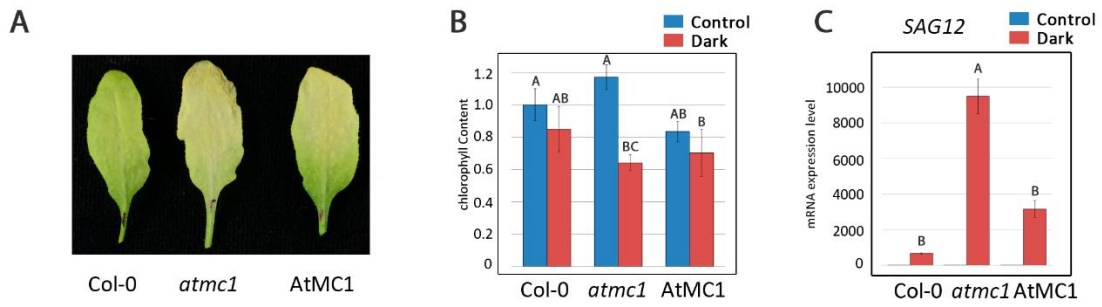
**Figure 16. Dark-Induced Leaf Senescence.** (A) Phenotypes of dark-induced leaves from 4-week-old Col-0, *atmc1* and *atmc1 P_{AtMC1}::AtMC1-HA* plants. (B) Relative chlorophyll contents in dark-induced leaves from 4-week-old Col-0, *atmc1* and AtMC1 plants (C) Quantitative real-time PCR analysis of the senescence marker gene *SAG12* in dark-induced senescing leaves of the indicated genotypes, normalized to β-tubulin. Letters indicate a significant difference following a one-way ANOVA with Bartlett's test (α=0.05). The experiment is representative of three independent replicates.

**DISCUSSION**

A healthy proteome is essential for cell survival. Protein misfolding in humans is associated with multiple diseases like Alzheimer, Huntington, and Parkinson, recently drawing a great extent of research attention (Knowles et al. 2014, Soto 2003). Accumulation of misfolded proteins in plant organelles can cause dysfunctions which lead to developmental defects and impaired environmental stress tolerance. Cells have evolved a sensitive system for protein quality control (PQC) to minimize the accumulation of misfolded proteins to manage proteome homeostasis. Cells manage the misfolded proteins by their spatial sequestration into several defined compartments, which plays a central role in protein quality control (Sontag et al. 2017). Misfolded cytosolic proteins have been shown to be sequestered in two evolutionarily conserved dynamic compartments, IPOD and JUNQ (Bagola et al. 2008). The IPOD is thought to terminally sequester toxic amyloid and prion proteins in the periphery of yeast cells near the vacuole (Hill et al. 2017). Misfolded and stress-damaged proteins are shuttled to dynamic compartments called Q-bodies, and rapidly cleared by the ubiquitin-proteasome pathway (Escusa-Toret et al. 2013, Ogrodnik et al. 2014, Spokoini et al. 2012). If clearance is impaired, these misfolded proteins are concentrated in the JUNQ. Proteins in JUNQ are more dynamic than IPOD and may act as a reservoir for the storage of misfolded proteins for subsequent refolding or clearance (Kaganovich, Kopito et al. 2008). Misfolded proteins can also accumulate in the nucleus. Less is known about nuclear PQC in yeast. The cytosolic misfolded proteins are suggested to be routed to an intranuclear quality control compartment (INQ), which is located just inside the nuclear membrane and next to the nucleolus and may aid in the clearance of misfolded proteins from the nucleus (Miller, Ho et al. 2015).

## 4.1 Protein quality control mechanisms and components are conserved between yeast and plants

Molecular chaperones are essential for misfolded protein recognition and sorting to the various PQC compartments, thus they can be used as sensitive molecule markers for different compartments (Alberti 2012, Hill, Hao et al. 2014). In yeast, ScHSP104 localizes

to both the JUNQ and IPOD in yeast. The ScHSP104 can solubilizes and reactivates proteins form denatured aggregates, and the bacterial homolog, ClpB possesses similar activity. There is no ScHSP104 homolog in metazoans, while the plant orthologue of ScHSP104 is AtHSP101. The mammalian cells uncover such activities analogous protein. Plants and yeast may have similar PQC components which are different from animals.In yeast, ScUBC9[TS] is used an JUNQ aggregate maker. In this study, we also generated plants carrying the ScUBC9 [TS] ortholog in plants AtSCE1[TS], which can be used as a new marker for protein aggregate formation upon heat stress.

Autophagy also plays a role in PQC networks, the whole protein quality control compartments may be targeted to vacuole via the autophagy pathway. The composition of RNP granules such as SGs and processing bodies in plant cells is similar to those protein quality control compartments in yeast and metazoans (Chantarachot et al. 2018). Our laboratory has shown that autophagic components and AtMC1 are required for clearance of protein aggregates, emerging as central players in the proteostasis network across species. In this study, we showed that AtMC1 is actively expressed in response to heat stress and aging and co-localized with cytosolic protein aggregates in yeast. This is similar to the yest ScMCA1, indicating a certain functional conservation across species. AtMC1 also participates in the degradation of misfolded proteins in yeast, and its catalytic activity is dispensable. Similar to yeast, AtMC1 and AtHSP101 also co-localize in the cytosol. In addition, AtMC1 could co-immunoprecipitate with AtHSP101, which didn't require the intact AtMC1 catalytic site and pro-domain.

## 4.2 The plant metacaspase AtMC1 may participate in clearance of protein aggregates.

ScMCA1 was observed to be a regulator of cell cycle progression; the loss of which reduced cellular fitness and abolished the G2/M cell cycle checkpoint upon microtubule disruption (Lee, Puente et al. 2008). ScMCA1 exerted a pro-life effect by contributing to proteostasis

maintenance (Hill, Hao et al. 2014). ScMCA1 was shown to mediate key interactions with known members of the proteostasis network such as Cdc48, ScHSP104, and the ScHSP70/40 chaperone systems (Shrestha, Puente et al. 2013). ScMCA1 has been observed to localize to distinct quality control compartments such as the JUNQ in aging yeast, which is at a time when proteostasis mechanisms are in a steady decline (Hill, Hao et al. 2014). The ubiquitination of various misfolded protein substrates has been suggested to be a limited sorting factor for JUNQ (Kaganovich, Kopito et al. 2008). Indeed, loss of ScMCA1 led to increased retention of insoluble protein material within the cell, coupled with an engagement of the compensatory autophagic response (Lee, Brunette et al. 2010). Finally, ScMCA1 has been shown to limit/prevent protein aggregation in daughter cells during yeast aging studies (Hill, Hao et al. 2014). ScMCA1 is ubiquitinated at multiple lysine residues, one of which (K355) oversees its protein regulatory role. Abrogation of this modification led to the altering of proteostasis safeguards within the cell. Rsp5 as the candidate E3 ligase which acts on ScMCA1 via an upstream phosphorylation site (S346). Rps31 as a substrate for ScMCA1, suggesting that this metacaspase regulates proteostasis (in part) by stimulating ubiquitin biogenesis (Shrestha, Brunette et al. 2019).

Compelling observations that link ScMCA1 to protein aggregate management, a similar role has been described for the plant metacaspase AtMC1, suggesting that proteome regulation is a conserved metacaspase function (Coll, Smidler et al. 2014). Our data show that transformation of the plant *AtMC1* gene into yeast *Scmca1* deletion mutant complemented clearance of unfolded proteins. In Arabidopsis, we have shown that *atmc1* plants accumulate more AtHSP101-containing aggregates than wild-type plants during heat stress response. In *atmc1 atg18a* plants, this phenotype is enhanced, indicating that the AtMC1 acts independently to autophagy in protein aggregate clearance. Furthermore, we also conducted pathogen infection to ascertain whether AtHSP101-containing protein foci also form as part of defense responses and what are their dynamics. Our data suggested that pathogen infection induced cellular protein aggregation, and AtHSP101 was involved in this process.

The increased AtHSP101-containing aggregates were observed in pathogen infected plants. Further, *atmc1* mutants and autophagy-deficient mutants accumulated more AtHSP101-containing aggregates than wild-type. Our hypothesis is that AtMC1 functions in aggregate clearance during heat stress and pathogen attack.

## 4.3 AtMC1 involved in AtHSP101-containing aggregates

In yeast ScMCA1 and ScHSP104 form foci and co-localize during heat stress and aging (Lee, Brunette et al. 2010). ScMCA1 interacts with ScHSP104 and other molecular chaperones to maintain proteostasis. Our data shows that in yeast AtMC1 and ScHSP104 co-localize in foci during heat stress and aging. In plants, the formation and co-localization of AtMC1 and AtHSP101 foci was observed in the Arabidopsis protoplast. Furthermore, AtMC1 co-immunoprecipitated with AtHSP101 in *N. benthamiana* after heat stress. *atmc1* plants accumulated more AtHSP101-containing aggregates than wild-type plants upon heat stress and pathogen attack. Together, these data suggest that AtMC1 may contribute to protein quality control by functionally interacting with the AtHSP101 protein or protein aggregates.

Analysis of heat stress-induced AtHSP101-containing aggregates degradation in the presence or absence of protesome inhibitor MG132 or autophagy inhibitor ConA revealed that most AtHSP101-containing aggregates are degraded through autophagy, with a much less than expected contribution from proteasome-dependent processes. A similar observation was made in yeast, where most ScHSP104 clients are disaggregated without proteasomal clearance  (Wallace et al. 2015). This result can also explain that heat stress induced AtHSP101-containing aggregates persisted longer after recovery in the autophagy mutant than wild-type and *atmc1* mutant plants, where autophagy occurs normally (Coll, Smidler et al. 2014). Our data shows that in the *atmc1* plants, the degradation of heat stress-induced AtHSP101-containing aggregates were inhibited by the autophagy inhibitor ConA, but not affected in autophagy mutants. Together, AtMC1 seems to be involved in protein

aggregation/clearance acting in a parallel pathway to the autophagy for protein quality control.

## 4.4 Heat stress and pathogen attack induced distinct aggregates

All living organisms experience environmental stress, which can alter protein homeostasis. In addition to environmental stress, aging also results in a decline in protein homeostasis efficiency (Hipp et al. 2019). Studies in *Caenorhabditis elegans* show that both osmotic stress and aging enhance the misfolding of numerous cellular proteins (Burkewitz et al. 2011, David et al. 2010). By studying the osmotic stress and aging-induced polyQ protein aggregates, it reveals that distinct protein aggregates were formed in response to different physiological conditions. It indicated that protein can adopt distinct aggregation states depending on the initiating stressor.

Yeast metacaspase ScMCA1 is recruited to chaperone-enriched aggregates during aging. Elevating ScMCA1 expression counteracted accumulation of proteins aggregates and extended yeast life-span (Hill, Hao et al. 2014). This life-span extension was partly dependent on the caspase activity of ScMCA1 but required the presence of the protein disaggregase ScHSP104. We defined the formation and co-localization of AtMC1and ScHSP104 foci in the yeast aging cells. Previous data from our lab showed that plants lacking a functional copy of *AtMC1* displayed an early senescence phenotype, and accumulated high level of insoluble aggregates in aging plants (Coll, Smidler et al. 2014). This early senescence phenotype was only partially complemented by re-introducing wild-type AtMC1. In the future it will be interesting to determine what is the exact role of AtMC1 in plant senescence related to protein quality control by clearance of insoluble aggregates in aging.

Beyond physiological aging, heat stress and pathogen attack are thought to strongly influence protein-folding processes in the plant. By taking advantage of both AtHSP101 and AtSCE1[TS] as reporter of protein aggregation in plant, we gained insights into these processes in several ways. First, different reporters do not associate with the same type of aggregates

during heat stress. AtHSP101-containing aggregates exhibit dynamic localization patterns and are highly mobile in the cytoplasm. In contrast, AtSCE1$^{TS}$-containing aggregates are immobile and smaller in comparison. Second, pathogen attack-induced protein aggregates are only associated with the reporter AtHSP101, but not with AtSCE1$^{TS}$.   Together, these data suggest that AtHSP101 and AtSCE1$^{TS}$ associate with different type of aggregates. Heat stress-induced aggregates may be intrinsically different from pathogen attack induced aggregates, in contents, size and dynamics.

NLR proteins are normally expressed at low levels and inactive states in the absence of pathogen triggers. During pathogen infection, plant NLR proteins recognize pathogen effector proteins to activate defense responses. NLR proteins may form aggregates and initiate HR cell death to prevent the spread of infection. The Arabidopsis NLR protein HR4$^{Fei-0}$, a homolog of RPW8, can autonomously form self-oligomers resembling amyloid-like aggregates, which in turn can directly kill cells in an RPP7b$^{Lerik1-3}$-independent manner (Li et al. 2019). These NLR proteins form a plant resistosome complex, shedding light on the mechanisms by which RPW8/HR proteins trigger cell death. Other plant NLRs have been shown to form cell death-inducing resistosomes (Wang, Hu et al. 2019). Whether AtMC1 participates in the regulation of NLR protein levels and resistosome formation remains to be elucidated.

# CONCLUSIONS

From the main goals of this thesis, we extract the following conclusions:

**Characterization of the AtMC1 protein quality control function in yeast cells.**

1. AtMC1 localizes in ScHSP104 and ScUB9$^{TS}$-containing foci during heat stress and aging in yeast.

2. AtMC1 participates in the degradation of misfolded proteins in yeast.

**Characterization of the AtMC1 protein quality control function in plants.**

3. AtHSP101 and AtSCE1$^{TS}$ are orthologues of yeast protein aggregate marker ScHSP104 and ScUB9$^{TS}$ in plant.

4. Plants form AtHSP101-containing protein aggregates foci during heat stress and pathogen attack. Plants lacking *atmc1* or *atg18a* are defective in protein aggregates clearance during stress responses.

5. Plants form AtSCE1$^{TS}$-containing protein aggregates foci during heat stress, but not in response to pathogen attack. AtSCE1$^{TS}$ -containing protein aggregates does not seem to be affected by the lack of *atmc1* or autophagy deficiency.

6. AtMC1 and AtHSP101 co-localize and co-immunoprecipitate in plants.

# MATERIALS AND METHODS

## 2.1 Yeast strains, media and growth conditions

### 2.1.1 Yeast strains, media and growth conditions are as follows:

The wild type BY4741 (Open Biosystems, ThermoFisher Scientific, USA) and *Scmca1Δ* (Lee, Puente et al. 2008) strains of *Saccharomyces cerevisiae* were grown in acidified YPD (Yeast extract Peptone Dextrose) medium (1% yeast extract, 2% peptone and 2% glucose, pH 3.5). Five ml starter cultures of YPD were inoculated with a single colony and grown overnight. Larger YPD cultures were then inoculated from the starter cultures and grown to mid-logarithmic phase ($OD_{600}$ 0.5-0.6) at 30ºC with orbital rotation. Cells were then collected via centrifugation at $1000 \times g$ for 2 minutes, washed with water and re-collected and then stored at -80ºC for future processing. For heat shock treatment, mid-logarithmic cultures were further incubated at 38ºC for 30 minutes before collection.

In addition to the strains listed above, we also utilized some strains provide by Thomas Nyström (Hill, Hao et al. 2014) (Table 3). Yeast strains were prepared from frozen glycerol stocks on solid medium in either YPD (1% yeast extract, 2% bactopeptone, 2% glucose supplemented with 2% agar) or on synthetic selective media lacking uracil (0.67% yeast nitrogen base without amino acids, 0.192% yeast synthetic dropout media supplement lacking uracil, 2% glucose supplemented with 2% agar) with incubation at 30°C.

### 2.1.2 Generation of new yeast strains

To complement the yeast metacaspase gene *ScMCA1* with Arabidopsis *AtMC1* (At1g02170), we constructed a gene replacement cassette by PCR-directed homologous recombination according to (Gardner et al. 2014). The cassette consisted of three fragments: 1) yeast 5'flanked with N-acetyltransferase (*NAT*) resistance gene and a GPD (glyceraldehyde-3-phosphate dehydrogenase) constitutive promoter, 2) Arabidopsis *AtMC1* gene fused to a C-terminal HA tag, 3) 3' flanking of the yeast *ScMCA1* gene. These three fragments were PCR-amplified from various plasmids using the Platinum Pfx DNA polymerase (ThermoFisher

Scientific) and fused into the final recombinant DNA by using the double-joint PCR method as previously described Yu et al. (2004). This recombinant DNA product (*NATNT2:pGPD::AtMC1-HA*) was transformed into the *Scmca1Δ* mutant strain *KanMX4*, by homologous recombination to generate the AtMC1-complemented *Scmca1Δ* yeast strain (Figure 3).



**Figure 3. Schematic representation of the construction of a gene replacement cassette.** A successful reaction will fuse DNA fragments of a 5' flanking sequence, a 3' flanking sequence and AtMC1. Primers 2 and 3 should carry 25–30 bases of homologous sequence overlapping with the ends of the AtMC1-HA. The arrows numbered from 1 to 10 represent primers for the PCRs and primers 2 and 3 are 45–60 bases long chimeric primers. If a polymerase that incorporates an A to the 3' end of the PCR product is used, it is strongly suggested that nested primers (7 and 8) are designed after a T in the genomic sequence. (A) First round PCR: amplification of the components using the specific and chimeric primers. (B) Second round PCR: the assembly reaction is carried out without using any specific primers, as the overhanging chimeric extensions act as primers. The first two cycles are shown in detail. (C) Third round PCR: amplification of the final product using nested

primers. (D) Confirmation of gene replacement: The AtMC1 replacing cassette was transformed into Sc*mca1Δ* strain (carrying the *Scmca1Δ::KanMX4+* allele) selecting for G418 resistance. Transformants were selected by NAT resistance (conferring resistance to the streptothricin antibiotic nourseothricin) and loss of the original G418 resistance.

**Table 2. Primers used in double joint PCR**

| Name | | Sequence | |
|------|-----|----------|-----|
| 1 | 5' | TTCTCCCAACAAATAGTACTCCAAC | 3' |
| 2 | 5' | GATGCTTGAGGGAGGTGGCGGGTACATCGATGAATTCTCTGTCGTCCG | 3' |
| 3 | 5' | CCCTTACGATGTTCCTGATTACGCTTAGAAATATATGAATGTGTACGTTG | 3' |
| 4 | 5' | GAAAGAACAGGAAGAGTCTGAAAAAGAT | 3' |
| 5 | 5' | ATGTACCCGCCACCTCCCT | 3' |
| 6 | 5' | CTAAGCGTAATCAGGAACATCG | 3' |
| 7 | 5' | TGTGGCTTAACAGTTCTCCTT | 3' |
| 8 | 5' | ATTTTTCTTTGGTTGAGGTGATG | 3' |

The plasmid pFE35 encoding the cytoplasmic fusion protein ΔssCL*MYC, C-terminally fused to Leu2 and a 13 myc tag and a pMT737 empty vector encoding URA were transformed into wild-type, *Scmca1Δ* and AtMC1-complemented *Scmca1Δ* strains.

**Table 3. Yeast strains and plasmid used in this study, showing the genotype and genetic background of the constructed strains with related references.**

| Experiment | Strain Name | Genotype | Backgound |
|---|---|---|---|
| AtMC1 localization | *Scmca1Δ* | *MATa Scmca1Δ::kanMX4 his3Δ1 leu2Δ0 met15Δ0 ura3Δ0* | BY4741 |
| | *Scmca1Δ ScHSP104-GFP* | *Scmca1Δ::KanMX4 + ScHSP104-GFP- HIS3* | BY4741 |
| Growth tests | *WT* | *MATa his3Δ1 leu2Δ0 met15Δ0 ura3Δ0* | BY4741 |
| | *Scmca1Δ* | *MATa Scmca1Δ::kanMX4 his3Δ1 leu2Δ0 met15Δ0 ura3Δ0* | BY4741 |
| | *Scmca1Δ AtMC1* | *MATa his3Δ1 leu2Δ0 met15Δ0 ura3Δ0 pGDP-natNT2-AtMC1-HA* | BY4741 |

| Plasmids | Description | Reference |
|---|---|---|
| pSIK1-RFP | CEN pRS416 SIK1-RFP URA3 AmpR | (Sung et al. 2007) |
| pUBC9-ts-CHFP | 2μ pESC: pGAL1-UBC9-ts-CHFP (mCherry) URA3 AmpR | Kaganovich, Kopito et al. (2008) |
| pAtMC1-mCherry | CEN pRS416 pAtMC1-mCherry URA3 AmpR | |
| pAtMC1-GFP | CEN pRS415 pAtMC1-GFP LEU2 AmpR | |
| pMT737 | CEN pRS416 URA3 AmpR | Tabuchi et al. (2009) |
| pFE35 | CEN ΔssCPY* - LEU2 - Myc Hph (Hygromicin) | Frederik Eisele, Sweden |

## 2.1.3 Yeast spot dilution assays

Yeast strains were grown to saturation. The $OD_{600}$ of a 1:20 dilution was measured and diluted to $OD_{600} =1$. Cells were centrifuged and washed 2 times with sterile water. Cells were resuspended and diluted in sterile water so that the final $OD_{600}=1$. Using a microtiter plate 10-fold serial dilutions (20 µl culture +180 µl water) were made, ranging from undiluted to a $10^5$ dilution. Five µl from each well were spotted onto the corresponding selective media. Plates were incubated at 37 ºC for 3 days before images were taken.

## 2.2 Plant materials

All Arabidopsis lines used in this study are in Columbia-0 (*Col-0*) background. The T-DNA insertion line of *atg18a* (Gabi_651D08) was described in (Xiong et al. 2005). The T-DNA insertion line of *atmc1* (At1g02170, GABI_096A10) was obtained from GABI-Kat Resource at Bielefeld University Coll *et al*. (2010). The *atmc1 atg18a* double mutant Arabidopsis plants were generated from single mutant Arabidopsis parental plants and described in (Coll, Smidler et al. 2014).

*Agrobacterium tumefaciens*-mediated transient assays were performed in *N. benthamiana* plant leaves.

### 2.2.1 Growth conditions

Arabidopsis plants were grown under short-day conditions (SD, 8 h light, 22 °C; 16 h dark, 20 °C) for most experiments. Arabidopsis seeds were surface-sterilized and plated on solid medium or planted directly on soil. For seed sterilization, all steps were performed in a fume hood. Arabidopsis seeds were put in 2 ml microcentrifuge tubes. The tubes were placed in a rack with the cap open and put into a plastic box with lid. Then a beaker with 40 ml of 25% hydrochloric acid (HCl) was put in the box. Subsequently, 1.25 ml of 5% bleach was put into the beaker and the lid of the box was closed immediately. After 4 h of incubation in the fume hood, the box was opened for 1 h. Then the lids of the tubes were closed and plated on 1/2 MS solid medium in the laminar flow bench. Seeds were stratified at 4 °C in darkness for 2 days. The seeds were transferred to the growth chamber under SD conditions. *N. benthamiana* plants were grown under long-day (LD) conditions (16 h light, 25 °C; 8 h dark, 22°C). Plants were grown for 6 weeks and fully developed leaves were used for *Agrobacterium tumefaciens*-mediated transient protein expression as described below.

## 2.2.2 Heat Stress Treatment

Arabidopsis plants were grown on soil for 2 weeks under SD conditions, or grown on solid medium for 6 days. For heat stress treatment, plants were transferred to an incubator set to 38ºC for 1 h. After heat treatment, plants were put back into the SD growth chamber for recovery. During recovery, Arabidopsis leaves were collected for microscopic imaging at 7 different time-points: 2 h, 4 h, 8 h, 24 h, 48 h, 72 h and 120 h.

*N. benthamiana* plants were grown 6 weeks under LD conditions before treatment. For heat stress treatment, *N. benthamiana* plants were transferred to an incubator set to 42 ºC for 1 h. After heat treatment, plants were put back into the LD growth chamber for recovery 2 h.

## 2.2.3 Infection of Arabidopsis with *P. syringae*

*P. syringae pv. tomato* DC3000 carrying *avrRpm1* glycerol stocks kept at -80 °C were used for preparing freshly grown single colonies on King´s B agar plates with 50 µg/ml kanamycin and 50 µg/ml rifampicin. Streaked *P. syringae* were incubated overnight at 28 °C.

Ten ml of a 10 mM $MgCl_2$ solution were added to the plate and bacteria were scrapped 10 min later. The plates were placed on the bench for 10 min. The bacteria were sucked up and transferred into an erlenmeyer flask with 100 ml 10 mM $MgCl_2$. The flask was stirred at low speed for 5 min. The $OD_{600}$ of the bacteria was measured and diluted to an $OD_{600}$ of 0.005 with 10mM $MgCl_2$. Silwet-L77 (0.02%) was added to the suspension and stirred at low speed for 5min.

For infection of Arabidopsis, 2-week-old plants grown under SD conditions were dipped in the *P. syringae* suspension for approximately 2 min, and the plants were put in a tray covered with a plastic lid. Control plants were dipped with 10 mM $MgCl_2$. The plants were placed back into the chamber for incubation. Arabidopsis leaves were collected for microscopic imaging after 6 h infection.

## 2.2.4 Induction of Senescence

Leaf senescence was induced according to the experimental design by (Keech et al. 2010). Briefly, Arabidopsis plants were grown under long-day conditions (LD, 16 h light, 22 °C; 8 h dark, 20 °C) for 5 weeks. Rosette leaves 7 to 8 were covered with aluminum foil for 4 days, while the rest of the plant remained under the light. These leaves are referred to as IDLs (individually darkened leaves). The IDLs and normal leaves were collected for quantitative real-time PCR and chlorophyll content analysis.

## 2.2.5 Generation of transgenic plants carrying GFP fusion to AtHSP101

A genomic fragment of the Arabidopsis *AtHSP101* gene (*At1g74310*) was cloned into the entry vector pDONR207 vector to make the plasmid *pDONR207-P$_{AtHSP101}$::AtHSP101*. This fragment contained 407 bp of the *AtHSP101* promoter (407bp) and the *AtHSP101* gene without stop codon. The *P$_{AtHSP101}$::AtHSP101* was recombined into the pDONR207 vector through BP reaction with Gateway BP Clonase ateway® BP Clonase II Enzyme Mix (Invitrogen, Darmstadt, Germany) according to the kit manual. Similarly, through an LR reaction, the target DNA fragments were cloned into pB7FWG vectors by utilizing the Gateway® LR Clonase II Enzyme Mix (Invitrogen, Darmstadt, Germany) as indicated in the manual. The vectors pB7FWG provide a C-terminal GFP fusion to AtHSP101 protein (Fujimoto et al. 2009). This plasmid was transformed into the *Agrobacterium tumefaciens* strain GV3101, and then used to generate stable Arabidopsis transformants using Col-0, *atmc1*, *atg18a* and *atmc1 atg18a* backgrounds by the floral dip method (Clough et al. 1998). Four independent homozygous transgenic lines were obtained in each background.

**Table 4. Transgenic lines generated in this work**

| Name | plasmid construct | antibiotics | background |
|------|-------------------|-------------|------------|
| Col-0 | pB7FWG - $P_{AtHSP101}$::*AtHSP101-GFP* | Basta | Col-0 |
| *atmc1* | pB7FWG - $P_{AtHSP101}$::*AtHSP101-GFP* | Basta | *atmc1* |
| *atg18* | pB7FWG - $P_{AtHSP101}$::*AtHSP101-GFP* | Basta | *atg18a* |
| *atmc1 atg18* | pB7FWG - $P_{AtHSP101}$::*AtHSP101-GFP* | Basta | *atmc1 atg18a* |
| Col-0 | pEarleyGate102-35S::*AtSCE1$^{TS}$-CFP* | Basta | Col-0 |
| *atmc1* | pEarleyGate102-35S::*AtSCE1$^{TS}$-CFP* | Basta | *atmc1* |
| *atg18* | pEarleyGate102-35S::*AtSCE1$^{TS}$-CFP* | Basta | *atg18a* |
| *atmc1 atg18* | pEarleyGate102-35S::*AtSCE1$^{TS}$-CFP* | Basta | *atmc1 atg18a* |

## 2.2.6 Generation of transgenic plants carrying CFP fusion to AtSCE1$^{TS}$

The plasmid pEarleyGate102-*35S::AtSCE1*-CFP was kindly provided by Aiming Wang (Xiong et al. 2013). We designed oligonucleotide primers to introduce a Y69L mutation into the *AtSCE1* gene by using Phusion Site-Directed Mutagenesis Kit. This mutated plasmid pEarleyGate102-*35S::AtSCE1$^{TS}$*-CFP was transformed into *Agrobacterium*, strain GV3101, and then used to transform the Col-0, *atmc1*, *atg18* and *atmc1 atg18a* Arabidopsis plants by the method described above.

## 2.2.7 Arabidopsis protoplast transformation

For preparation of Arabidopsis protoplasts, leaves were collected from 2-week-old-plants. Leaves of approximately 20 Arabidopsis plants were cut using a sharp razor blade to small strips of approximately 1 mm width and immediately transferred to a 9 mm petri dish containing 10 ml of enzyme solution [1.5% cellulase 'Onozuka' R10 (Yakult, Tokyo, Japan), 0.3% macerozyme 'Onozuka' R10 (Yakult), 0.4 M mannitol, 10 mM $CaCl_2$, 20 mM KCl and 20 mM MES, pH 5.6]. Leaves were gently shaken under the light for up to 90 min until the protoplasts were released into the enzyme solution. The mixture was filtered to a 50 ml

falcon tube by a 70 µm falcon cell strainer (Thermo-Fisher Scientific, Waltham, MA,). The residue in the petri dish was washed with 10 ml W5 solution (154 mM NaCl, 125 mM $CaCl_2$, 5 mM KCl, 5 mM glucose, and 2 mM MES, pH 5.6) and filtered using the same piece of falcon cell strainer. The protoplasts were centrifuged at $100 \times g$ for 3 min, washed twice with 25 ml of pre-chilled modified W5 solution and incubated on ice for 30 min. During the incubation period, protoplasts were counted using a Neubauer chamber under a light microscope.

The W5 solution covering the protoplasts was discarded carefully and the protoplast pellet was re-suspended in MMg solution (0.4 M mannitol, 15 mM $MgCl_2$, and 4 mM MES, pH 5.6) to a final concentration of $2 \times 10^5$ cells/ml. For each transformation, 20 µg of plasmid DNA at a concentration of 2-4 µg/µl was mixed with 1.5 ml protoplast suspension. 1.5 ml of a freshly-prepared polyethylene glycol (PEG) solution [40% (w/v) PEG 4000, 0.1 M $CaCl_2$ and 0.2 M mannitol] was added and mixed gently, and the mixture was incubated at room temperature for 5 min. After incubation, 6 ml of W5 solution were added slowly, the solution was mixed, and protoplasts were pelleted by centrifugation at $200 \times g$ for 2 min. The supernatant was removed as completely as possible without disturbing the protoplast pellet. Washing with W5 solution was repeated once more. The protoplasts were re-suspended gently in 1 ml of W5 solution and were incubated at room temperature for 16 h in constant low light conditions.

### 2.2.8 Transient protein expression in *N. benthamiana*

*Agrobacterium* strains carrying *Dex::AtMC1-HA*, *Dex::AtMC$_{CACA}$-HA* or *Dex::AtMC1-ΔN-HA* (Coll, Vercammen et al. 2010), *P$_{AtHSP101}$::AtHSP101-GFP* and the strain carrying anti-silencing vector *35S::p19* (Voinnet, Rivas et al. 2003) were grown to $OD_{600}$ 0.5-0.8, and collected by centrifugation at $4000 \times g$ for 10 min. The pellets were then resuspended in infiltration buffer (10 mM $MgCl_2$, 10 mM MES and 150 µM acetosyringone). The *Agrobacterium* strains were mixed together with final $OD_{600}$ at *Dex::AtMC1-HA*

(*Dex::AtMC$_{CACA}$-HA* or *Dex::AtMC1-ΔN-HA*) 0.2, *P$_{AtHSP101}$::AtHSP101-GFP* 0.4 and 35S::p19 0.1. The suspension was then infiltrated into the abaxial leaf epidermis of *N. benthamiana* with a 1 ml needleless syringe. Plants were maintained in the greenhouse under normal conditions after infiltration. Three well-expanded leaves were infiltrated for each construct. Samples were collected for either microscopic imaging or protein extraction 2 days after infiltration. For *Dex* promoter gene expression had to be induced, leaves were treated with 0.2 µM dexamethasone 24 hours before sample collection. To induce *P$_{AtHSP101}$::AtHSP101-GFP AtHSP101* gene expression, the *N. benthamiana* plants were treated with heat stress at 38 °C for 1 h after dexamethasone treatment.

## 2.2.9 RNA isolation and quantitative real-time PCR (qPCR) analysis

Six-week-old Arabidopsis rosette leaves 7 to 8 were covered with aluminum foil for 4 days were collected and frozen in liquid nitrogen. The same stage of Arabidopsis rosette leaves grow under the light were harvest as a control. Subsequently, approximately 50-100 mg Arabidopsis leaves were ground to a fine powder with a mortar and pestle. Total mRNA was extracted with the RNeasy Mini Kit (Qiagen) according to the kit manual. For the cDNA synthesis, an aliquot of 1 µg RNA was used and the genomic DNA from the RNA preparations was removed with DNase I treatment (Thermo Fisher Scientific) according to the manual. The reverse strand cDNA was then synthesized by using the DNase I treated RNA aliquot as template with the High-Capacity cDNA Reverse Transcription Kit (Thermo Fisher Scientific) according to the kit manual.

Rosette leaves 7 to 8 were covered with aluminum foil for 4 days, while the rest of the plant remained under the light. These leaves are referred to as IDLs (individually darkened leaves). The IDLs and normal leaves were collected for quantitative real-time PCR and chlorophyll content analysis.

For quantification of cDNA qRT-PCR using the Life Technologies SYBR Green PCR Master Mix in a total volume of 15 µl: 7.5 µl of SYBR Green PCR Master Mix, 2.5 µl of diluted cDNA, 1 µl of primer mix (forward and reverse primers: 10 pmol/µl each) and 4 µlof $H_2O$. The reaction was run at 95 °C for 5 min, followed by 40 cycles at 95 °C for 15 s, 55 °C for 30 s and 72°C for 30 s. All qPCR reaction was prepared in triplicates and performed with ABI PRISM 7000 Sequence Detection System (Applied Biosystems). Relative expression of *AtSAG12* (*At5G45890*) was calculated using the ΔΔCT method. *AtSAG12* expression was first normalized to expression of the housekeeping tubulin gene *TUB2* (*At5g62690*).

## 2.3 Protein analysis

### 2.3.1 Extraction of yeast protein

After yeast cells were grown to exponential phase in selective medium, 1 ml of a yeast culture of $OD_{600}$ of 1 was centrifuged for 30 seconds (sec) at $112000 \times g$. Cells were resuspended in 1 ml of 0.2 M NaOH, and incubated for 20 min on ice, followed by centrifugation for 30 sec at $11200 \times g$. The pelleted cells were resuspended in 50 µl of HU buffer (8 M urea, 5%SDS, 1mM EDTA, 100 mM DTT, 0.005% bromophenol blue, 0.2 M Tris-HCl, pH 6.8) containing protease inhibitor mixture (Sigma-Aldrich), and heated for 10 minutes at 70 °C. After centrifugation for 5 (min) at $112000 \times g$, 10 µl of supernatant were subjected to 12% SDS-PAGE and blotted against anti-myc antibodies (Sigma-Aldrich).

### 2.3.2 Extraction of plant total protein

Frozen leaf samples were ground in a mortar with a pestle in liquid nitrogen, Total protein extracts were prepared by grinding plant tissues in mortar with a pestle in liquid nitrogen. Approximately 100 mg of grinded tissue were transferred in a 1.5 ml microtube, and incubated with 200 µl of homogenization buffer (20 mM Tris-HCl, pH 8.0, 0.1% SDS, 150 mM NaCl, 1 mM EDTA, and 1 % Triton X-100, 5 mM dithiothreitol, protease inhibitor cocktail). After vortexing for 1 min, each sample was centrifuged at $10000 \times g$ for 15 min

at 4°C. The supernatant was transferred to a new tube, 2 µl of supernatant was used for a Bradford Protein concentration measure. The protein suspension was added protein loading dye and boiled 3 min in the heat block at 95 °C before loading the SDS-PAGE gel.

## 2.3.2 Co-immunoprecipitation assays and protein analysis

One g of frozen *N. benthamiana* leaves were ground in a mortar with a pestle in liquid nitrogen. Two ml of lysis buffer (200 mM K-HEPES pH 7.4, 1.1 M $C_2H_3KO$, 20 mM $MgCl_2$, 1% Tween-20, 10 µM $CaCl_2$, 2% PVP40, 5 mM dithiothreitol, protease inhibitor cocktail) was added and vortexed thoroughly. Each sample was centrifuged at 2000 × $g$ for 15 min at 4°C. The supernatant was filtered through miracloth (Millipore) and collected in 15 ml tubes. Then, the supernatant was centrifuged again at 7000 × $g$ for 15 min at 4°C. The supernatant was transferred to a new tube and the protein concentration was measured. For co-immunoprecipitation, 2 ml of pre-adjusted total protein extracts at 3 mg/ml were collected and incubated with 50 µl of anti-green fluorescent protein (GFP) magnetic beads (MACS; Miltenyi Biotec, Bergisch, Gladbach, Germany), for 2 h at 4 °C under constant rotation. Bound proteins were eluted according to the manufacturer's instructions.

Twenty-five µg of total protein (input) and 20 µl of eluate were loaded onto an SDS-PAGE gel and electroblotted onto a PVDF membrane (Bio-Rad). Accumulation of GFP-tagged protein was detected by immunoblotting with 1: 5000 anti-GFP mouse monoclonal antibody (clone B-2; Santa Cruz Biotechnology, Dallas, TX, USA) and subsequently 1:2000 diluted anti-Mouse Ig-HRP (Amersham). Detection of HA-tagged protein was performed by incubating the blots in 1: 5000 monoclonal anti-HA-HRP (clone 3F10; Roche). Supersignal West Femto Chemiluminescent Substrate (Thermo Scientific) was used for signal development. Equal loading was demonstrated by staining the membrane with coomassie brilliant blue.

### 2.3.4 Confocal laser scanning microscopy

Confocal laser scanning microscopy was performed on a Leica SP2 AOBS inverted confocal microscope (Leica Microsystems, Wetzlar, Germany) equipped with a $\times$ 40, numerical aperture-1.2 water objective. GFP fusion was excited with a 488 nm Argon laser and detected using a 505-530 bandpass emission filter. RFP fusion was excited using a 561 nm He-Ne laser and detected using a custom 595-620 nm bandpass emission filter. CFP fusion was excited using a 364 nm Ar-UV laser and detected using a custom 434-474 nm bandpass emission filter. DAPI was excited using a 345 nm He-Cd laser and detected using a 358-461 nm bandpass emission filter. Microscopy images were processed using the LSM510 image browser (http://www.zeiss.com/lsm) and ImageJ converted to TIFF (for images) or AVI (for movies) formats.

### 2.3.5 Chemical treatments

Six-day-old seedlings grown on 1/2 MS solid medium under SD photoperiod and exposed to the heat stress regimes described above, were transferred to 1/2 MS liquid medium containing either 1 µM Concanamycin A, 50 µM of the proteasome inhibitor MG132 or an equivalent volume of DMSO and incubated in the dark for 16 h. Subsequently, images were obtained with a Leica SP2 AOBS inverted confocal microscope as described above.

The plant nuclei were stained with 4', 6-diamidino-2-phenylindole (DAPI), which stains the nucleus blue. Arabidopsis leaves were stained with freshly-prepared 1µg/ml DAPI solution for 10 min in the dark. The leaves were washed with phosphate-buffered saline (137 mM NaCl, 2.7 mM KCl, 10 mM $Na_2HPO_4$, 1.8 mM $KH_2PO_4$) two times. Subsequently, the leaves were observed with fluorescence microscope (Leica SP2 AOBS) as described above.

**2.3.6 Measurement of the chlorophyll content**

Arabidopsis fully expanded leaves were collected leaf discs were punched out using a metallic cork borer (n. 3 $\varnothing$). Each sample consisted of 3 combined leaf discs (0.033g total fresh weight leaf material). Chlorophyll was extracted and homogenized in 1 ml of 80% acetone then maintained on ice. Following homogenization, samples were centrifuged at $10000 \times g$ for 2 min at 4 °C and 1 ml of supernatant was transferred to a 1 ml plastic cuvette. AB470 nm, AB662 nm and AB647 nm were measured using a UV spectrophotometer. The concentration of chlorophylls a and b, as well as the major carotenoids, comprising xanthophyll and carotene, was calculated as described by Lichtenthaler (1987).

**REFERENCES**

Abramov, A. Y., E. V. Potapova, V. V. Dremin and A. V. Dunaev (2020). "Interaction of oxidative stress and misfolded proteins in the mechanism of neurodegeneration." Life **10**(7): 101.

Alberti, S. (2012). "Molecular mechanisms of spatial protein quality control." Prion **6**(5): 437-442.

Ambit, A., N. Fasel, G. H. Coombs and J. C. Mottram (2008). "An essential role for the Leishmania major metacaspase in cell cycle progression." Cell Death & Differentiation **15**(1): 113-122.

Ameisen, J. C. (2002). "On the origin, evolution, and nature of programmed cell death: a timeline of four billion years." Cell Death & Differentiation **9**(4): 367-393.

An, H., A. Ordureau, J. A. Paulo, C. J. Shoemaker, V. Denic and J. W. Harper (2019). "TEX264 is an ER-resident ATG8-interacting protein critical for endoplasmic reticulum remodeling during nutrient stress." Molecular cell **74**(5): 891.

Arrasate, M., S. Mitra, E. S. Schweitzer, M. R. Segal and S. Finkbeiner (2004). "Inclusion body formation reduces levels of mutant huntingtin and the risk of neuronal death." nature **431**(7010): 805-810.

Axe, E. L., S. A. Walker, M. Manifava, P. Chandra, H. L. Roderick, A. Habermann, G. Griffiths and N. T. Ktistakis (2008). "Autophagosome formation from membrane compartments enriched in phosphatidylinositol 3-phosphate and dynamically connected to the endoplasmic reticulum." The Journal of cell biology **182**(4): 685-701.

Bagola, K. and T. Sommer (2008). "Protein quality control: on IPODs and other JUNQ." Current Biology **18**(21): R1019-R1021.

Balint-Kurti, P. (2019). "The plant hypersensitive response: concepts, control and consequences." Molecular plant pathology **20**(8): 1163-1178.

Becker, L. A., B. Huang, G. Bieri, R. Ma, D. A. Knowles, P. Jafar-Nejad, J. Messing, H. J. Kim, A. Soriano and G. Auburger (2017). "Therapeutic reduction of ataxin-2 extends lifespan and reduces pathology in TDP-43 mice." Nature **544**(7650): 367-371.

Betting, J. and W. Seufert (1996). "A yeast Ubc9 mutant protein with temperature-sensitive in vivo function is subject to conditional proteolysis by a ubiquitin-and proteasome-dependent pathway." Journal of Biological Chemistry **271**(42): 25790-25796.

Bhandawat, A., K. Jayaswall, H. Sharma and J. Roy (2020). "Sound as a stimulus in associative learning for heat stress in Arabidopsis." Communicative & Integrative Biology **13**(1): 1-5.

Bösl, B., V. Grimminger and S. Walter (2006). "The molecular chaperone Hsp104—a molecular machine for protein disaggregation." Journal of structural biology **156**: 139-148.

Brockwell, D. J. and S. E. Radford (2007). "Intermediates: ubiquitous species on folding energy landscapes?" Current opinion in structural biology **17**(1): 30-37.

Bukau, B. and A. L. Horwich (1998). "The Hsp70 and Hsp60 chaperone machines." Cell **92**(3): 351-366.

Burkewitz, K., K. Choe and K. Strange (2011). "Hypertonic stress induces rapid and widespread protein damage in C. elegans." American Journal of Physiology-Cell Physiology **301**(3): C566-C576.

Cai, Y. M., J. Yu, Y. Ge, A. Mironov and P. Gallois (2018). "Two proteases with caspase-3-like activity, cathepsin B and proteasome, antagonistically control ER-stress-induced programmed cell death in Arabidopsis." New Phytologist **218**(3): 1143-1155.

Cashikar, A. G., M. Duennwald and S. L. Lindquist (2005). "A chaperone pathway in protein disaggregation Hsp26 alters the nature of protein aggregates to facilitate reactivation by Hsp104." Journal of Biological Chemistry **280**(25): 23869-23875.

Cashikar, A. G., E. C. Schirmer, D. A. Hattendorf, J. R. Glover, M. S. Ramakrishnan, D. M. Ware and S. L. Lindquist (2002). "Defining a pathway of communication from the C-terminal peptide binding domain to the N-terminal ATPase domain in a AAA protein." Molecular cell **9**(4): 751-760.

Castanys-Muñoz, E., E. Brown, G. H. Coombs and J. C. Mottram (2012). "Leishmania mexicana metacaspase is a negative regulator of amastigote proliferation in mammalian cells." Cell death & disease **3**(9): e385-e385.

Chamachi, N. G. and S. Chakrabarty (2017). "Temperature-induced misfolding in prion protein: evidence of multiple partially disordered states stabilized by non-native hydrogen bonds." Biochemistry **56**(6): 833-844.

Chantarachot, T. and J. Bailey-Serres (2018). "Polysomes, stress granules, and processing bodies: a dynamic triumvirate controlling cytoplasmic mRNA fate and function." Plant physiology **176**(1): 254-269.

Chapin, L. J., Y. Moon and M. L. Jones (2017). "Downregulating a type I metacaspase in petunia accelerates flower senescence." Journal of the American Society for Horticultural Science **142**(5): 405-414.

Chen, L. and K. Madura (2014). "Degradation of specific nuclear proteins occurs in the cytoplasm in Saccharomyces cerevisiae." Genetics **197**(1): 193-197.

Chen, S. and M. B. Dickman (2004). "Bcl-2 family members localize to tobacco chloroplasts and inhibit programmed cell death induced by chloroplast-targeted herbicides." Journal of Experimental Botany **55**(408): 2617-2623.

Chung, T., A. Suttangkakul and R. D. Vierstra (2009). "The ATG autophagic conjugation system in maize: ATG transcripts and abundance of the ATG8-lipid adduct are regulated by development and nutrient availability." Plant physiology **149**(1): 220-234.

Clerico, E. M., J. M. Tilitsky, W. Meng and L. M. Gierasch (2015). "How hsp70 molecular machines interact with their substrates to mediate diverse physiological functions." Journal of molecular biology **427**(7): 1575-1588.

Clough, S. J. and A. F. Bent (1998). "Floral dip: a simplified method for Agrobacterium-mediated transformation of Arabidopsis thaliana." The plant journal **16**(6): 735-743.

Cohen, E., J. Bieschke, R. M. Perciavalle, J. W. Kelly and A. Dillin (2006). "Opposing activities protect against age-onset proteotoxicity." Science **313**(5793): 1604-1610.

Coll, N. S., A. Smidler, M. Puigvert, C. Popa, M. Valls and J. L. Dangl (2014). "The plant metacaspase AtMC1 in pathogen-triggered programmed cell death and aging: functional linkage with autophagy." Cell Death & Differentiation **21**(9): 1399-1408.

Coll, N. S., D. Vercammen, A. Smidler, C. Clover, F. Van Breusegem, J. L. Dangl and P. Epple (2010). "Arabidopsis type I metacaspases control cell death." Science **330**(6009): 1393-1397.

Cui, F., L. Liu, Q. Zhao, Z. Zhang, Q. Li, B. Lin, Y. Wu, S. Tang and Q. Xie (2012). "Arabidopsis ubiquitin conjugase UBC32 is an ERAD component that functions in brassinosteroid-mediated salt stress tolerance." The Plant Cell **24**(1): 233-244.

Dahiya, R., T. Mohammad, M. F. Alajmi, M. Rehman, G. M. Hasan, A. Hussain and M. Hassan (2020). "Insights into the Conserved Regulatory Mechanisms of Human and Yeast Aging." Biomolecules **10**(6): 882.

David, D. C., N. Ollikainen, J. C. Trinidad, M. P. Cary, A. L. Burlingame and C. Kenyon (2010). "Widespread protein aggregation as an inherent part of aging in C. elegans." PLoS Biol **8**(8): e1000450.

Di Gregorio, S. E. and M. L. Duennwald (2018). "Yeast as a model to study protein misfolding in aged cells." FEMS yeast research **18**(6): foy054.

Dick, S. A. and L. A. Megeney (2013). "Cell death proteins: an evolutionary role in cellular adaptation before the advent of apoptosis." Bioessays **35**(11): 974-983.

Dickman, M. B. and R. Fluhr (2013). "Centrality of host cell death in plant-microbe interactions." Annual review of phytopathology **51**: 543-570.

Dickman, M. B., Y. K. Park, T. Oltersdorf, W. Li, T. Clemente and R. French (2001). "Abrogation of disease development in plants expressing animal antiapoptotic genes." Proceedings of the National Academy of Sciences **98**(12): 6957-6962.

Dinner, A. R., A. Šali, L. J. Smith, C. M. Dobson and M. Karplus (2000). "Understanding protein folding via free-energy surfaces from theory and experiment." Trends in biochemical sciences **25**(7): 331-339.

Dobson, C. M. (2003). "Protein folding and misfolding." Nature **426**(6968): 884-890.

Doelling, J. H., J. M. Walker, E. M. Friedman, A. R. Thompson and R. D. Vierstra (2002). "The APG8/12-activating enzyme APG7 is required for proper nutrient recycling and senescence in Arabidopsis thaliana." Journal of Biological Chemistry **277**(36): 33105-33114.

Dooley, H. C., M. Razi, H. E. J. Polson, S. E. Girardin, M. I. Wilson and S. A. Tooze (2014). "WIPI2 links LC3 conjugation with PI3P, autophagosome formation, and pathogen clearance by recruiting Atg12–5-16L1." Molecular cell **55**(2): 238-252.

Eisele, F. and D. H. Wolf (2008). "Degradation of misfolded protein in the cytoplasm is mediated by the ubiquitin ligase Ubr1." FEBS letters **582**(30): 4143-4146.

Ellis, R. J. and A. P. Minton (2006). "Protein aggregation in crowded environments." Biological chemistry **387**(5): 485-497.

Escamez, S. and H. Tuominen (2014). "Programmes of cell death and autolysis in tracheary elements: when a suicidal cell arranges its own corpse removal." Journal of Experimental Botany **65**(5): 1313-1321.

Escusa-Toret, S., W. I. M. Vonk and J. Frydman (2013). "Spatial sequestration of misfolded proteins by a dynamic chaperone pathway enhances cellular fitness during stress." Nature cell biology **15**(10): 1231-1243.

Fagundes, D., B. Bohn, C. Cabreira, F. Leipelt, N. Dias, M. H. Bodanese-Zanettini and A. Cagliari (2015). "Caspases in plants: metacaspase gene family in plant stress responses." Functional & integrative genomics **15**(6): 639-649.

Feder, M. E. and G. E. Hofmann (1999). "Heat-shock proteins, molecular chaperones, and the stress response: evolutionary and ecological physiology." Annual review of physiology **61**(1): 243-282.

Fendrych, M., T. Van Hautegem, M. Van Durme, Y. Olvera-Carrillo, M. Huysmans, M. Karimi, S. Lippens, C. J. Guérin, M. Krebs and K. Schumacher (2014). "Programmed cell death controlled by ANAC033/SOMBRERO determines root cap organ size in Arabidopsis." Current Biology **24**(9): 931-940.

Finley, D. (2009). "Recognition and processing of ubiquitin-protein conjugates by the proteasome." <u>Annual review of biochemistry</u> **78**: 477-513.

Fu, H., N. Reis, Y. Lee, M. H. Glickman and R. D. Vierstra (2001). "Subunit interaction maps for the regulatory particle of the 26S proteasome and the COP9 signalosome." <u>The EMBO journal</u> **20**(24): 7096-7107.

Fujimoto, M., S. i. Arimura, S. Mano, M. Kondo, C. Saito, T. Ueda, M. Nakazono, A. Nakano, M. Nishimura and N. Tsutsumi (2009). "Arabidopsis dynamin-related proteins DRP3A and DRP3B are functionally redundant in mitochondrial fission, but have distinct roles in peroxisomal fission." <u>The Plant Journal</u> **58**(3): 388-400.

Furuta, N., N. Fujita, T. Noda, T. Yoshimori and A. Amano (2010). "Combinational soluble N-ethylmaleimide-sensitive factor attachment protein receptor proteins VAMP8 and Vti1b mediate fusion of antimicrobial and canonical autophagosomes with lysosomes." <u>Molecular biology of the cell</u> **21**(6): 1001-1010.

Gallina, I., C. Colding, P. Henriksen, P. Beli, K. Nakamura, J. Offman, D. P. Mathiasen, S. Silva, E. Hoffmann and A. Groth (2015). "Cmr1/WDR76 defines a nuclear genotoxic stress body linking genome integrity and protein quality control." <u>Nature communications</u> **6**(1): 1-16.

Galluzzi, L., I. Vitale, J. M. Abrams, E. S. Alnemri, E. H. Baehrecke, M. V. Blagosklonny, T. M. Dawson, V. L. Dawson, W. S. El-Deiry and S. Fulda (2012). "Molecular definitions of cell death subroutines: recommendations of the Nomenclature Committee on Cell Death 2012." <u>Cell Death & Differentiation</u> **19**(1): 107-120.

Garapati, P., G.-P. Xue, S. Munné-Bosch and S. Balazadeh (2015). "Transcription factor ATAF1 in Arabidopsis promotes senescence by direct regulation of key chloroplast maintenance and senescence transcriptional cascades." <u>Plant Physiology</u> **168**(3): 1122-1139.

Gardner, J. M. and S. L. Jaspersen (2014). Manipulating the yeast genome: deletion, mutation, and tagging by PCR. <u>Yeast Genetics</u>, Springer**:** 45-78.

Gidalevitz, T., F. Stevens and Y. Argon (2013). "Orchestration of secretory protein folding by ER chaperones." Biochimica et Biophysica Acta (BBA)-Molecular Cell Research **1833**(11): 2410-2424.

Glover, J. R. and S. Lindquist (1998). "Hsp104, Hsp70, and Hsp40: a novel chaperone system that rescues previously aggregated proteins." Cell **94**(1): 73-82.

Goldberg, A. L. (2003). "Protein degradation and protection against misfolded or damaged proteins." Nature **426**(6968): 895-89.

Goodman, R. N. and A. J. Novacky (1994). The hypersensitive reaction in plants to pathogens: a resistance phenomenon, American Phytopathological Society (APS).

Green, D. R. (2019). "The coming decade of cell death research: five riddles." Cell **177**(5): 1094-1107.

Guha, M., F. Xia, C. M. Raskett and D. C. Altieri (2010). "Caspase 2-mediated tumor suppression involves survivin gene silencing." Oncogene **29**(9): 1280-1292.

Hamilton, K. S., B. Phong, C. Corey, J. Cheng, B. Gorentla, X. Zhong, S. Shiva and L. P. Kane (2014). "T cell receptor–dependent activation of mTOR signaling in T cells is mediated by Carma1 and MALT1, but not Bcl10." Science signaling **7**(329): ra55-ra55.

Hanaoka, H., T. Noda, Y. Shirano, T. Kato, H. Hayashi, D. Shibata, S. Tabata and Y. Ohsumi (2002). "Leaf senescence and starvation-induced chlorosis are accelerated by the disruption of an Arabidopsis autophagy gene." Plant physiology **129**(3): 1181-1193.

Hander, T., Á. D. Fernández-Fernández, R. P. Kumpf, P. Willems, H. Schatowitz, D. Rombaut, A. Staes, J. Nolf, R. Pottie and P. Yao (2019). "Damage on plants activates Ca2+-dependent metacaspases for release of immunomodulatory peptides." Science **363**(6433).

Hardesty, B. and G. Kramer (2001). "Folding of a nascent peptide on the ribosome." Progress in nucleic acid research and molecular biology **66**: 41-66.

Hartl, F. U. (1996). "Molecular chaperones in cellular protein folding." Nature **381**(6583): 571-580.

Hartl, F. U., A. Bracher and M. Hayer-Hartl (2011). "Molecular chaperones in protein folding and proteostasis." Nature **475**(7356): 324-332.

Hatsugai, N., S. Iwasaki, K. Tamura, M. Kondo, K. Fuji, K. Ogasawara, M. Nishimura and I. Hara-Nishimura (2009). "A novel membrane fusion-mediated plant immunity against bacterial pathogens." Genes & development **23**(21): 2496-2506.

Hatsugai, N., K. Yamada, S. Goto-Yamada and I. Hara-Nishimura (2015). "Vacuolar processing enzyme in plant programmed cell death." Frontiers in plant science **6**: 234.

He, R., G. E. Drury, V. I. Rotari, A. Gordon, M. Willer, T. Farzaneh, E. J. Woltering and P. Gallois (2008). "Metacaspase-8 modulates programmed cell death induced by ultraviolet light and H2O2 in Arabidopsis." Journal of Biological Chemistry **283**(2): 774-783.

Helms, M. J., A. Ambit, P. Appleton, L. Tetley, G. H. Coombs and J. C. Mottram (2006). "Bloodstream form Trypanosoma brucei depend upon multiple metacaspases associated with RAB11-positive endosomes." Journal of cell science **119**(6): 1105-1117.

Hershko, A. and A. Ciechanover (1998). "The ubiquitin system." Annual review of biochemistry **67**(1): 425-479.

Higuchi-Sanabria, R., P. A. Frankino, J. W. Paul Iii, S. U. Tronnes and A. Dillin (2018). "A futile battle? Protein quality control and the stress of aging." Developmental cell **44**(2): 139-163.

Hill, S. M., S. Hanzén and T. Nyström (2017). "Restricted access: spatial sequestration of damaged proteins during stress and aging." EMBO reports **18**(3): 377-391.

Hill, S. M., X. Hao, J. Grönvall, S. Spikings-Nordby, P. O. Widlund, T. Amen, A. Jörhov, R. Josefson, D. Kaganovich and B. Liu (2016). "Asymmetric inheritance of aggregated proteins and age reset in yeast are regulated by Vac17-dependent vacuolar functions." Cell reports **16**(3): 826-838.

Hill, S. M., X. Hao, B. Liu and T. Nyström (2014). "Life-span extension by a metacaspase in the yeast Saccharomyces cerevisiae." Science **344**(6190): 1389-1392.

Hill, S. M. and T. Nyström (2015). "The dual role of a yeast metacaspase: What doesn't kill you makes you stronger." BioEssays **37**(5): 525-531.

Hipp, M. S., P. Kasturi and F. U. Hartl (2019). "The proteostasis network and its decline in ageing." Nature reviews Molecular cell biology **20**(7): 421-435.

Hofius, D., L. Li, A. Hafrén and N. S. Coll (2017). "Autophagy as an emerging arena for plant–pathogen interactions." Current opinion in plant biology **38**: 117-123.

Hong, S. W. and E. Vierling (2001). "Hsp101 is necessary for heat tolerance but dispensable for development and germination in the absence of stress." The Plant Journal **27**(1): 25-35.

Hoskins, J. R., S. M. Doyle and S. Wickner (2009). "Coupling ATP utilization to protein remodeling by ClpB, a hexameric AAA+ protein." Proceedings of the National Academy of Sciences **106**(52): 22233-22238.

Ishida, H., K. Yoshimoto, M. Izumi, D. Reisen, Y. Yano, A. Makino, Y. Ohsumi, M. R. Hanson and T. Mae (2008). "Mobilization of rubisco and stroma-localized fluorescent proteins of chloroplasts to the vacuole by an ATG gene-dependent autophagic process." Plant physiology **148**(1): 142-155.

Ishizaki, Y., M. D. Jacobson and M. C. Raff (1998). "A role for caspases in lens fiber differentiation." The Journal of cell biology **140**(1): 153-158.

Itakura, E., C. Kishi-Itakura, I. Koyama-Honda and N. Mizushima (2012). "Structures containing Atg9A and the ULK1 complex independently target depolarized mitochondria at initial stages of Parkin-mediated mitophagy." Journal of cell science **125**(6): 1488-1499.

Jeltsch, K. M., D. Hu, S. Brenner, J. Zöller, G. A. Heinz, D. Nagel, K. U. Vogel, N. Rehage, S. C. Warth and S. L. Edelmann (2014). "Cleavage of roquin and regnase-1 by the paracaspase MALT1 releases their cooperatively repressed targets to promote TH 17 differentiation." Nature immunology **15**(11): 1079-1089.

Johansen, T. and T. Lamark (2011). "Selective autophagy mediated by autophagic adapter proteins." Autophagy **7**(3): 279-296.

Johnston, J. A., C. L. Ward and R. R. Kopito (1998). "Aggresomes: a cellular response to misfolded proteins." The Journal of cell biology **143**(7): 1883-1898.

Jones, J. D. G. and J. L. Dangl (2006). "The plant immune system." Nature **444**(7117): 323.

Kabbage, M., W. Li, S. Chen and M. B. Dickman (2010). "The E3 ubiquitin ligase activity of an insect anti-apoptotic gene (SfIAP) is required for plant stress tolerance." Physiological and Molecular Plant Pathology **74**(5-6): 351-362.

Kaganovich, D., R. Kopito and J. Frydman (2008). "Misfolded proteins partition between two distinct quality control compartments." Nature **454**(7208): 1088-1095.

Karanasios, E., S. A. Walker, H. Okkenhaug, M. Manifava, E. Hummel, H. Zimmermann, Q. Ahmed, M.-C. Domart, L. Collinson and N. T. Ktistakis (2016). "Autophagy initiation by ULK complex assembly on ER tubulovesicular regions marked by ATG9 vesicles." Nature communications **7**(1): 1-17.

Keech, O., E. Pesquet, L. Gutierrez, A. Ahad, C. Bellini, S. M. Smith and P. Gardeström (2010). "Leaf senescence is accompanied by an early disruption of the microtubule network in Arabidopsis." Plant Physiology **154**(4): 1710-1720.

Kirstein, J., H. Strahl, N. Molière, L. W. Hamoen and K. Turgay (2008). "Localization of general and regulatory proteolysis in Bacillus subtilis cells." Molecular microbiology **70**(3): 682-694.

Klaips, C. L., G. G. Jayaraj and F. U. Hartl (2018). "Pathways of cellular proteostasis in aging and disease." Journal of Cell Biology **217**(1): 51-63.

Klemm, S., J. Gutermuth, L. Hültner, T. Sparwasser, H. Behrendt, C. Peschel, T. W. Mak, T. Jakob and J. r. Ruland (2006). "The Bcl10–Malt1 complex segregates FcεRI-mediated nuclear factor κB activation and cytokine production from mast cell degranulation." The Journal of experimental medicine **203**(2): 337-347.

Klionsky, D. J. (2005). "Autophagy." Current Biology **15**(8): R282-R283.

Kloppsteck, P., C. A. Ewens, A. Förster, X. Zhang and P. S. Freemont (2012). "Regulation of p97 in the ubiquitin–proteasome system by the UBX protein-family." Biochimica et Biophysica Acta (BBA)-Molecular Cell Research **1823**(1): 125-129.

Knowles, T. P. J., M. Vendruscolo and C. M. Dobson (2014). "The amyloid state and its association with protein misfolding diseases." Nature reviews Molecular cell biology **15**(6): 384-396.

Komander, D. and M. Rape (2012). "The ubiquitin code." Annual review of biochemistry **81**: 203-229.

Kumar, S., G. Stecher, M. Li, C. Knyaz and K. Tamura (2018). "MEGA X: molecular evolutionary genetics analysis across computing platforms." Molecular biology and evolution **35**(6): 1547-1549.

Kumpf, R. P. and M. K. Nowack (2015). "The root cap: a short story of life and death." Journal of experimental botany **66**(19): 5651-5662.

Kurepa, J., J. M. Walker, J. Smalle, M. M. Gosink, S. J. Davis, T. L. Durham, D.-Y. Sung and R. D. Vierstra (2003). "The small ubiquitin-like modifier (SUMO) protein modification system in Arabidopsis accumulation of sumo1 and-2 conjugates is increased by stress." Journal of Biological Chemistry **278**(9): 6862-6872.

Kwon, S. I. and O. K. Park (2008). "Autophagy in plants." Journal of Plant Biology **51**(5): 313-320.

Labbadia, J. and R. I. Morimoto (2015). "The biology of proteostasis in aging and disease." Annual review of biochemistry **84**: 435-464.

Lai, Z., F. Wang, Z. Zheng, B. Fan and Z. Chen (2011). "A critical role of autophagy in plant resistance to necrotrophic fungal pathogens." The Plant Journal **66**(6): 953-968.

Lamkanfi, M. (2011). "Emerging inflammasome effector mechanisms." Nature Reviews Immunology **11**(3): 213-220.

Lamkanfi, M., W. Declercq, M. Kalai, X. Saelens and P. Vandenabeele (2002). Alice in caspase land. A phylogenetic analysis of caspases from worm to man, Nature Publishing Group.

Lane, J. D., V. I. Korolchuk, J. T. Murray, M. Zachari and I. G. Ganley (2017). "The mammalian ULK1 complex and autophagy initiation." Essays in biochemistry **61**(6): 585-596.

Längst, G. and L. Manelyte (2015). "Chromatin remodelers: from function to dysfunction." Genes **6**(2): 299-324.

Laverriere, M., J. J. Cazzulo and V. E. Alvarez (2012). "Antagonic activities of Trypanosoma cruzi metacaspases affect the balance between cell proliferation, death and differentiation." Cell Death & Differentiation **19**(8): 1358-1369.

Lee, J., N. Sung, J. M. Mercado, C. F. Hryc, C. Chang, S. Lee and F. T. F. Tsai (2017). "Overlapping and specific functions of the Hsp104 N domain define its role in protein disaggregation." Scientific reports **7**(1): 1-11.

Lee, R. E. C., S. Brunette, L. G. Puente and L. A. Megeney (2010). "Metacaspase Yca1 is required for clearance of insoluble protein aggregates." Proceedings of the National Academy of Sciences **107**(30): 13348-13353.

Lee, R. E. C., L. G. Puente, M. Kærn and L. A. Megeney (2008). "A non-death role of the yeast metacaspase: Yca1p alters cell cycle dynamics." PloS one **3**(8): e2956.

Lee, R. E. C., L. G. Puente, M. Kærn and L. A. Megeney (2008). "A non-death role of the yeast metacaspase: Yca1p alters cell cycle dynamics." PloS one **3**(8).

Lenz, H. D., E. Haller, E. Melzer, K. Kober, K. Wurster, M. Stahl, D. C. Bassham, R. D. Vierstra, J. E. Parker and J. Bautor (2011). "Autophagy differentially controls plant basal immunity to biotrophic and necrotrophic pathogens." The Plant Journal **66**(5): 818-830.

Levine, B. and J. Yuan (2005). "Autophagy in cell death: an innocent convict?" The Journal of clinical investigation **115**(10): 2679-2688.

Li, L., A. Habring, K. Wang and D. Weigel (2019). "Oligomerization of NLR immune receptor RPP7 triggered by atypical resistance protein RPW8/HR as ligand." BioRxiv: 682807.

Li, W., M. Kabbage and M. B. Dickman (2010). "Transgenic expression of an insect inhibitor of apoptosis gene, SfIAP, confers abiotic and biotic stress tolerance and delays tomato fruit ripening." Physiological and Molecular Plant Pathology **74**(5-6): 363-375.

Lichtenthaler, H. K. (1987). "[34] Chlorophylls and carotenoids: pigments of photosynthetic biomembranes." Methods in enzymology **148**: 350-382.

Lindner, A. B., R. Madden, A. Demarez, E. J. Stewart and F. Taddei (2008). "Asymmetric segregation of protein aggregates is associated with cellular aging and rejuvenation." Proceedings of the National Academy of Sciences **105**(8): 3076-3081.

Liu, Y., J. S. Burgos, Y. Deng, R. Srivastava, S. H. Howell and D. C. Bassham (2012). "Degradation of the endoplasmic reticulum by autophagy during endoplasmic reticulum stress in Arabidopsis." The plant cell **24**(11): 4635-4651.

Liu, Y., M. Schiff, K. Czymmek, Z. Tallóczy, B. Levine and S. P. Dinesh-Kumar (2005). "Autophagy regulates programmed cell death during the plant innate immune response." Cell **121**(4): 567-577.

Liu, Y., Y. Xiong and D. C. Bassham (2009). "Autophagy is required for tolerance of drought and salt stress in plants." Autophagy **5**(7): 954-963.

Mackay, R. G., C. W. Helsen, J. M. Tkach and J. R. Glover (2008). "The C-terminal extension of Saccharomyces cerevisiae Hsp104 plays a role in oligomer assembly." Biochemistry **47**(7): 1918-1927.

Maeda, S., C. Otomo and T. Otomo (2019). "The autophagic membrane tether ATG2A transfers lipids between membranes." Elife **8**: e45777.

McLoughlin, F., M. Kim, R. S. Marshall, R. D. Vierstra and E. Vierling (2019). "HSP101 interacts with the proteasome and promotes the clearance of ubiquitylated protein aggregates." Plant Physiology **180**(4): 1829-1847.

Medicherla, B., Z. Kostova, A. Schaefer and D. H. Wolf (2004). "A genomic screen identifies Dsk2p and Rad23p as essential components of ER-associated degradation." EMBO reports **5**(7): 692-697.

Meng, F., I. Na, L. Kurgan and V. Uversky (2016). "Compartmentalization and functionality of nuclear disorder: intrinsic disorder and protein-protein interactions in intra-nuclear compartments." International journal of molecular sciences **17**(1): 24.

Miller, S. B. M., C. T. Ho, J. Winkler, M. Khokhrina, A. Neuner, M. Y. H. Mohamed, D. L. Guilbride, K. Richter, M. Lisby and E. Schiebel (2015). "Compartment-specific aggregases direct distinct nuclear and cytoplasmic aggregate deposition." The EMBO journal **34**(6): 778-797.

Minina, E. A., J. Staal, V. E. Alvarez, J. A. Berges, I. Berman-Frank, R. Beyaert, K. D. Bidle, F. Bornancin, M. Casanova and J. J. Cazzulo (2020). "Classification and nomenclature of metacaspases and paracaspases: no more confusion with caspases." Molecular cell **77**(5): 927-929.

Mizushima, N., T. Yoshimori and Y. Ohsumi (2011). "The role of Atg proteins in autophagosome formation." Annual review of cell and developmental biology **27**: 107-132.

Neef, D. W., M. L. Turski and D. J. Thiele (2010). "Modulation of heat shock transcription factor 1 as a therapeutic target for small molecule intervention in neurodegenerative disease." PLoS Biol **8**(1): e1000291.

Noda, T. (2017). "Autophagy in the context of the cellular membrane-trafficking system: the enigma of Atg9 vesicles." Biochemical Society Transactions **45**(6): 1323-1331.

O'Driscoll, J., D. Clare and H. Saibil (2015). "Prion aggregate structure in yeast cells is determined by the Hsp104-Hsp110 disaggregase machinery." Journal of Cell Biology **211**(1): 145-158.

Ogrodnik, M., H. Salmonowicz, R. Brown, J. Turkowska, W. Średniawa, S. Pattabiraman, T. Amen, A.-c. Abraham, N. Eichler and R. Lyakhovetsky (2014). "Dynamic JUNQ inclusion bodies are asymmetrically inherited in mammalian cell lines through the asymmetric partitioning of vimentin." Proceedings of the National Academy of Sciences **111**(22): 8049-8054.

Park, S.-H., Y. Kukushkin, R. Gupta, T. Chen, A. Konagai, M. S. Hipp, M. Hayer-Hartl and F. U. Hartl (2013). "PolyQ proteins interfere with nuclear degradation of cytosolic proteins by sequestering the Sis1p chaperone." Cell **154**(1): 134-145.

Parsell, D. A., A. S. Kowal, M. A. Singer and S. Lindquist (1994). "Protein disaggregation mediated by heat-shock protein Hspl04." Nature **372**(6505): 475-478.

Parselt, D. A., Y. Sanchez, J. D. Stitzel and S. Lindquist (1991). "Hspl04 is a highly conserved protein with two essential nucleotide-binding sites." Nature **353**(6341): 270-273.

Patel, S. and S. P. Dinesh-Kumar (2008). "Arabidopsis ATG6 is required to limit the pathogen-associated cell death response." Autophagy **4**(1): 20-27.

Pickart, C. M. (2001). "Mechanisms underlying ubiquitination." Annual review of biochemistry **70**.

Pitsili, E., U. J. Phukan and N. S. Coll (2020). "Cell death in plant immunity." Cold Spring Harbor Perspectives in Biology **12**(6): a036483.

Powers, E. T., R. I. Morimoto, A. Dillin, J. W. Kelly and W. E. Balch (2009). "Biological and chemical approaches to diseases of proteostasis deficiency." Annual review of biochemistry **78**: 959-991.

Queitsch, C., S.-W. Hong, E. Vierling and S. Lindquist (2000). "Heat shock protein 101 plays a crucial role in thermotolerance in Arabidopsis." The Plant Cell **12**(4): 479-492.

Ravikumar, B., S. Sarkar, J. E. Davies, M. Futter, M. Garcia-Arencibia, Z. W. Green-Thompson, M. Jimenez-Sanchez, V. I. Korolchuk, M. Lichtenberg and S. Luo (2010). "Regulation of mammalian autophagy in physiology and pathophysiology." Physiological reviews **90**(4): 1383-1435.

Richie, D. L., M. D. Miley, R. Bhabhra, G. D. Robson, J. C. Rhodes and D. S. Askew (2007). "The Aspergillus fumigatus metacaspases CasA and CasB facilitate growth under conditions of endoplasmic reticulum stress." Molecular microbiology **63**(2): 591-604.

Rojo, E., R. Martın, C. Carter, J. Zouhar, S. Pan, J. Plotnikova, H. Jin, M. Paneque, J. J. Sánchez-Serrano and B. Baker (2004). "VPEγ exhibits a caspase-like activity that contributes to defense against pathogens." Current Biology **14**(21): 1897-1906.

Rubinsztein, D. C. (2006). "The roles of intracellular protein-degradation pathways in neurodegeneration." Nature **443**(7113): 780-786.

Rüdiger, S., A. Buchberger and B. Bukau (1997). "Interaction of Hsp70 chaperones with substrates." Nature structural biology **4**(5): 342-349.

Ruland, J., G. S. Duncan, A. Wakeham and T. W. Mak (2003). "Differential requirement for Malt1 in T and B cell antigen receptor signaling." Immunity **19**(5): 749-758.

Ruland, J. and L. Hartjes (2019). "CARD–BCL-10–MALT1 signalling in protective and pathological immunity." Nature Reviews Immunology **19**(2): 118-134.

Saarikangas, J. and Y. Barral (2015). "Protein aggregates are associated with replicative aging without compromising protein quality control." Elife **4**: e06197.

Salguero-Linares, J. and N. S. Coll (2019). "Plant proteases in the control of the hypersensitive response." Journal of experimental botany **70**(7): 2087-2095.

Sanchez, Y., J. Taulien, K. A. Borkovich and S. Lindquist (1992). "Hsp104 is required for tolerance to many forms of stress." The EMBO journal **11**(6): 2357-2364.

Sarwat, M., A. R. Naqvi, P. Ahmad, M. Ashraf and N. A. Akram (2013). "Phytohormones and microRNAs as sensors and regulators of leaf senescence: assigning macro roles to small molecules." Biotechnology advances **31**(8): 1153-1171.

Sathyanarayanan, U., M. Musa, P. B. Dib, N. Raimundo, I. Milosevic and A. Krisko (2020). "ATP hydrolysis by yeast Hsp104 determines protein aggregate dissolution and size in vivo." Nature communications **11**(1): 1-17.

Schapire, A. L. and L. M. Lois (2016). A simplified and rapid method for the isolation and transfection of Arabidopsis leaf mesophyll protoplasts for large-scale applications. Plant Signal Transduction, Springer**:** 79-88.

Schirmer, E. C., S. Lindquist and E. Vierling (1994). "An Arabidopsis heat shock protein complements a thermotolerance defect in yeast." The Plant Cell **6**(12): 1899-1909.

Schirmer, E. C., D. M. Ware, C. Queitsch, A. S. Kowal and S. L. Lindquist (2001). "Subunit interactions influence the biochemical and biological properties of Hsp104." Proceedings of the National Academy of Sciences **98**(3): 914-919.

Schwartz, A. L. and A. Ciechanover (2009). "Targeting proteins for destruction by the ubiquitin system: implications for human pathobiology." Annual review of pharmacology and toxicology **49**: 73-96.

Shin, J.-H., K. Yoshimoto, Y. Ohsumi, J.-s. Jeon and G. An (2009). "OsATG10b, an autophagosome component, is needed for cell survival against oxidative stresses in rice." Molecules and cells **27**(1): 67-74.

Shorter, J. and D. R. Southworth (2019). "Spiraling in control: structures and mechanisms of the Hsp104 disaggregase." Cold Spring Harbor perspectives in biology **11**(8): a034033.

Shrestha, A., S. Brunette, W. L. Stanford and L. A. Megeney (2019). "The metacaspase Yca1 maintains proteostasis through multiple interactions with the ubiquitin system." Cell discovery **5**(1): 1-13.

Shrestha, A., L. G. Puente, S. Brunette and L. A. Megeney (2013). "The role of Yca1 in proteostasis. Yca1 regulates the composition of the insoluble proteome." Journal of proteomics **81**: 24-30.

Slavikova, S., S. Ufaz, T. Avin-Wittenberg, H. Levanony and G. Galili (2008). "An autophagy-associated Atg8 protein is involved in the responses of Arabidopsis seedlings to hormonal controls and abiotic stresses." Journal of Experimental Botany **59**(14): 4029-4043.

Slepenkov, S. V. and S. N. Witt (2002). "The unfolding story of the Escherichia coli Hsp70 DnaK: is DnaK a holdase or an unfoldase?" Molecular microbiology **45**: 1197-1206.

Smeal, T., J. Claus, B. Kennedy, F. Cole and L. Guarente (1996). "Loss of transcriptional silencing causes sterility in old mother cells of S. cerevisiae." Cell **84**(4): 633-642.

Smith, M. H., H. L. Ploegh and J. S. Weissman (2011). "Road to ruin: targeting proteins for degradation in the endoplasmic reticulum." Science **334**(6059): 1086-1090.

Solier, S., M. Fontenay, W. Vainchenker, N. Droin and E. Solary (2017). "Non-apoptotic functions of caspases in myeloid cell differentiation." Cell Death & Differentiation **24**(8): 1337-1347.

Sontag, E. M., R. S. Samant and J. Frydman (2017). "Mechanisms and functions of spatial protein quality control." Annual review of biochemistry **86**: 97-122.

Sontag, E. M., W. I. M. Vonk and J. Frydman (2014). "Sorting out the trash: the spatial nature of eukaryotic protein quality control." Current opinion in cell biology **26**: 139-146.

Soto, C. (2003). "Unfolding the role of protein misfolding in neurodegenerative diseases." Nature Reviews Neuroscience **4**(1): 49-60.

Soudry, E., S. Ulitzur and S. Gepstein (2005). "Accumulation and remobilization of amino acids during senescence of detached and attached leaves: in planta analysis of tryptophan levels by recombinant luminescent bacteria." Journal of experimental botany **56**(412): 695-702.

Spokoini, R., O. Moldavski, Y. Nahmias, J. L. England, M. Schuldiner and D. Kaganovich (2012). "Confinement to organelle-associated inclusion structures mediates asymmetric inheritance of aggregated protein in budding yeast." Cell reports **2**(4): 738-747.

Su, W., H. Ma, C. Liu, J. Wu and J. Yang (2006). "Identification and characterization of two rice autophagy associated genes, OsAtg8 and OsAtg4." Molecular biology reports **33**(4): 273-278.

Sung, M. K. and W. K. Huh (2007). "Bimolecular fluorescence complementation analysis system for in vivo detection of protein–protein interaction in Saccharomyces cerevisiae." Yeast **24**(9): 767-775.

Swatek, K. N. and D. Komander (2016). "Ubiquitin modifications." Cell research **26**(4): 399-422.

Sweeny, E. A., M. E. Jackrel, M. S. Go, M. A. Sochor, B. M. Razzo, M. E. DeSantis, K. Gupta and J. Shorter (2015). "The Hsp104 N-terminal domain enables disaggregase plasticity and potentiation." Molecular cell **57**(5): 836-849.

Tabuchi, M., Y. Kawai, M. Nishie-Fujita, R. Akada, T. Izumi, I. Yanatori, N. Miyashita, K. Ouchi and F. Kishi (2009). "Development of a novel functional high-throughput

screening system for pathogen effectors in the yeast Saccharomyces cerevisiae." Bioscience, biotechnology, and biochemistry **73**(10): 2261-2267.

Tamás, M. J., B. Fauvet, P. Christen and P. Goloubinoff (2018). "Misfolding and aggregation of nascent proteins: a novel mode of toxic cadmium action in vivo." Current genetics **64**(1): 177-181.

Tenreiro, S., V. Franssens, J. Winderickx and T. F. Outeiro (2017). "Yeast models of Parkinson's disease-associated molecular pathologies." Current opinion in genetics & development **44**: 74-83.

Tessarz, P., A. Mogk and B. Bukau (2008). "Substrate threading through the central pore of the Hsp104 chaperone as a common mechanism for protein disaggregation and prion propagation." Molecular microbiology **68**(1): 87-97.

Thompson, A. R., J. H. Doelling, A. Suttangkakul and R. D. Vierstra (2005). "Autophagic nutrient recycling in Arabidopsis directed by the ATG8 and ATG12 conjugation pathways." Plant physiology **138**(4): 2097-2110.

Tkach, J. M. and J. R. Glover (2008). "Nucleocytoplasmic trafficking of the molecular chaperone Hsp104 in unstressed and heat-shocked cells." Traffic **9**(1): 39-56.

Tooze, S. A. and T. Yoshimori (2010). "The origin of the autophagosomal membrane." Nature cell biology **12**(9): 831.

Tran, V., D. Weier, R. Radchuk, J. Thiel and V. Radchuk (2014). "Caspase-like activities accompany programmed cell death events in developing barley grains." PloS one **9**(10): e109426.

Tummers, B. and D. R. Green (2017). "Caspase-8: regulating life and death." Immunological reviews **277**(1): 76-89.

Tyedmers, J., A. Mogk and B. Bukau (2010). "Cellular strategies for controlling protein aggregation." Nature reviews Molecular cell biology **11**(11): 777-788.

Tyedmers, J., S. Treusch, J. Dong, J. M. McCaffery, B. Bevis and S. Lindquist (2010). "Prion induction involves an ancient system for the sequestration of aggregated proteins and

heritable changes in prion fragmentation." Proceedings of the National Academy of Sciences **107**(19): 8633-8638.

Uehata, T., H. Iwasaki, A. Vandenbon, K. Matsushita, E. Hernandez-Cuellar, K. Kuniyoshi, T. Satoh, T. Mino, Y. Suzuki and D. M. Standley (2013). "Malt1-induced cleavage of regnase-1 in CD4+ helper T cells regulates immune activation." Cell **153**(5): 1036-1049.

Uren, A. G., K. O'Rourke, L. Aravind, M. T. Pisabarro, S. Seshagiri, E. V. Koonin and V. M. Dixit (2000). "Identification of paracaspases and metacaspases: two ancient families of caspase-like proteins, one of which plays a key role in MALT lymphoma." Molecular cell **6**(4): 961-967.

Vabulas, R. M., S. Raychaudhuri, M. Hayer-Hartl and F. U. Hartl (2010). "Protein folding in the cytoplasm and the heat shock response." Cold Spring Harbor perspectives in biology **2**(12): a004390.

Van Hautegem, T., A. J. Waters, J. Goodrich and M. K. Nowack (2015). "Only in dying, life: programmed cell death during plant development." Trends in plant science **20**(2): 102-113.

Vaux, D. L. and S. J. Korsmeyer (1999). "Cell death in development." Cell **96**(2): 245-254.

Vembar, S. S. and J. L. Brodsky (2008). "One step at a time: endoplasmic reticulum-associated degradation." Nature reviews Molecular cell biology **9**(12): 944.

Ventura, S. and A. Villaverde (2006). "Protein quality in bacterial inclusion bodies." Trends in biotechnology **24**(4): 179-185.

Voges, D., P. Zwickl and W. Baumeister (1999). "The 26S proteasome: a molecular machine designed for controlled proteolysis." Annual review of biochemistry **68**(1): 1015-1068.

Voinnet, O., S. Rivas, P. Mestre and D. Baulcombe (2003). "Retracted: An enhanced transient expression system in plants based on suppression of gene silencing by the p19 protein of tomato bushy stunt virus." The Plant Journal **33**(5): 949-956.

Wagner, S. A., P. Beli, B. T. Weinert, M. L. Nielsen, J. Cox, M. Mann and C. Choudhary (2011). "A proteome-wide, quantitative survey of in vivo ubiquitylation sites reveals widespread regulatory roles." Molecular & Cellular Proteomics **10**(10).

Wallace, E. W. J., J. L. Kear-Scott, E. V. Pilipenko, M. H. Schwartz, P. R. Laskowski, A. E. Rojek, C. D. Katanski, J. A. Riback, M. F. Dion and A. M. Franks (2015). "Reversible, specific, active aggregates of endogenous proteins assemble upon heat stress." Cell **162**(6): 1286-1298.

Wang, J., M. Hu, J. Wang, J. Qi, Z. Han, G. Wang, Y. Qi, H.-W. Wang, J.-M. Zhou and J. Chai (2019). "Reconstitution and structure of a plant NLR resistosome conferring immunity." Science **364**(6435).

Wang, J., J. Wang, M. Hu, S. Wu, J. Qi, G. Wang, Z. Han, Y. Qi, N. Gao and H.-W. Wang (2019). "Ligand-triggered allosteric ADP release primes a plant NLR complex." Science **364**(6435).

Watanabe, N. and E. Lam (2011). "Arabidopsis metacaspase 2d is a positive mediator of cell death induced during biotic and abiotic stresses." The Plant Journal **66**(6): 969-982.

Watanabe, N. and E. Lam (2011). "Calcium-dependent activation and autolysis of Arabidopsis metacaspase 2d." Journal of Biological Chemistry **286**(12): 10027-10040.

Weaver, L. M. and R. M. Amasino (2001). "Senescence is induced in individually darkened Arabidopsis leaves, but inhibited in whole darkened plants." Plant Physiology **127**(3): 876-886.

Weibezahn, J., P. Tessarz, C. Schlieker, R. Zahn, Z. Maglica, S. Lee, H. Zentgraf, E. U. Weber-Ban, D. A. Dougan and F. T. F. Tsai (2004). "Thermotolerance requires refolding of aggregated proteins by substrate translocation through the central pore of ClpB." Cell **119**(5): 653-665.

Winkler, J., A. Seybert, L. König, S. Pruggnaller, U. Haselmann, V. Sourjik, M. Weiss, A. S. Frangakis, A. Mogk and B. Bukau (2010). "Quantitative and spatio-temporal features of protein aggregation in Escherichia coli and consequences on protein quality control and cellular ageing." The EMBO journal **29**(5): 910-923.

Winkler, J., A. Seybert, L. König, S. Pruggnaller, U. Haselmann, V. Sourjik, M. Weiss, A. S. Frangakis, A. Mogk and B. Bukau (2010). "Quantitative and spatio-temporal features

of protein aggregation in Escherichia coli and consequences on protein quality control and cellular ageing." The EMBO journal **29**(5): 910-923.

Wong, A. H.-H., C. Yan and Y. Shi (2012). "Crystal structure of the yeast metacaspase Yca1." Journal of biological chemistry **287**(35): 29251-29259.

Xiong, R. and A. Wang (2013). "SCE1, the SUMO-conjugating enzyme in plants that interacts with NIb, the RNA-dependent RNA polymerase of Turnip mosaic virus, is required for viral infection." Journal of virology **87**(8): 4704-4715.

Xiong, Y., A. L. Contento and D. C. Bassham (2005). "AtATG18a is required for the formation of autophagosomes during nutrient stress and senescence in Arabidopsis thaliana." The Plant Journal **42**(4): 535-546.

Xu, P., D. M. Duong, N. T. Seyfried, D. Cheng, Y. Xie, J. Robert, J. Rush, M. Hochstrasser, D. Finley and J. Peng (2009). "Quantitative proteomics reveals the function of unconventional ubiquitin chains in proteasomal degradation." Cell **137**(1): 133-145.

Yan, X. X., J. Najbauer, C. C. Woo, K. Dashtipour, C. E. Ribak and M. Leon (2001). "Expression of active caspase-3 in mitotic and postmitotic cells of the rat forebrain." Journal of Comparative Neurology **433**(1): 4-22.

Yang, P., H. Fu, J. Walker, C. M. Papa, J. Smalle, Y.-M. Ju and R. D. Vierstra (2004). "Purification of the Arabidopsis 26 S proteasome biochemical and molecular analyses revealed the presence of multiple isoforms." Journal of Biological Chemistry **279**(8): 6401-6413.

Yang, X., R. Srivastava, S. H. Howell and D. C. Bassham (2016). "Activation of autophagy by unfolded proteins during endoplasmic reticulum stress." The Plant Journal **85**(1): 83-95.

Yoshimoto, K., H. Hanaoka, S. Sato, T. Kato, S. Tabata, T. Noda and Y. Ohsumi (2004). "Processing of ATG8s, ubiquitin-like proteins, and their deconjugation by ATG4s are essential for plant autophagy." The Plant Cell **16**(11): 2967-2983.

Yu, J.-H., Z. Hamari, K.-H. Han, J.-A. Seo, Y. Reyes-Domínguez and C. Scazzocchio (2004). "Double-joint PCR: a PCR-based molecular tool for gene manipulations in filamentous fungi." Fungal genetics and biology **41**(11): 973-981.

Zhang, B., B. Sztojka, S. Escamez, R. Vanholme, M. Hedenström, Y. Wang, H. Turumtay, A. Gorzsás, W. Boerjan and H. Tuominen (2020). "PIRIN2 suppresses S-type lignin accumulation in a noncell-autonomous manner in Arabidopsis xylem elements." New Phytologist **225**(5): 1923-1935.

Zheng, Z., S. A. Qamar, Z. Chen and T. Mengiste (2006). "Arabidopsis WRKY33 transcription factor is required for resistance to necrotrophic fungal pathogens." The Plant Journal **48**(4): 592-605.

Zhu, P., X.-H. Yu, C. Wang, Q. Zhang, W. Liu, S. McSweeney, J. Shanklin, E. Lam and Q. Liu (2020). "Structural basis for Ca 2+-dependent activation of a plant metacaspase." Nature communications **11**(1): 1-9.

# ANNEX

# SCIENTIFIC REPORTS

# The effector AWR5 from the plant pathogen *Ralstonia solanacearum* is an inhibitor of the TOR signalling pathway

Crina Popa[1,2], Liang Li[1], Sergio Gil[2], Laura Tatjer[3], Keisuke Hashii[4], Mitsuaki Tabuchi[4], Núria S. Coll[1], Joaquín Ariño[3] & Marc Valls[1,2]

Bacterial pathogens possess complex type III effector (T3E) repertoires that are translocated inside the host cells to cause disease. However, only a minor proportion of these effectors have been assigned a function. Here, we show that the T3E AWR5 from the phytopathogen *Ralstonia solanacearum* is an inhibitor of TOR, a central regulator in eukaryotes that controls the switch between cell growth and stress responses in response to nutrient availability. Heterologous expression of *AWR5* in yeast caused growth inhibition and autophagy induction coupled to massive transcriptomic changes, unmistakably reminiscent of TOR inhibition by rapamycin or nitrogen starvation. Detailed genetic analysis of these phenotypes in yeast, including suppression of AWR5-induced toxicity by mutation of *CDC55* and *TPD3*, encoding regulatory subunits of the PP2A phosphatase, indicated that AWR5 might exert its function by directly or indirectly inhibiting the TOR pathway upstream PP2A. We present evidence *in planta* that this T3E caused a decrease in TOR-regulated plant nitrate reductase activity and also that normal levels of TOR and the Cdc55 homologues in plants are required for *R. solanacearum* virulence. Our results suggest that the TOR pathway is a bona fide T3E target and further prove that yeast is a useful platform for T3E function characterisation.

Many bacterial pathogens use a type III secretion system (T3SS) to inject a suite of proteins inside the host cell[1]. These proteins are referred to as type III effectors (T3Es), and play a central role in bacterial survival and disease development[2]. T3Es manipulate host cell pathways by mimicking key host proteins or mediating changes in their subcellular localization, by targeting plant-specific transcription factors, by inhibiting translation and metabolic stress pathways or exploiting a specific form of host-mediated fatty acid modification[3–5]. The functional study of T3Es from phytopathogenic bacteria has raised a tremendous interest in the last years[6,7]. The number of T3Es identified is growing at a very fast pace as more bacterial genomes become available, revealing complex repertoires that feature internal redundancy, which complicates their study[6]. However, only in a few cases the function of this kind of effectors *in planta* has been identified.

Heterologous production in *Saccharomyces cerevisiae* has offered promising and effective strategies to characterize bacterial T3Es[8]. Seminal work with YopE showed that this T3E caused specific growth inhibition and cytoskeletal alteration, an activity conserved in yeast and mammalian cells[9]. Functional analyses of plant-associated T3E in yeast have revealed other effector-triggered phenotypes including cell death, suppression of apoptosis or perturbation of host cellular processes, such as MAPK signalling or sphingolipid synthesis[10–12]. All these findings strengthen the premise that many bacterial T3E target universal eukaryotic processes so that *S. cerevisiae* can be exploited to elucidate their molecular function and to investigate target-effector interactions[8,13].

The TOR complex 1 (TORC1) is a central regulator of cell growth in response to nutrient availability and stress conditions by controlling diverse cellular processes, including transcriptional activation, ribosome biogenesis or autophagy[14] (Fig. 1a). This complex contains the Tor1 or Tor2 protein kinases and can be inhibited by the

[1]Centre for Research in Agricultural Genomics (CSIC-IRTA-UAB-UB), Bellaterra, Catalonia, Spain. [2]Genetics Department, Universitat de Barcelona, Barcelona, Catalonia, Spain. [3]Institut de Biotecnologia i Biomedicina and Departament de Bioquímica i Biologia Molecular, Universitat Autònoma de Barcelona, Cerdanyola del Vallès, Catalonia, Spain. [4]Laboratory of Applied Molecular and Cell Biology, Kagawa University, Kagawa, Japan. Correspondence and requests for materials should be addressed to N.S.C. (email: nuria.sanchez-coll@cragenomica.es)

drug rapamycin. In yeast, TORC1 acts by controlling three major cell components: the kinase Sch9, Tap42 and its associated phosphatases and the ATG1 complex[14,15]. Thus, TORC1 modulates nitrogen catabolite repression and diverse stress responses by controlling the activity of several phosphatases, such as protein phosphatase 2A (PP2A) or Sit 4, often by modifying their interaction with regulatory subunits (Fig. 1a[15]).

*Ralstonia solanacearum* is emerging as a model system to study plant-pathogen molecular interactions and T3E function[16]. This soil-borne bacterium is the causing agent of bacterial wilt, a disease caused when the bacterium growing in plant extracellular spaces (apoplast) infects the xylem vessels, where it multiplies extensively and blocks water flow[17]. *R. solanacearum* has been ranked as the second most important bacterial plant pathogen[18], due to its high persistence and wide geographical distribution and host range, as it infects more than 200 plant species, including important agricultural crops such as tomato and potato[19]. Of more than 70 T3Es identified in the reference strain GMI1000, only for two of them a defined role *in planta* has been assigned[16]. AWRs (named after a conserved alanine-tryptophan-arginine tryad and also called RipAs) are one of the multigenic families of T3Es conserved in all *R. solanacearum* strains[17], with orthologues in other bacterial pathogens such as *Xanthomonas* strains, *Acidovorax avenae* or *Burkholderia* spp.[20]. A low protein similarity has also been described between AWRs and the *Xanthomonas oryzae pv. oryzae* effector XopZ, which was shown to be involved in virulence and suppression of host basal defence[21]. Translocation assays have proven AWRs as *bona fide R. solanacearum* type III secreted effectors[20,22,23]. However, sequence information on AWR proteins gives no clue on their putative function. In a previous study, we showed that the AWR T3E family collectively contributes to *R. solanacearum* virulence, as a mutant bacterium devoid of all AWRs multiplies 50-fold less than the wild-type strain on eggplant and tomato plants. Functional analysis of AWRs also demonstrated that their expression in different plant species triggers varying defence responses[20]. Functional analyses for each AWR showed that AWR5 had an important contribution in virulence and also caused the most dramatic plant responses. In addition, we have recently found that *awr5* is one of the most highly expressed genes when *R. solanacearum* grows inside the plant host (Marina Puigvert, unpublished results). Association genetics combining genomic data from *R. solanacearum* strains and their pathogenicity on eggplant, pepper and tomato accessions identified AWR5 amongst the three T3Es highly associated to virulence[24].

In this work we take advantage of the yeast system to characterize AWR5 function. Heterologous expression of *AWR5* in *S. cerevisiae* resulted in dramatic growth inhibition of yeast cells. We show that this effect on yeast growth is caused by inhibition of the central regulatory TOR pathway. Importantly, AWR5 impact on the TOR pathway is conserved in both yeast and plants, revealing a previously unknown T3E mode of action maintained in evolutionary distant organisms. Moreover, our work further validates yeast as an excellent platform to uncover T3E function.

## Results

### Expression of the *R. solanacearum awr* type III effector family in yeast causes growth inhibition.

To investigate the function of the AWR bacterial effectors in eukaryotic cells, we expressed the five *awr* genes from *R. solanacearum* GMI1000 in *S. cerevisiae.* In a first step, *awr*s were cloned in the high-copy-number vector pAG-426GAL, where they are transcribed from the strong galactose-inducible *GAL1* promoter. The resulting plasmids were introduced in yeast and the transformed strains grown overnight, then serially diluted and plated either in repressing media (glucose) or inducing media (galactose). It was observed that, except for AWR4, these effectors inhibited growth to different extents, as observed by the inability to form macroscopic colonies on inducing media (Supplementary Fig. S1). AWR1, 2, 3 and 5 caused a strong toxicity upon induction, but AWR5 showed the most dramatic effect, inhibiting yeast growth even in non-inducing conditions. The phenotype seemed specific for AWR effectors, as it was not observed when a control gene (GFP) was expressed (Supplementary Fig. S1). The full-length AWR5 protein was required for functionality, as expression of split variants of AWR5 (N-terminal or C-terminal halves, or the central region) did not cause toxicity (Supplementary Fig. S1).

To evaluate the phenotype in more physiological conditions and ensure construct stability and tight control of effector transcription, we integrated the bacterial genes in the yeast genome under the control of a repressible Tet-Off promoter. When the resulting strains bearing *awr*s or a control GUS gene were plated in the absence of the repressor doxycycline, only expression of *awr5* reproduced the dramatic growth arrest (Fig. 1b). The absence of toxicity for AWR1, 2 and 4 could not be attributed to a lack of expression, as the full-length proteins were readily detected in yeast cells (Supplementary Fig. S2). Thus, we concentrated on the characterization of the growth inhibition caused by *awr5* expression.

### Characterization of the AWR5-dependent growth inhibition phenotype.

Yeast growth inhibition was also apparent upon AWR5 production in liquid cultures as indicated by a rapid stagnation of cell density over time (not shown) and a clear decrease in the number of growing cells (Fig. 1c). Growth inhibition kinetics paralleled with an increase in *awr5* RNA (Supplementary Fig. S3) and protein levels (Fig. 1d). Microscopic observation of strains producing AWR5 revealed the presence of budding cells at similar proportions to cells not producing the bacterial effector (Supplementary Fig. S4a). Thus, it could be ruled out that this protein specifically alters the cell cycle.

Expression of *awr5* caused strong growth inhibition but not cell death, as deduced from methylene blue staining of cells bearing *awr5* in the absence of doxycycline (Supplementary Fig. S4a) and from counting of viable cells able to form colonies after 6 h of *awr5* expression (Supplementary Fig. S4b). Similarly, growth arrest in cells expressing *awr5* was not likely caused by defects in cell wall construction leading to cell lysis, since it was not eliminated by osmotic stabilization with 10% sorbitol (Supplementary Fig. S5). In contrast, determination of cell size upon expression of *awr5* showed significant changes, visible after 8 h of induction, with AWR5-producing cells showing an average diameter of $4.96 \pm 0.03\,\mu m$, while that of non-expressing cells was over $5.3 \pm 0.06\,\mu m$ (Supplementary Fig. S4c).
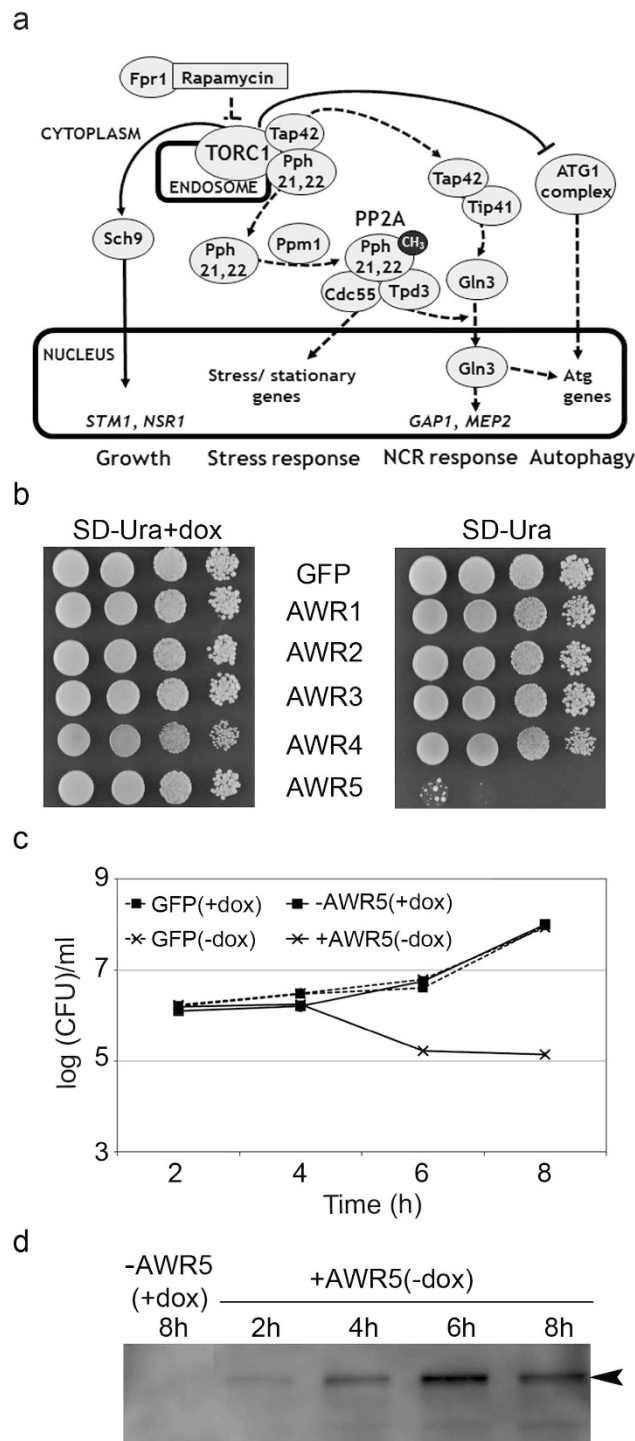
**Figure 1. Expression of *awr5* effector inhibits yeast growth. (a)** Schematic view of the *Saccharomyces cerevisiae* TORC1-regulated pathways. The TORC1 complex is a central growth regulator, controlling the balance between growth and quiescence. Continuous and dotted lines represent, respectively, signaling events regulated by active and inactive TORC1. (**b**) Growth on solid medium of yeast strains expressing *awr* effectors. Yeast strains bearing *awr* genes fused to GFP tag or a GFP control were subjected to serial 10-fold dilutions and spotted onto solid SD-Ura+doxycycline (repressing medium) and SD-Ura (inducing medium). Photographs were taken after 2 days of growth. (**c**) Growth kinetics in liquid medium of yeast cells harboring *awr5* or a GFP control. Yeast cells harboring *awr5* or a GFP control were grown in SD-Ura+dox (−AWR5) and SD-Ura (+AWR5) liquid media and dispersed on SD-Ura+dox plates. The logarithm of colony forming units (CFU) per ml is shown over time. Error bars indicate standard errors for 2 biological replicates. (**d**) Immunoblot analysis of AWR5 protein levels. Total protein was extracted from cultures shown in Fig. 1c and immunoblotted using an anti-GFP antibody. The black arrowhead indicates AWR5-GFP protein. All experiments were performed at least three times, with similar results.

Previous reports studying effectors from *Pseudomonas syringae* or *Xanthomonas euvesicatoria* had shown that some of them caused growth arrest when yeast was forced to respire[10,11]. To verify if respiration affected AWR5 toxicity in yeast, we grew serial dilutions of the strain producing this protein or a control gene (β-glucuronidase, GUS) onto solid medium containing the non-fermentable carbon sources ethanol and glycerol. As observed in Supplementary Fig. S5, the toxic effect due to AWR5 was maintained under these conditions.

In summary, we established that production of the full-length AWR5 protein in yeast targeted a cellular process leading to growth inhibition and decreased cell size, but not involving an evident cell cycle arrest or cell death.

### Expression of *awr5* mimics the transcriptional changes induced by the TORC1 inhibitor rapamycin.
To understand the molecular basis of *awr5* toxicity in yeast and to highlight putative functional targets, we considered the identification of possible changes at the mRNA level caused by expression of the effector. To this end, we carried out a genome-wide transcriptomic analysis using DNA microarrays in yeast cells with *awr5* expression induced for 2, 4 and 6 h. This time-course was selected according to the previously characterized growth effect (Fig. 1c). DNA microarray analysis yielded 3763 genes with valid data for all 3 time-points. We observed that induction of *awr5* expression produced relevant time-dependent changes in the transcriptomic profile that, in most cases, could be observed after 4 and 6 h of induction. The mRNA level of 766 genes was modified at least 2-fold, with 319 genes induced and 447 repressed. The functional assignment of induced genes revealed a striking excess of genes subjected to nitrogen catabolite repression (NCR)[25], such as *MEP2*, *GAP1*, *DAL5*, *CPS1* or *DUR1,2*, whereas among the repressed genes there was a vast excess of genes encoding ribosomal proteins or involved in ribosome biogenesis. This profile was reminiscent of that reported by several laboratories for inhibition of the TORC1 pathway[15].

We took advantage of recent work in our laboratory in which the transcriptomic profile in response to 1 h of exposure to rapamycin had been generated[26]. Combination of this data with that obtained here after *awr5* expression yielded 2774 genes with expression information in both conditions. Figure 2a shows the correspondence between changes produced in response to *awr5* with those caused by rapamycin. It can be observed that whereas the correlation is relatively poor shortly after *awr5* induction (correlation coefficient = 0.402), the similarity between both responses becomes evident after 4 h and, particularly, after 6 h of *awr5* induction (correlation coefficients 0.569 and 0.739, respectively). We then selected among the 766 genes whose expression changed at least 2-fold those with data for the rapamycin treatment (596 genes) and subjected this set of genes to clustering analysis. Figure 2b clearly documents that the time-dependent transcriptional response to expression of *awr5* matches that provoked by rapamycin treatment (correlation coefficient of 0.872 when compared with *awr5* data after 6 h of expression). It can be observed that clusters 1 and 2 -and to some extent also cluster 3- are enriched in induced genes related to metabolism of nitrogen (mostly amino acids), whereas regarding the repressed genes, cluster 5 includes genes involved in translation and cluster 6 is enriched in genes encoding ribosomal proteins or members of the RiBi (ribosome biogenesis) regulon. All these results indicate that expression of bacterial *awr5* in yeast triggers a response that mimics the inhibition of the TORC1 pathway.

These transcriptomic data were validated by performing quantitative RT-PCR analysis on a subset of genes from different TORC1-regulated pathways, which showed altered expression levels in response to *awr5* (Fig. 3b). As expected, *awr5* expression resulted in a decrease of the levels of the TOR-activated *STM1* and *NSR1* genes, which are involved in yeast growth[27,28]. In contrast, the levels of the TOR-repressed *GAP1* and *MEP2*, which control nitrogen catabolite repression[29], increased in response to *awr5* expression. Similar results were obtained when promoter activity was measured using fusions to the β-galactosidase reporter: *awr5* expression resulted in increased *GAP1* and *MEP2* promoter output (Fig. 3b).

### Mutations in two genes involved in the TORC1 pathway rescue the yeast growth inhibition caused by AWR5.
Since AWR5 mimicked rapamycin treatment in yeast, we tested whether disruption of *FPR1*-encoding the rapamycin-binding protein Fpr1 that inhibits the TORC1 kinase in the presence of rapamycin[15] rescued the AWR5-triggered phenotype. Growth inhibition caused by AWR5 was maintained in the *fpr1* strain (Fig. 4a), indicating that the bacterial effector acts on TORC1 through a different mechanism than rapamycin.

In order to ascertain which point of the TOR-controlled pathways was targeted by AWR5 we analysed yeast strains with altered levels of different genes mediating TORC1 signalling. Interestingly, the strains mutated in the PP2A regulatory or scaffold subunits *cdc55* or *tpd3* did not show AWR5-triggered growth inhibition (Fig. 4b). This indicated that these PP2A subunits are essential for AWR5 to cause its phenotype. These results were also corroborated by testing promoter activity of *GAP1* fused to the β-galactosidase reporter in wild type and *cdc55* mutant strains. Our results clearly showed that *CDC55* was required for the increase in *GAP1* promoter activity that occurs in response to *awr5* expression (Fig. 4c).

On the contrary, AWR5 did not seem to target the PP2A catalytic subunit, since AWR5-mediated growth inhibition could not be rescued by overexpression or conditional mutation of the two redundant genes (*pph21, 22*) encoding this subunit (Supplementary Fig. S6a,b). Any other mutant (*rts1*, *tip41*, *ppm1* and *gln3*) or overexpressor (*SIT4*) in genes related to signalling through the TORC1 pathway that we tested did not show reversion of AWR5-mediated growth inhibition. However, we could not detect interaction between Cdc55 or Tpd3 and AWR5 in yeast using co-immunoprecipitation (Supplementary Fig. S7a,b). Although the transcription profile was specifically compatible with TORC1 inhibition, we checked whether AWR5 had any impact on TORC2. As shown in supplementary Fig. S8, AWR5 does not interfere with TORC2, because a dominant active *ypk2* mutant (one of the major downstream components of the TORC2 pathway) did not rescue growth inhibition caused by AWR5 (Fig. S8a) and expression of the effector did not alter the actin cytoskeleton, a target of the TORC2 pathway (Fig. S8b).
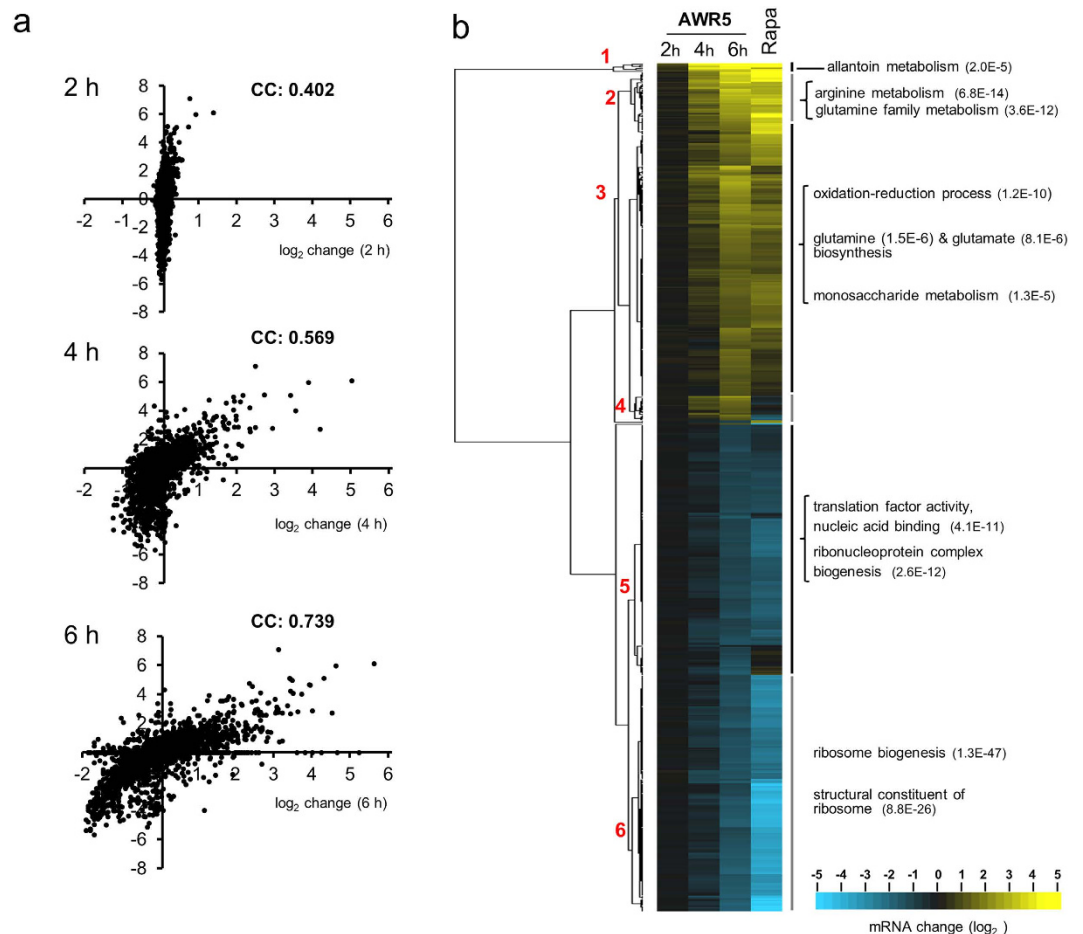
**Figure 2. Expression of bacterial *awr5* in yeast mimics the transcriptomic changes caused by inhibition of the TORC1 pathway.** (**a**) Changes in mRNA levels caused by expression of *awr5* (X-axis, log2 space) for the set of 2774 genes with valid data for all three time-points were plotted against the corresponding values after 1 h treatment with 200 ng/ml rapamycin (Y axis, log2 space). "CC" figures indicate the calculated correlation coefficient among both sets of data for each time-point. (**b**) The set of 596 genes presenting at least 2-fold changes in mRNA levels upon expression of *awr5* and with valid data for the rapamycin treatment were clustered (Euclidean distance, average linkage) using Cluster 3.0 software[57] and are represented with the Java Treeview software, version 1.1.6r4[58]. Numbers in red denote selected clusters referred to in the main text and number between parentheses designate the p-value for the indicated GO annotations.

In addition, AWR5 also did not co-immunoprecipitate with the Lst8, a shared component of TORC1 and TORC2[30] (Supplementary Fig. S7c).

To determine whether Cdc55 was required for downstream AWR5-mediated responses, we carried out a new transcriptomic analysis, in this case by direct sequencing of RNAs (RNA-seq) in wild type and *cdc55* cells expressing *awr5* for 6 h. Analysis of the wild type strain showed a response congruent with that observed previously using DNA microarrays, with a correlation coefficient of 0.63 in the genes detected as induced by both methodologies (Supplementary Fig. S9). In addition, among the top 25 most induced genes detected by microarray analysis, 13 were also ranked as such by RNA-seq. Comparison of the profiles of the wild type and the *cdc55* strains after 6 h of *awr5* induction showed that mutation in *CDC55* dramatically attenuated the transcriptomic effects caused by *awr5* expression. As illustrated in Fig. 5a, 512 genes were induced in the wild type strain upon *awr5* expression and only 212 in the *cdc55* strain (of which only 144 were also induced in wild type cells). This effect was particularly evident in repressed genes, since the *cdc55* mutation affected almost 90% of the genes repressed by *awr5* expression in the wild type strain. The attenuation of the transcriptional response to AWR5 could clearly be observed by plotting the 100 genes showing highest induction (Fig. 5b, upper panel) or repression (Fig. 5b, lower panel) in wild-type cells and comparing to their expression in *cdc55* cells.

It was apparent that many of the highly induced genes in response to AWR5 expression, which belong to the NCR and the mitochondrial retrograde pathways, decreased their expression in the absence of the regulatory subunit of PP2A. Indeed, 26 out of 28 NCR and *RTG* genes[31] ranking as top 100 induced decreased their expression more than 50% in *cdc55* cells. Similarly, a significant number of genes whose expression was decreased in response to AWR5 were clearly no longer repressed in *cdc55* cells. However, the effect was not homogeneous. For instance the transcripts showing little or no change in *awr5*-induced repression upon deletion of *CDC55* are
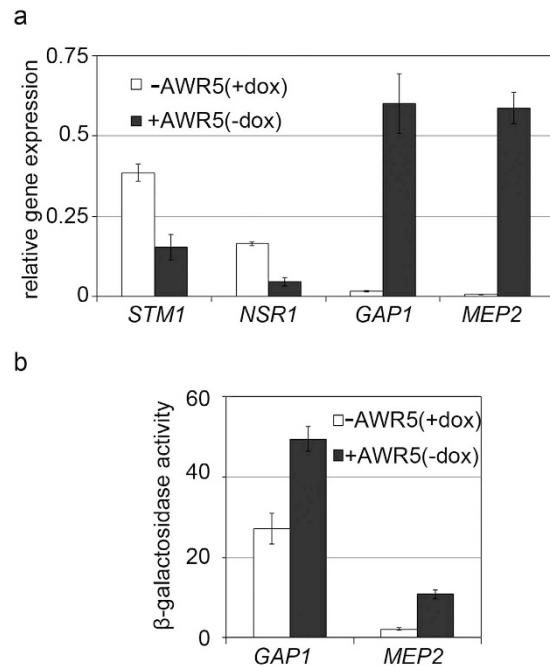
a



b



**Figure 3. Transcriptional response of TORC1-related genes to *awr5* expression.** (**a**) qRT-PCR experiments showing relative gene expression of TORC1 downstream targets. Gene expression of nitrogen catabolite repression (NCR)-sensitive *GAP1* and *MEP2* and ribosomal biogenesis *STM1* and *NSR1* genes was tested in yeast strains expressing *awr5* (+AWR5 (−dox)) 6 hours after induction. Error bars represent standard errors from 2 biological replicates. (**b**) β-galactosidase activities from yeast cells bearing *awr5*. Promoter activities of *GAP1* and *MEP2* were determined 6 hours after growth in SD-Ura+dox (−AWR5) and SD-Ura (+AWR5). Data represent the means and standard errors of 4 independent clones. All assays were repeated at least twice with similar results.

. . . . . . . . . . . . . . . . . . . . . . . . . . . . . . . . . . . . . . . . . . . . . . . . . . . . . . . . . . . . . . . . . . . . . . . . . . . . . . . . . . . . . . . . . . . . . . . . . . . . . . . . . . . . . . . . . . . . . . . .

largely enriched in genes involved in ribosome biogenesis and rRNA processing (Supplementary Fig. S10). This could be expected, as TOR-regulated expression of these genes is mostly PP2A-independent.

Taken together, these results indicate that the inability to form PP2A complexes containing Cdc55 not only neutralizes the severe growth defect caused by expression of *awr5*, but also substantially minimizes the transcriptional alterations derived from such expression. These data further supported the notion that the PP2A complex might mediate the phenotype caused by the AWR5 effector.

**awr5 expression constitutively activates autophagy.** It is known that TORC1 regulates autophagy in yeast via inhibition of the ATG1 complex (Fig. 1a and[32]). Our microarray data showed that expression of *awr5* increased the expression of diverse autophagy genes, such as *ATG8* or *ATG14,* which indicates activation of this process. In order to confirm whether autophagy was affected by *awr5* expression, autophagic flux was monitored in yeast cells constitutively expressing *GFP-ATG8* (Fig. 6). Proteolysis of GFP-ATG8 in the vacuole during autophagy results in the accumulation of the GFP moiety. Hence, detection of free GFP levels by western blot analysis can be used as readout of the autophagic rate[33]. Expression of *awr5* led to a dramatic accumulation of GFP in yeast cells, indicating an increased autophagic flux (Fig. 6a). As a control, we subjected yeast cells to nitrogen starvation, which resulted, as expected, in an increase of free GFP levels (Fig. 6b). Interestingly, free GFP levels in *awr5*-expressing cells relative to GFP-ATG8 were higher than in nitrogen-starved cells, indicating that AWR5 expression induces autophagy more potently than nitrogen starvation does. Next, we tested whether Cdc55 was involved in AWR5-triggered autophagy in yeast. Although GFP-ATG8 levels were slightly higher in *cdc55* mutant cells expressing *awr5*, autophagy was similarly induced in both strains (Fig. 6a). *awr5* expression was analysed and similar levels were detected in wild type and *cdc55* mutant cells (Fig. 6c). These findings indicated that AWR5-mediated autophagy induction occurs independently of Cdc55 in yeast.

**AWR5 alters the TOR pathway in plants.** Since heterologous expression of a T3E from *R. solanacearum* in yeast altered the TORC1 pathway, it was plausible that the effector had a similar effect in its natural context, i.e. when translocated inside the cells of plants infected by the pathogen. In plants, it has been shown that TOR silencing results in activation of nitrogen recycling activities and reduces primary nitrogen assimilation, measured by nitrate reductase activity[34]. In order to test whether *awr5* expression resulted in TOR inhibition in plants we thus used this activity as readout. Transient expression of *awr5* in *Nicotiana benthamiana* leaves resulted in a significant reduction of nitrate reductase activity compared to the control (GUS) (Fig. 7a). Leaky expression of *awr5* prior to induction may account for the slightly lower nitrate reductase activity values in leaves transformed with *awr5*. *awr5* expression did not significantly affect the activity of the TOR-independent, constitutive enzyme
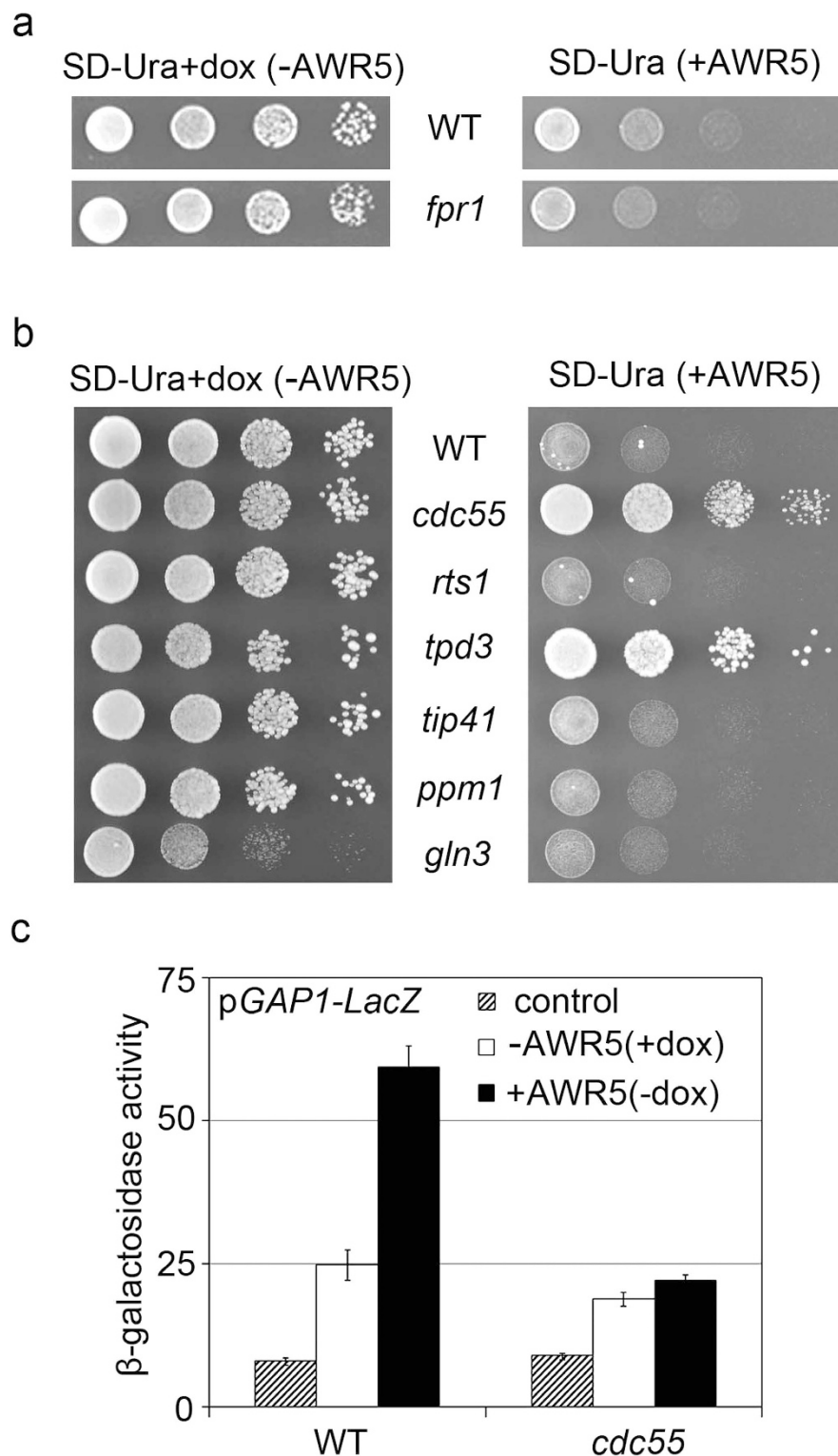
**Figure 4. cdc55 and tpd3 mutations affecting PP2A protein phosphatase activity suppress AWR5-induced yeast growth inhibition.** (**a**) Growth on solid medium of control (WT) and an *fpr1* mutant carrying *awr5* under the control of a Tet-Off promoter. Serial 10-fold dilutions were spotted onto solid SD-Ura+doxycycline (−AWR5) and SD-Ura (+AWR5). (**b**) Growth on solid medium of control (WT) and TORC1-related yeast mutants containing plasmid carrying *awr5*. Serial 10-fold dilutions were spotted onto solid SD-Ura+ doxycycline (−AWR5) and SD-Ura (+AWR5). Photographs were taken after 3 days of growth. (**c**) *GAP1* promoter activity from plasmid *pGAP1-LacZ* in wild-type (WT) and mutant *cdc55* yeast cells bearing *awr5* or a control gene (*GFP*). β-galactosidase activity was measured 6 hours after growth in SD-Ura+dox (−AWR5) and SD-Ura (+AWR5). Values represent the means and standard errors of 4 independent clones. All experiments were performed three times with similar results.
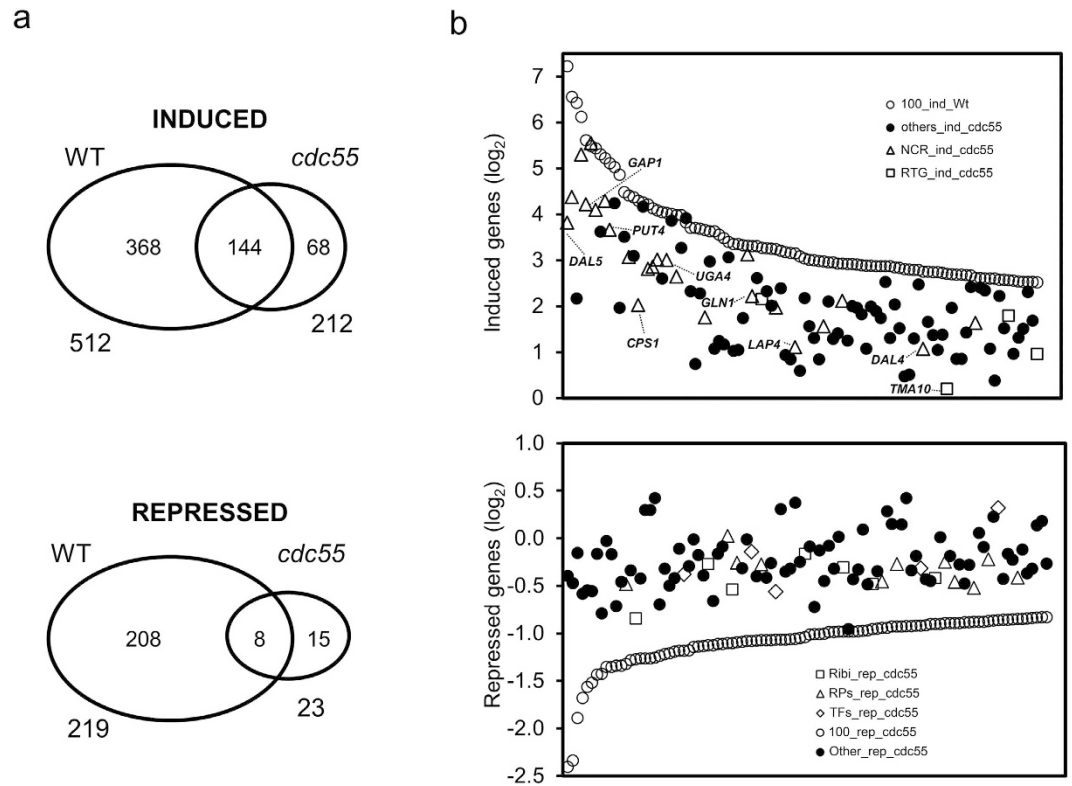
**Figure 5. Mutation of *CDC55* greatly attenuates AWR5 impact on the yeast transcriptional profile.** (**a**) Venn diagram showing the number of genes whose expression was considered to be induced (top) or repressed (bottom) by expression of AWR5 in wild-type and *cdc55* cells for a set of 5732 genes with valid data for both strains. (**b**) Plots of the log2 values for the changes in the level of expression induced by expression of AWR5 in both wild-type (open circles) and *cdc55* strains for the 100 most upregulated (top) and 100 most downregulated (bottom) genes in the wild-type strain (open circles). Symbols for the expression values for the *cdc55* strain are depicted as follows. For the induced genes: open triangles, the NCR family, as defined previously[25]; the RTG group (open squares) comprises the genes described as documented targets for the Rtg1 or Rtg3 transcription factors as defined in[59]. Genes not included in these categories are designated as "others" (closed circles). The genes downregulated in the wild-type strain are classified into one of three possible families: Ribi regulon (open squares), ribosomal proteins (open triangles), protein translation (open diamonds), and others (closed circles), as defined in[59].

glucose-6-phosphate dehydrogenase (Fig. 7b). This clearly indicates that the decrease in the TOR- dependent nitrate reductase activity is specifically caused by *awr5* expression in plants.

The mechanisms by which AWR5 alters the TOR pathway in plants remains to be determined. Transient expression of *awr5* did not result in autophagy induction in *N. benthamiana* leaves expressing the autophagy marker GFP:ATG8a (Supplementary Fig. S11a). In addition, we could not detect direct interaction between AWR5 and TOR1 by co-immunoprecipitation using *N. benthamiana* leaves transiently over-expressing tagged versions of the two proteins (Supplementary Fig. S11b).

To further prove that AWR5 impacts the plant TOR pathway we infected *Arabidopsis thaliana* wild-type Col-0 plants, TOR1-silenced plants (*TOR* RNAi)[35] and two mutant lines disrupted in the genes encoding either of the *CDC55* homologues (*b55α* and *b55β*)[36] with *R. solanacearum* and recorded the appearance of wilting symptoms over time. TOR1-silenced lines were slightly more resistant to bacterial infection (Fig. 7c) and the two lines mutated in the *CDC55* homologues showed a striking resistance to infection as compared to the wild-type *Arabidopsis* (Fig. 7d), indicating that AWR5 effector may be targeting the TOR pathway in both plants and yeast. Although TOR RNAi lines have been previously reported to be slightly reduced in growth compared[35], in our growing conditions both TOR RNAi and b55 mutants were indistinguishable from wild-type plants (Fig. S12), ruling out the possibility that their altered response to *R. solanacearum* infection was due to reduced surface of interaction.

## Discussion

In this work, we have produced *R. solanacearum* AWR effectors in yeast and have found that AWR5 impacts the TORC1 pathway, an essential component of eukaryotic cells. The premise for using *Saccharomyces cerevisiae* was that this organism carries out most eukaryotic processes and, unlike the host cells where T3E are naturally injected, it shows less gene redundancy and lacks resistance components that counteract and mask effector
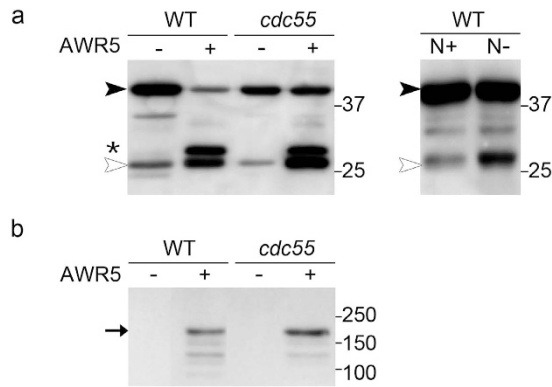
**Figure 6. a*wr5* expression induces constitutive autophagy, independently of Cdc55-PP2A activity. (a)** Immunodetection of GFP-ATG8 processing in wild-type and mutant *cdc55* yeast strains expressing *awr5*. Wild-type (WT) and mutant *cdc55* yeast cells bearing *awr5* gene were grown in SD-Ura+dox (−AWR5) and SD-Ura (+AWR5). Total protein extracts were immunoblotted using anti-GFP antibody. The black and the empty arrowhead indicate, respectively, GFP-ATG8 fusion protein and cleaved GFP. The asterisk denotes a degradation product of AWR5-GFP protein. (**b**) Wild-type cells carrying GFP-ATG8 grown in nitrogen-rich (N+) or nitrogen-depleted (N−) medium were used as a control of GFP-ATG8 processing and induction of autophagy in N− conditions. (**c**) AWR5 protein levels in wild-type and mutant *cdc55* yeast cells. Total protein was extracted and immunoblotted using anti-GFP antibody. The black arrow indicates AWR5-GFP protein. All experiments were performed at least three times, with similar results.
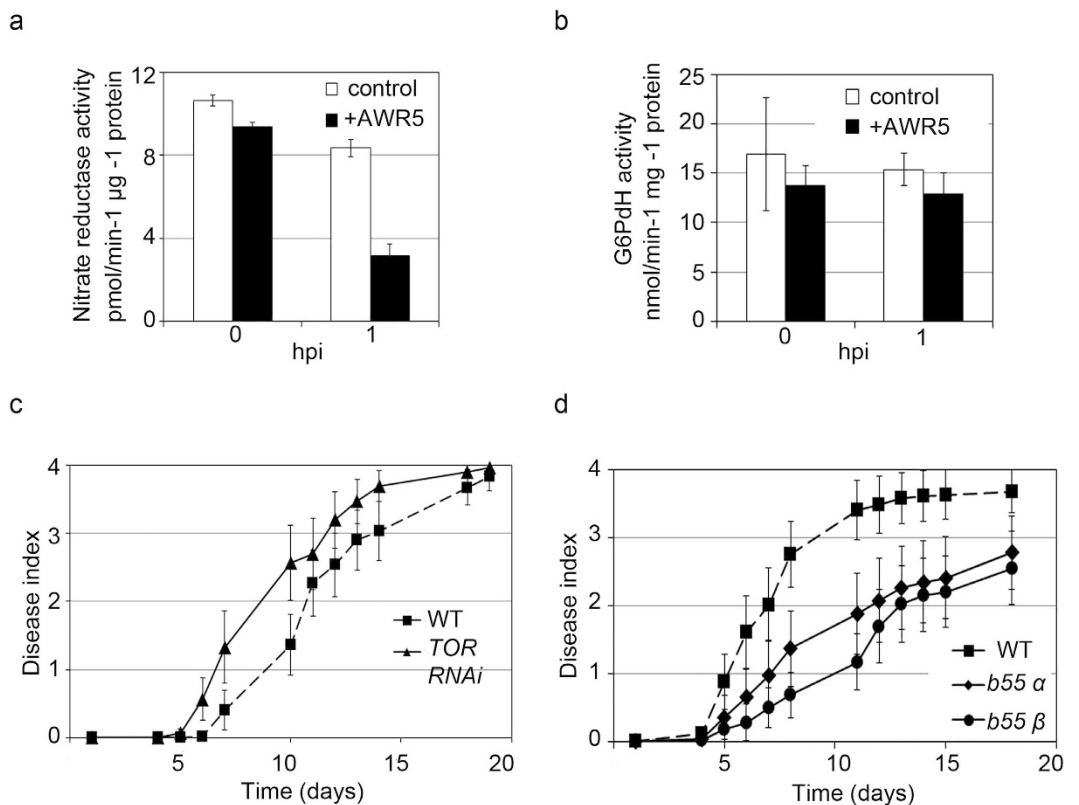


**Figure 7. Interplay between AWR5 and TOR *in planta*.** Effect of *awr5* transient expression on (**a**) nitrate reductase (NR) activity or (**b**) glucose-6-phosphate dehydrogenase (G6PdH) in *Nicotiana benthamiana*. Full leaves of *N. benthamiana* were agroinfiltrated with constructs bearing *awr5* or a control gene (*GUS*). Total protein extracts were used to determine NR and G6PdH activity at 0 and 1 hours post-estradiol induction (hpi). Error bars indicate standard errors of 2 biological replicates for NR and 3 for G6PdH. TOR (**c**) and its signalling component B55 (**d**) are involved in plant defence responses against *R. solanacearum* invasion. Five-week old plants grown in Jiffy pots were inoculated with *R. solanacearum* GMI1000 at an $OD_{600} = 0.1$ and wilting symptoms were recorded over time according to a disease index scale (0: no wilting, 1: 25% wilted leaves, 2: 50%, 3: 75%, 4: death). The experiment was repeated twice using at least 20 plants in each. Error bars indicate standard errors.

function[37]. For instance, gain-of-function analyses of T3E in plants are often hampered by a hypersensitive response (HR), a programmed cell death associated with recognition of effectors or effector virulence activities[38].

A number of studies have successfully used *S. cerevisiae* as a model to identify T3E targets[8,13]. Toxicity -ranging from growth arrest to cell death- is the most common phenotype observed in these studies. However, this is not a widespread phenomenon when *R. solanacearum* T3E are expressed in yeast, as only 6 out of 36 effectors representing the repertoire of strain GMI1000 caused substantial growth inhibition (this work and[39]). Interestingly, four out of the six toxic T3E encode AWR proteins, suggesting a distinct function for this effector family in bacterial-host interactions. Cell growth inhibition caused by T3E has been traced back to interference on vesicle trafficking, disruption of the cytoskeleton or MAP Kinase alteration[8], providing important clues on T3E function. In the case of AWR5, we show that it targets a novel cellular process, namely, the TORC1 pathway.

As mentioned above, the TORC1 protein complex regulates the transition between growth and quiescence in response to nutrient status and can be inhibited by rapamycin. TORC1 acts by controlling three major cell components: the kinase Sch9, Tap42, its associated phosphatases and the ATG1 complex[14,15]. Active TORC1 directly phosphorylates Sch9 -the orthologue of the mammalian S6 kinase-, which induces RiBi genes, such as *STM1* and *NSR1*, to increase translation and promote growth (Fig. 1a). In addition, when TORC1 is active, the essential downstream regulatory protein, Tap42, is phosphorylated and associates with the catalytic subunits of the PP2A and PP2A-like phosphatases, which are retained in membranes interacting with TORC1[14]. Finally, active TORC1 can inhibit autophagy by phosphorylation of ATG13, which prevents association with the ATG1 kinase and subsequent autophagy induction[32]. On the contrary, when TORC1 is inactivated by rapamycin treatment or nitrogen starvation, Tap42 and the PP2A and PP2A-like phosphatases are released to the cytosol and activated, allowing expression of stress genes and NCR genes such as *GAP1* and *MEP2*[15] (Fig. 1a). This gene reprogramming takes place through PP2A-mediated inhibition of nuclear export of the Msn2/4 factors and PP2A/Sit4-mediated dephosphorylation and subsequent translocation of Gln3 to the nucleus. Our gene expression analyses and biochemical characterizations showed that the bacterial effector AWR5 interferes with the TORC1-regulated pathways, repressing ribosome biogenesis and translation and activating autophagy and stress responses. Activation of the latter, which are incompatible with growth, could explain the dramatic growth defects triggered by AWR5 in yeast. Our findings that mutants in two PP2A subunits (*cdc55* and *tpd3*) totally rescued this phenotype strongly support that AWR5 impacts TORC1-regulated pathways in eukaryotic cells.

As mentioned before, most TORC1-controlled effects occur through two major effector branches, mediated by the Sch9 kinase and by complexes of Tap42 and the phosphatases (mainly PP2A and Sit4). The wide transcriptomic impact of AWR5 on all TORC1-controlled pathways, mimicking the effect of rapamycin or nitrogen starvation, could be explained by assuming that AWR5 targets multiple hits downstream the pathway. Along this line, downstream components of the TOR pathway have already been involved in plant defense: PP2A was found to negatively regulate pathogen perception[40] and PP1A is targeted by a *Phytophtora infestans* effector[41,42]. However, the most likely scenario is that AWR5 would target a few or even a single target controlling all these processes. If this were the case, AWR5 would exert its function inhibiting TORC1 upstream of PP2A, thus causing Sch9 inhibition, autophagy activation and the release of Tap42 and PP2A phosphatase subunits. The notion of a single target is reinforced by the fact that only a limited number of T3E molecules are injected into the host cell to exert their function. Along this line, leaky expression of *awr5* from a tet-off promoter in the presence of the repressor doxycycline had a detectable effect on yeast growth.

The observation that deletion of genes encoding two components of the PP2A heterotrimeric forms, *CDC55* and *TPD3*, abolishes the dramatic growth defect of cells expressing *awr5* suggests that in spite of the wide transcriptional effect caused by *awr5* expression, the major reason for AWR5 toxicity lies downstream PP2A and indicates that the formation of this heterotrimer is essential for the negative effect of AWR5 to take place. In this regard, it is worth noting that deletion of *TPD3* and of *CDC55* yields yeast cells resistant to rapamycin, whereas that of *RTS1* does not. Moreover, it has been proposed that an active TORC1 pathway promotes the association of Tap42 with PP2A catalytic subunits Pph21/22 to form complexes necessary for sustaining cell growth, whereas Cdc55 and Tpd3 would inhibit such association[43]. Although our study does not allow pointing to a specific TOR-regulated event to explain the inhibitory effect of AWR5, the observation that deletion of *CDC55* only normalizes the expression of specific subsets of genes altered by *awr5* expression (i.e. NCR genes but not ribosomal protein encoding genes) or the fact that AWR5-mediated autophagy promotion was not dependent on Cdc55 contribute to narrow the possible candidates.

Interestingly, during the course of this work, the *cdc55* mutant has been also isolated in a screen for suppressors of the yeast growth inhibition caused by the *Erwinia amylovora* T3E DspA[12]. This could suggest that the PP2A phosphatase has evolved as a cellular hub, targeted by different pathogens to interfere with plant host cell homeostasis. However, DspA caused a specific alteration of the yeast sphingolipid biosynthesis, showing no overlap with AWR5-triggered phenotypes other than the Cdc55-dependent growth inhibition. In addition, AWR5 still caused its toxicity on strains with mutations in the small GTPase *rho2* and in the sphingolipid biosynthesis gene *sur1* (data not shown), which strongly supressed DspA-triggered growth defects[12]. All these data support a different mode of action for these T3Es, only sharing Cdc55 as an intermediate in signal transduction.

TOR functions are conserved across kingdoms; in plants TOR is also a master regulator of the cell, controlling the switch between stress and growth[44,45]. Our data clearly supports the idea that AWR5 alters the TOR pathway in plants.

First, *awr5* expression *in planta* results in nitrate reductase activity inhibition. This enzyme has a central role in nitrogen metabolism and its inhibition has been previously linked to TOR deficiency and activated nitrogen recycling[34]. Noteworthy, even a minimal escape in *awr5* expression visibly impacted plant nitrate reductase activity, similar to the yeast growth inhibition caused by leaky expression of *awr5*. This strengthens the notion of a conserved AWR5 function as an extremely efficient modulator of the TOR pathway in disparate eukaryotic contexts. Second, TOR-deficient plants were more susceptible to *R. solanacearum* infection and plants lacking the *CDC55*

homologues *B55α* or *B55β*, showed enhanced resistance to the pathogen. These opposite results are expected if the bacterium inhibits TOR signalling, as the B55 activity is repressed by TOR, and demonstrate a novel role for the TOR complex in plant defence.

In the context of *Ralstonia solanacearum* infection it remains a mystery why a bacterial T3E would mimic the effect of nitrogen starvation on infected tissues. Interestingly, there are several instances in the literature showing modulation of the host metabolism by T3Es. For example, the *R. solanacearum* effector RipTPS was shown to possess trehalose-6-phosphate synthase activity[46] and the effector WtsE from *Pantoea stewartii* was shown to alter phenylpropanoid metabolism[47].

Furthermore, group A *Streptococcus* enhances its growth by activation of asparagine metabolism via ER stress induction in mammalian cells[48]. Since ER stress responses are intimately connected with TOR signalling[49], it is tempting to speculate that AWR5 modulates the TOR pathway to induce ER stress responses and stimulate growth by an analogous mechanism to the one proposed in *Streptococcus*. On an alternative hypothetic scenario, AWR5-mediated inhibition of TOR (nitrogen recycling, autophagy, inhibition of protein synthesis…) would be beneficial for the bacterium during the last stages of infection, as it would facilitate plant cell dismissal and consequently nutrient availability.

## Methods

**Plasmids, strains and gene cloning.** All strains and plasmids used in this study are described in Supplementary Table S1. For heterologous expression of *awr*s under the control of the galactose inducible promoter (*GAL1*), expression vectors were constructed by recombining entry clones carrying each of the *awr* ORFs into the Gateway destination vector pAG426GAL-ccdb-HA[50] through a Gateway LR reaction (Invitrogen, Waltham, Massachusetts, USA). For expression of *awr5* fragments in yeast, N-terminal (1368 bp) and C-terminal (1821 bp) halves of *awr5* as well as a central (1425 bp) fragment overlapping them were amplified from genomic DNA.

For integration of the *awr* genes fused to a C-terminal GFP tag at the locus of *URA3* gene in the yeast chromosome, each of them was cloned by Gateway recombination or ligation into the integrative vector pYI-GWY, a *URA3* plasmid in which the heterologous genes are under the control of a Tet-off promoter created in this study. Following linearization with *Bst*BI that cuts inside in *URA3* cassette, pYI-GWY derivatives carrying genes *awr1* to *awr5* were integrated into the yeast chromosome by double recombination into the *URA3* locus in yeast. To this end, the wild type strain JA-100 containing a *ura3* point mutation was used as recipient, giving rise to uracyl autotrophs after *awr* integration. For expression of *awr5* gene in the *cdc55Δ* mutant yeast strain, cloning was performed in two steps. Firstly, a *cdc55::KanMX4* cassette from the *cdc55Δ* strain in the BY4741 background was amplified and subsequently introduced into the genome of strain JA-100. Secondly, the *awr5* gene fused to the C-terminal GFP was integrated into the newly constructed *cdc55* strain as described above.

**Yeast strains and growth conditions.** For expression of *awrs* or their fragments under the control of the galactose promoter, yeast cells were grown for 2 days in SD-Ura + raffinose 2%, then diluted to optical density at 600 nm of 0.4 in water and plated either in repressing media (glucose) or inducing media (galactose) to monitor the effects of AWRs in cell growth/viability. For standard growth inhibition experiments on plates, strains were incubated overnight with shaking in selective medium with doxycycline 20 μg/ml. Cultures were then normalized to $OD_{600} = 0.1$–0.2 and grown until exponential phase. 1 $OD_{600}$ of cells were then harvested, washed 2 times with sterile water, re-suspended in 1 ml water and 10-fold serially diluted in water four times. Each suspension (5 or 10 μl) was dropped either in non-inducing media (+doxycycline) or inducing media (no doxycycline) onto agar plates and then incubated for 2–3 days before photographs were taken.

To test growth viability in liquid media over time and for sample harvesting for RNA isolation, yeast strains were grown overnight in rich YPD medium with doxycycline 15 μg/ml (repressing conditions), then normalized to $OD_{600} = 0.05$ and grown for 2, 4, 6 or 8 hours in YPD+dox (non-inducing conditions) and YPD (inducing conditions). Similar growth conditions were carried out for protein extraction and beta-galactosidase assays, using selective medium in this case. To test viability of yeast cells expressing *awr5* after doxycycline addition, strains were grown overnight in either SD-Ura+dox (non-inducing conditions) or SD-Ura (inducing). Cells were recovered and normalized to $OD_{600} = 0.05$ and grown in liquid in SD-Ura+dox. Samples were harvested at different time points, serially 10-fold diluted and plated onto solid SD-Ura+dox and incubated for 2 days at 28 °C until colonies were counted.

For methylene blue staining, yeast cells carrying *awr5* were harvested at 6 hours after induction and stained for 5 minutes with a 0.01% methylene blue solution in glycine buffer. In parallel, the same cells were fixed with formaldehyde 37% for 10 mins before methylene blue addition as a positive staining control. Images were obtained using a Dapi 395–440/FT 460/LP470 filterset.

To measure yeast cell size, wild-type yeast strains (JA-100) and strains bearing *awr5* were grown overnight in YPD medium with and without doxycycline (15 μg/ml). The next day, cultures were normalized to $OD_{600} = 0.05$ and grown in liquid either in YPD+dox or YPD during 6 and 8 hours. Cells were analyzed with a Scepter Handheld Automated Cell Counter (Merck Millipore, Darmstadt, Germany).

To measure induction of autophagy, wild-type and *cdc55Δ* strains carrying *awr5* and ATG8-GFP were grown overnight in selective media plus doxycycline. Cultures were then normalized to an $OD_{600} = 0.2$, grown until exponential phase, normalized again to $OD_{600} = 0.05$ and finally grown overnight with or without doxycycline until samples were harvested. For autophagy induction after nitrogen starvation JA-100 cells were grown overnight in SD medium without ammonium sulfate (BD Difco, Franklin Lakes, NJ, USA) and 2% glucose.

**DNA microarray analysis.** Aliquots of the same samples harvested to test viability of cells expressing *awr5* in liquid media at 2, 4 and 6 hours after induction were used for microarray analysis. For microarray

hybridization, total RNA (8 μg) was employed for cDNA synthesis and labelling using the indirect labelling kit (CyScribe Post-Labeling kit; GE Healthcare, Wauwatosa, WI, USA) with Cy3–dUTP and Cy5–dUTP fluorescent nucleotides. The cDNA obtained was dried, re-suspended in hybridization buffer and evaluated with a Nanodrop spectrophotometer (Nanodrop Technologies, Thermo Scientific, Waltham, MA, USA). The combined fluorescently labelled cDNAs were hybridized to yeast genomic microchips constructed in our laboratory by arraying 6014 different PCR-amplified open reading frames from *S. cerevisiae*[51]. Microarrays were processed as described previously[52], scanned with a ScanArray 4000 apparatus (Packard BioChip Technologies, Perkin Elmer, Waltham, MA, USA) and the output was analysed using GenePix Pro 6.0 software. Data collected from 2 biological replicates (two microarrays each, with dye swap) after 2, 4 and 6 h of doxycycline removal (thus triggering expression of *awr5*) were combined. Genes were considered induced or repressed by AWR5 expression when the minus/plus doxycycline ratio was ≥2.0 or ≤0.5, respectively, for both biological replicates. All data has been added to the Gene Expression Omnibus (GEO) database under numbers GSE70202, GSE70331 and GSE70835.

**qRT-PCR.** Two independent biological replicas of the strain carrying *awr5* grown in inducing and non-inducing conditions were harvested at 4 and 6 hours after induction and subjected to RNA extraction to quantify *awr5* mRNA levels, whereas of *GAP1, MEP2, STM1* and *NSR1* levels were only tested from samples obtained 6 h after induction. For quantitative real-time PCR, a Light Cycler 480 (Roche, Basel, Switzerland) with SYBR Green chemistry was used with three technical replicas. Actin was used as a housekeeping gene to normalize samples.

**RNA-seq experiments.** Libraries were prepared with the QuantSeq 3′ mRNA kit (Lexogen, Greenland, NH, USA) using 0.5 μg of total RNA purified as above. Sequencing was performed in an Illumina MiSeq machine with Reagent Kit v3 (single end, 80–125 nt/read). Two biological replicates were sequenced, obtaining a total number of 8.4–12.9 million reads per condition. Mapping of fastq files to generate SAM files was carried out with the Bowtie2 software[53] in local mode (95.1–97.3% mapped reads). The SAM files were analyzed with the SeqMonk software (www.bioinformatics.bbsrc.ac.uk/projects/seqmonk). Mapped reads were counted using CDS probes (extended 100 nt downstream the open reading frame because the library is biased towards the 3′-end of mRNAs) and corrected for the largest dataset. Raw data was subjected to diverse filters to remove sequences with a low number of reads.

**Protein assays.** For immunoblots, 30 or 40 $OD_{600}$ units from overnight yeast cultures grown in non-inducing or inducing conditions were were resuspended in 500 μl of extraction buffer (50 mM Tris-HCl pH7.5, 1 mM EDTA, 0.1% Nonidet P-40, 1% glycerol, with complete protease inhibitor (Roche, Basel, Switzerland) and subjected to 10 cycles of 1 minute sonication and 1 minute pauses. Supernatants were recovered after centrifugation at 500 g for 10 min at 4 °C. 125 μg of total protein extracts were separated on polyacrylamide gels and immunoblot was performed using anti-GFP mouse monoclonal antibody (clone B-2; Santa Cruz Biotechnology, Dallas, TX, USA).

Beta-galactosidase activity was measured from, 2 ml of cultures pelleted 6 hours after induction as described[54].

**Plant material.** Wild type (Wt) Columbia 0, TOR-silenced 35-7 (*TOR* RNAi)[35], *b55α* and *b55β Arabidopsis* mutant lines[36] were used. 3 to 4-week-old *N. benthamiana* plants were used for transient expression experiments.

**Enzymatic activity determinations.** To measure nitrate reductase activity, *N. benthamiana* plants were treated two times a week with 2mM-15mM $KNO_3$, then, transient *Agrobacterium*-mediated transformation was performed as previously described[20] using the estradiol-inducible vector pMDC7 carrying AWR5 or GUS. Protein expression was induced by painting the leaves 14 hours post-agrobacterium infiltration with 20 μM estradiol and Silwet L-77 adjuvant. Whole leaves (1 g) were harvested at 0 and 1 hour after post-estradiol induction and homogenized in 3 ml of 0.1 M HEPES-KOH, pH 7.5, 3% polyvinylpolypyrrolidone, 1 mM EDTA and 10 mM cysteine. The extracts were filtered through four layers of Miracloth (Merk Millipore, Billerica, USA) and centrifuged for 15 minutes at 30,000 × g at 4 °C and nitrate reductase activity measured as described in[55].

To measure glucose-6-phosphate dehydrogenase activity *N. benthamiana* leaves were transiently transformed as previously described[20] using the estradiol-inducible vector pMDC7 carrying AWR5 or GUS. Protein expression was induced by painting the leaves with 20 μM estradiol and Silwet L-77 adjuvant 14 hours post-agrobacterium infiltration. Half-leaves (500 mg) were harvested at 0 and 1 hour after post-estradiol induction and homogenized in 500 μl of 20 mM imidazol, pH 7. The extracts were centrifuged 15 minutes at 1000 × g at 4 °C and the supernatant was transferred to a new tube and kept on ice. To determine the activity of glucose-6-phosphate dehydrogenase activity 170 μl of 2x assay buffer (0.1 M imidazol, 0.2 M KCl, 20 mM MgCl2, 2 mM EDTA), 131 μl $H_2O$, 7 μl of 10 mM NADP and 25 μl of cell-free extract were sequentially added to a spectrophotometer cuvette and the $A_{340}$ was monitored for a few minutes until stabilization. Then 7 μl of 50 mM glucose-6-phosphate were added and the $A_{340}$ was recorded, as a measure of Glucose-6-phosphate dehydrogenase activity (expressed as nmoles $min^{-1}$ $mg^{-1}$ protein).

**Pathogenicity assays.** *R. solanacearum* pathogenicity tests were carried out using the soil-drench method as described[56].

# References
1. Charro, N. & Mota, L. J. Approaches targeting the type III secretion system to treat or prevent bacterial infections. *Expert Opin Drug Discov* **10**, 373–387, doi: 10.1517/17460441.2015.1019860 (2015).
2. Macho, A. P. & Zipfel, C. Targeting of plant pattern recognition receptor-triggered immunity by bacterial type-III secretion system effectors. *Curr Opin Microbiol* **23**, 14–22, doi: 10.1016/j.mib.2014.10.009 (2015).

3. Dean, P. Functional domains and motifs of bacterial type III effector proteins and their roles in infection. *FEMS Microbiol Rev* **35,** 1100–1125, doi: 10.1111/j.1574-6976.2011.00271.x (2011).
4. Boch, J., Bonas, U. & Lahaye, T. TAL effectors–pathogen strategies and plant resistance engineering. *New Phytol* **204,** 823–832 (2014).
5. Boyle, P. C. & Martin, G. B. Greasy tactics in the plant-pathogen molecular arms race. *J Exp Bot* **66,** 1607–1616, doi: 10.1093/jxb/erv059 (2015).
6. Deslandes, L. & Rivas, S. Catch me if you can: bacterial effectors and plant targets. *Trends Plant Sci* **17,** 644–655, doi: 10.1016/j.tplants.2012.06.011 (2012).
7. Marin, M. & Ott, T. Intrinsic disorder in plant proteins and phytopathogenic bacterial effectors. *Chem Rev* **114,** 6912–6932, doi: 10.1021/cr400488d (2014).
8. Popa, C., Coll, N. S., Valls, M. & Sessa, G. Yeast as a Heterologous Model System to Uncover Type III Effector Function. *PLoS pathogens* **12,** e1005360, doi: 10.1371/journal.ppat.1005360 (2016).
9. Von Pawel-Rammingen, U. *et al.* GAP activity of the Yersinia YopE cytotoxin specifically targets the Rho pathway: a mechanism for disruption of actin microfilament structure. *Mol Microbiol* **36,** 737–748 (2000).
10. Munkvold, K. R., Martin, M. E., Bronstein, P. A. & Collmer, A. A survey of the Pseudomonas syringae pv. tomato DC3000 type III secretion system effector repertoire reveals several effectors that are deleterious when expressed in Saccharomyces cerevisiae. *Mol Plant Microbe Interact* **21,** 490–502 (2008).
11. Salomon, D., Bosis, E., Dar, D., Nachman, I. & Sessa, G. Expression of Pseudomonas syringae type III effectors in yeast under stress conditions reveals that HopX1 attenuates activation of the high osmolarity glycerol MAP kinase pathway. *Microbiology* **158,** 2859–2869, doi: 10.1099/mic.0.062513-0 (2012).
12. Siamer, S. *et al.* Expression of the bacterial type III effector DspA/E in Saccharomyces cerevisiae down-regulates the sphingolipid biosynthetic pathway leading to growth arrest. *The Journal of biological chemistry* **289,** 18466–18477, doi: 10.1074/jbc.M114.562769 (2014).
13. Curak, J., Rohde, J. & Stagljar, I. Yeast as a tool to study bacterial effectors. *Curr Opin Microbiol* **12,** 18–23 (2009).
14. Eltschinger, S. & Loewith, R. TOR Complexes and the Maintenance of Cellular Homeostasis. *Trends Cell Biol* **26,** 148–159, doi: 10.1016/j.tcb.2015.10.003 (2016).
15. Conrad, M. *et al.* Nutrient sensing and signaling in the yeast Saccharomyces cerevisiae. *FEMS Microbiol Rev* **38,** 254–299, doi: 10.1111/1574-6976.12065 (2014).
16. Coll, N. S. & Valls, M. Current knowledge on the Ralstonia solanacearum type III secretion system. *Microb Biotechnol* **6,** 614–620, doi: 10.1111/1751-7915.12056 (2013).
17. Peeters, N., Guidot, A., Vailleau, F. & Valls, M. Ralstonia solanacearum, a widespread bacterial plant pathogen in the post-genomic era. *Mol Plant Pathol* **14,** 651–662, doi: 10.1111/mpp.12038 (2013).
18. Mansfield, J. *et al.* Top 10 plant pathogenic bacteria in molecular plant pathology. *Mol Plant Pathol* **13,** 614–629, doi: 10.1111/j.1364-3703.2012.00804.x (2012).
19. Salanoubat, M. *et al.* Genome sequence of the plant pathogen Ralstonia solanacearum. *Nature* **415,** 497–502, doi: 10.1038/415497a (2002).
20. Sole, M. *et al.* The awr gene family encodes a novel class of Ralstonia solanacearum type III effectors displaying virulence and avirulence activities. *Mol Plant Microbe Interact* **25,** 941–953, doi: 10.1094/MPMI-12-11-0321 (2012).
21. Song, C. & Yang, B. Mutagenesis of 18 type III effectors reveals virulence function of XopZ(PXO99) in Xanthomonas oryzae pv. oryzae. *Mol Plant Microbe Interact* **23,** 893–902, doi: 10.1094/MPMI-23-7-0893 (2010).
22. Cunnac, S., Occhialini, A., Barberis, P., Boucher, C. & Genin, S. Inventory and functional analysis of the large Hrp regulon in Ralstonia solanacearum: identification of novel effector proteins translocated to plant host cells through the type III secretion system. *Mol Microbiol* **53,** 115–128, doi: 10.1111/j.1365-2958.2004.04118.x (2004).
23. Mukaihara, T., Tamura, N. & Iwabuchi, M. Genome-wide identification of a large repertoire of Ralstonia solanacearum type III effector proteins by a new functional screen. *Mol Plant Microbe Interact* **23,** 251–262, doi: 10.1094/MPMI-23-3-0251 (2010).
24. Pensec, F. *et al.* Towards the identification of Type III effectors associated to Ralstonia solanacearum virulence on tomato and eggplant. *Phytopathology*, doi: 10.1094/PHYTO-06-15-0140-R (2015).
25. Godard, P. *et al.* Effect of 21 different nitrogen sources on global gene expression in the yeast Saccharomyces cerevisiae. *Mol Cell Biol* **27,** 3065–3086, doi: 10.1128/MCB.01084-06 (2007).
26. Gonzalez, A., Casado, C., Arino, J. & Casamayor, A. Ptc6 is required for proper rapamycin-induced down-regulation of the genes coding for ribosomal and rRNA processing proteins in S. cerevisiae. *PLoS One* **8,** e64470, doi: 10.1371/journal.pone.0064470 (2013).
27. Homma, T., Iwahashi, H. & Komatsu, Y. Yeast gene expression during growth at low temperature. *Cryobiology* **46,** 230–237 (2003).
28. Van Dyke, N., Chanchorn, E. & Van Dyke, M. W. The Saccharomyces cerevisiae protein Stm1p facilitates ribosome preservation during quiescence. *Biochem Biophys Res Commun* **430,** 745–750, doi: 10.1016/j.bbrc.2012.11.078 (2013).
29. Conway, M. K., Grunwald, D. & Heideman, W. Glucose, nitrogen, and phosphate repletion in Saccharomyces cerevisiae: common transcriptional responses to different nutrient signals. *G3 (Bethesda)* **2,** 1003–1017, doi: 10.1534/g3.112.002808 (2012).
30. Maegawa, K., Takii, R., Ushimaru, T. & Kozaki, A. Evolutionary conservation of TORC1 components, TOR, Raptor, and LST8, between rice and yeast. *Mol Genet Genomics* **290,** 2019–2030, doi: 10.1007/s00438-015-1056-0 (2015).
31. Dilova, I., Chen, C. Y. & Powers, T. Mks1 in concert with TOR signaling negatively regulates RTG target gene expression in S. cerevisiae. *Curr Biol* **12,** 389–395 (2002).
32. Kamada, Y. *et al.* Tor directly controls the Atg1 kinase complex to regulate autophagy. *Mol Cell Biol* **30,** 1049–1058, doi: 10.1128/MCB.01344-09 (2010).
33. Cheong, H. & Klionsky, D. J. Biochemical methods to monitor autophagy-related processes in yeast. *Methods Enzymol* **451,** 1–26, doi: 10.1016/S0076-6879(08)03201-1 (2008).
34. Ahn, C. S., Han, J. A., Lee, H. S., Lee, S. & Pai, H. S. The PP2A regulatory subunit Tap46, a component of the TOR signaling pathway, modulates growth and metabolism in plants. *Plant Cell* **23,** 185–209, doi: 10.1105/tpc.110.074005 (2011).
35. Deprost, D. *et al.* The Arabidopsis TOR kinase links plant growth, yield, stress resistance and mRNA translation. *EMBO Rep* **8,** 864–870, doi: 10.1038/sj.embor.7401043 (2007).
36. Heidari, B. *et al.* Protein phosphatase 2A B55 and A regulatory subunits interact with nitrate reductase and are essential for nitrate reductase activation. *Plant Physiol* **156,** 165–172, doi: 10.1104/pp.111.172734 (2011).
37. Costanzo, M. *et al.* The genetic landscape of a cell. *Science* **327,** 425–431, doi: 10.1126/science.1180823 (2010).
38. Coll, N. S., Epple, P. & Dangl, J. L. Programmed cell death in the plant immune system. *Cell Death Differ* **18,** 1247–1256, doi: 10.1038/cdd.2011.37 (2011).
39. Fujiwara, S. *et al.* RipAY, a plant pathogen effector protein exhibits robust gamma-glutamyl cyclotransferase activity when stimulated by eukaryotic thioredoxins. *The Journal of biological chemistry*, doi: 10.1074/jbc.M115.678953 (2016).
40. Segonzac, C. *et al.* Negative control of BAK1 by protein phosphatase 2A during plant innate immunity. *EMBO J* **33,** 2069–2079, doi: 10.15252/embj.201488698 (2014).
41. Boevink, P. C. *et al.* A Phytophthora infestans RXLR effector targets plant PP1c isoforms that promote late blight disease. *Nat Commun* **7,** 10311, doi: 10.1038/ncomms10311 (2016).
42. Yerlikaya, S. *et al.* TORC1 and TORC2 work together to regulate ribosomal protein S6 phosphorylation in Saccharomyces cerevisiae. *Mol Biol Cell* **27,** 397–409, doi: 10.1091/mbc.E15-08-0594 (2016).

43. Jiang, Y. & Broach, J. R. Tor proteins and protein phosphatase 2A reciprocally regulate Tap42 in controlling cell growth in yeast. *EMBO J* **18**, 2782–2792, doi: 10.1093/emboj/18.10.2782 (1999).
44. Dobrenel, T. *et al.* TOR Signaling and Nutrient Sensing. *Annu Rev Plant Biol*, doi: 10.1146/annurev-arplant-043014-114648 (2016).
45. Xiong, Y. & Sheen, J. Novel links in the plant TOR kinase signaling network. *Curr Opin Plant Biol* **28**, 83–91, doi: 10.1016/j.pbi.2015.09.006 (2015).
46. Poueymiro, M. *et al.* A Ralstonia solanacearum type III effector directs the production of the plant signal metabolite trehalose-6-phosphate. *MBio* **5**, doi: 10.1128/mBio.02065-14 (2014).
47. Asselin, J. A. *et al.* Perturbation of maize phenylpropanoid metabolism by an AvrE family type III effector from Pantoea stewartii. *Plant Physiol* **167**, 1117–1135, doi: 10.1104/pp.114.253120 (2015).
48. Baruch, M. *et al.* An extracellular bacterial pathogen modulates host metabolism to regulate its own sensing and proliferation. *Cell* **156**, 97–108, doi: 10.1016/j.cell.2013.12.007 (2014).
49. Crespo, J. L. BiP links TOR signaling to ER stress in Chlamydomonas. *Plant Signal Behav* **7**, 273–275, doi: 10.4161/psb.18767 (2012).
50. Alberti, S., Gitler, A. D. & Lindquist, S. A suite of Gateway cloning vectors for high-throughput genetic analysis in Saccharomyces cerevisiae. *Yeast* **24**, 913–919, doi: 10.1002/yea.1502 (2007).
51. Alberola, T. M. *et al.* A new set of DNA macrochips for the yeast Saccharomyces cerevisiae: features and uses. *Int Microbiol* **7**, 199–206 (2004).
52. Hegde, P. *et al.* A concise guide to cDNA microarray analysis. *Biotechniques* **29**, 548–550, 552–544, 556 passim (2000).
53. Langmead, B. & Salzberg, S. L. Fast gapped-read alignment with Bowtie 2. *Nat Methods* **9**, 357–359, doi: 10.1038/nmeth.1923 (2012).
54. Reynolds, A., Lundblad, V., Dorris, D. & Keaveney, M. Yeast vectors and assays for expression of cloned genes. *Curr Protoc Mol Biol* Chapter 13, Unit13 16, doi: 10.1002/0471142727.mb1306s39 (2001).
55. Reed, A. J. & Hageman, R. H. Relationship between Nitrate Uptake, Flux, and Reduction and the Accumulation of Reduced Nitrogen in Maize (Zea mays L.): II. Effect of nutrient nitrate concentration. *Plant Physiol* **66**, 1184–1189 (1980).
56. Monteiro, F., Genin, S., van Dijk, I. & Valls, M. A luminescent reporter evidences active expression of Ralstonia solanacearum type III secretion system genes throughout plant infection. *Microbiology* **158**, 2107–2116, doi: 10.1099/mic.0.058610-0 (2012).
57. de Hoon, M. J., Imoto, S., Nolan, J. & Miyano, S. Open source clustering software. *Bioinformatics* **20**, 1453–1454, doi: 10.1093/bioinformatics/bth078 (2004).
58. Saldanha, A. J. Java Treeview–extensible visualization of microarray data. *Bioinformatics* **20**, 3246–3248, doi: 10.1093/bioinformatics/bth349 (2004).
59. Gonzalez, A., Ruiz, A., Casamayor, A. & Arino, J. Normal function of the yeast TOR pathway requires the type 2C protein phosphatase Ptc1. *Mol Cell Biol* **29**, 2876–2888, doi: 10.1128/MCB.01740-08 (2009).

## Acknowledgements

## Author Contributions

C.P. performed and designed the experiments, analyzed data and wrote the manuscript. L.L. performed the experiments. S.G. performed the experiments. L.T. performed the experiments. K.H. performed the experiments. M.T. designed the research. N.S.C. designed the experiments, analyzed data and wrote the manuscript. J.A. designed the experiments, analyzed data and wrote the manuscript. M.V. designed the experiments, analyzed data and wrote the manuscript. All authors reviewed the manuscript.

## Additional Information

**Supplementary information** accompanies this paper at http://www.nature.com/srep

**Competing financial interests:** The authors declare no competing financial interests.

**How to cite this article**: Popa, C. *et al.* The effector AWR5 from the plant pathogen *Ralstonia solanacearum* is an inhibitor of the TOR signalling pathway. *Sci. Rep.* **6**, 27058; doi: 10.1038/srep27058 (2016).

# Autophagy as an emerging arena for plant–pathogen interactions

Daniel Hofius[1], Liang Li[2], Anders Hafrén[1] and Nuria S Coll[2]

Autophagy is a highly conserved degradation and recycling process that controls cellular homeostasis, stress adaptation, and programmed cell death in eukaryotes. Emerging evidence indicates that autophagy is a key regulator of plant innate immunity and contributes with both pro-death and pro-survival functions to antimicrobial defences, depending on the pathogenic lifestyle. In turn, several pathogens have co-opted and evolved strategies to manipulate host autophagy pathways to the benefit of infection, while some eukaryotic microbes require their own autophagy machinery for successful pathogenesis. In this review, we present and discuss recent advances that exemplify the important role of pro- and antimicrobial autophagy in plant–pathogen interactions.

**Addresses**
[1] Department of Plant Biology, Uppsala BioCenter, Swedish University of Agricultural Sciences and Linnean Center of Plant Biology, SE-75007 Uppsala, Sweden
[2] Centre for Research in Agricultural Genomics (CSIC-IRTA-UAB-UB), Bellaterra-Cerdanyola del Valles, 08193 Catalonia, Spain

Corresponding authors: Hofius, Daniel (daniel.hofius@slu.se), Coll, Nuria S (nuria.sanchez-coll@cragenomica.es)

## Introduction

Autophagy is an evolutionary conserved process in eukaryotes that employs double-membrane vesicular structures, termed autophagosomes, to enclose and deliver cytoplasmic material for vacuolar/lysosomal degradation and recycling [1]. Depending on how the cellular cargo is recruited to the developing autophagosomes, autophagy can act as an unspecific (bulk) catabolic pathway for nutrient remobilization and energy supply, or as selective mechanism to eliminate superfluous and harmful compounds including aggregated proteins and damaged organelles [2]. While basal levels of autophagy serves mainly cellular homeostasis and quality control, increased autophagy activity allows adaptation to stressful conditions caused by a large variety of developmental and environmental cues [3]. Besides the significant contribution to cellular and organismal survival, autophagy has been implicated in the regulation and execution of programmed cell death (PCD) in various eukaryotic organisms [4]. In plants, autophagy is increasingly recognized for its central importance in development, reproduction, metabolism, senescence and tolerance to abiotic and biotic stresses [5,6]. In this review, we focus on the role of autophagy during plant–pathogen interactions. In particular, we discuss the most recent evidence showing that plant autophagy may benefit either the host by participating in immune responses, or the invading agent, by contributing to infection.

The plant immune system has evolved several layers to fend off pathogenic organisms [7]. Perception of conserved microbial-associated molecular patterns (MAMPs) by surface receptors leads to activation of basal defenses known as MAMP-triggered immunity (MTI). Adapted pathogens interfere with MTI by secreting effectors that, in turn, can be recognized by resistance ($R$) genes to initiate effector-triggered immunity (ETI). ETI often culminates in a local PCD reaction at the site of pathogen attack, termed the hypersensitive response (HR) [8]. During the last years, it has become evident that autophagy is engaged in various aspects of plant immunity [9]. Most notably, autophagy was shown to regulate basal resistance as well as immunity- and disease-related cell death responses to microbial pathogens with different infection strategies. However, due to the concomitant involvement of plant autophagy in homeostatic, metabolic and developmental processes, the dissection of autophagic mechanisms underlying host immunity and microbial pathogenesis is still in its infancy.

Most plant pathogens except viruses do not enter the cytoplasmic space, and there is limited evidence for direct autophagic targeting of pathogens or their individual components in in a process resembling xenophagy in metazoans. Interestingly, similar to microbes in other host organisms [10,11], an increasing number of examples indicate that phytopathogens are able to manipulate plant autophagy to their own advantage. As detailed below, these include inhibition of autophagy mechanisms contributing to immunity [12,13,14•] and the activation of autophagy pathways to target defense compounds or to potentially enhance nutrient acquisition [15••,16,17•].

## The role of autophagy in eukaryotic plant pathogens

It is well established that autophagy components and pathways in eukaryotic microbes are important for pathogenesis and plant invasion. Several studies published in the last decade and summarized in [18] showed that microbial autophagy mediates the development of appressoria, which are specialized infection structures used by fungi and oomycetes to enter the plant tissue. More recently, new components mediating autophagy-dependent plant infection by fungi have been discovered (Figure 1). The conserved retromer complex is involved in protein trafficking from endosomes to the trans-Golgi network, and was shown to be essential for autophagy-dependent host penetration by the rice blast fungus *Magnaporthe oryzae* [19]. Interestingly, retromer also contributes to the regulation of autophagy-dependent immune cell death in plants [20]. Furthermore, the *M. oryzae* Rab GTPase MoYpt7 is required for fungal autophagy, appressoria development and pathogenicity [21]. Autophagy is also involved in hyphal fusion and positively regulates the virulence of *Fusarium oxysporum* [22]. In *Botrytis cinerea* the autophagy gene BcATG1 is essential for pathogenesis, besides playing a critical role in numerous developmental processes [23]. In several other phytopathogenic fungi, autophagic regulation of organelle quantity has been shown to play a major role in the metabolic switch responsible for the transition to virulence [24].

## The role of autophagy in plant immunity

Despite some remaining controversy, both pro-death and pro-survival functions of autophagy are now generally recognized to contribute to anti-microbial defenses and disease resistance, depending on the pathosystem and pathogenic lifestyle.

Autophagy can have a positive regulatory role during HR [25] (Figure 1). Several Arabidopsis mutants disrupted in core autophagy (*ATG*) genes or related pathway components displayed significantly reduced HR upon infection with avirulent strains of the bacterium *Pseudomonas syringae* pathovar (pv) *tomato* (*Pst* DC3000) harboring the effector proteins AvrRps4 or AvrRpm1 [20,26,27,28•]. However, autophagy defects seemed to compromise *R* gene-mediated disease resistance only in case of *Pst* DC3000 AvrRps4 [20,29], supporting the earlier observed decoupling of HR from growth restriction for AvrRpm1-containing bacteria [30]. Knock-down of *ATG6* homologs in wheat further revealed the engagement of autophagy in broad-spectrum immunity conditioned by the *Pm21 R* gene towards the powdery mildew fungus *Blumeria graminis* f. sp. *tritici* (*Bgt*) [31]. Intriguingly, constitutive activation of autophagy in *Nicotiana benthamiana* due to silencing of the ATG3-interacting cytosolic glyceraldehyde-3-phosphate dehydrogenase (GAPC) enhanced *N* gene-mediated HR and resistance against *Tobacco mosaic virus* (TMV) [32••]. This finding substantiates the death-promoting effect of enhanced autophagy during ETI [33], and explains the increased TMV accumulation previously noted in HR lesions of autophagy-deficient *N. benthamiana* leaves [34]. Furthermore, it adds to the emerging picture that the positive role of autophagy in immunity-related PCD is opposite to its function in preventing premature senescence and runaway cell death outside of the primary infection sites [28•,35].

How autophagy exerts the dual roles during HR activation and containment is not well understood. The influence of autophagy on cellular survival is likely linked to homeostatic functions required to counterbalance infection-induced systemic responses such as ROS production, salicylic acid (SA) signaling, accumulation of misfolded/aggregated proteins, and endoplasmic reticulum stress [26,28•,36]. In contrast, the pro-death mechanism of autophagy remains largely undefined, but may also involve the regulation of SA homeostasis and/or the level of NON-EXPRESSOR OF PATHOGENESIS-RELATED GENES 1 (NPR1), that negatively impacts HR [26,28•,37]. Future work could further address the potential engagement of selective autophagic processes, for example, in the removal of negative HR regulators [35].

There is compelling evidence and a broad consensus that autophagy positively controls plant resistance to necrotrophic pathogens (Figure 1). Autophagy deficiency in Arabidopsis mutants resulted in spreading necrotic lesions and enhanced fungal growth upon infection with *B. cinerea*, *Alternaria brassicicola*, and *Plectosphaerella cucumerina* [38–40], and restored susceptibility to a non-pathogenic mutant strain of *Sclerotinia sclerotiorum* [13]. Notably, autophagy-mediated disease resistance to *B. cinerea* engages the upstream regulator BAG6 (BCL2-ASSOCIATED ATHANOGENE FAMILY PROTEIN 6) [41••]. While Arabidopsis *bag6* mutants were defective in autophagy induction and hypersusceptible to *B. cinerea*, ectopic expression of BAG6 in *N. benthamiana* leaves activated autophagy and cell death, which prevented fungal infection [41••]. Hence, pathogen-induced necrotic cell death and disease development is restricted by autophagy and/or immunity-related (autophagic) PCD. This mechanism agrees with the inhibition of necrosis by autophagy during execution of vacuolar cell death in development [42]. The molecular basis of the crosstalk remains largely unknown, although it is evident that protection from *B. cinerea* infection occurs independently of selective autophagy mediated by the cargo receptor NEXT TO BRCA1 GENE 1 (NBR1) [29]. Resistance to necrotrophs may be also mediated by autophagy via modulation of hormone homeostasis, for example, to stimulate jasmonic acid (JA) defence signaling, or removal of plant- and pathogen-derived toxic cellular constituents [39].

Figure 1
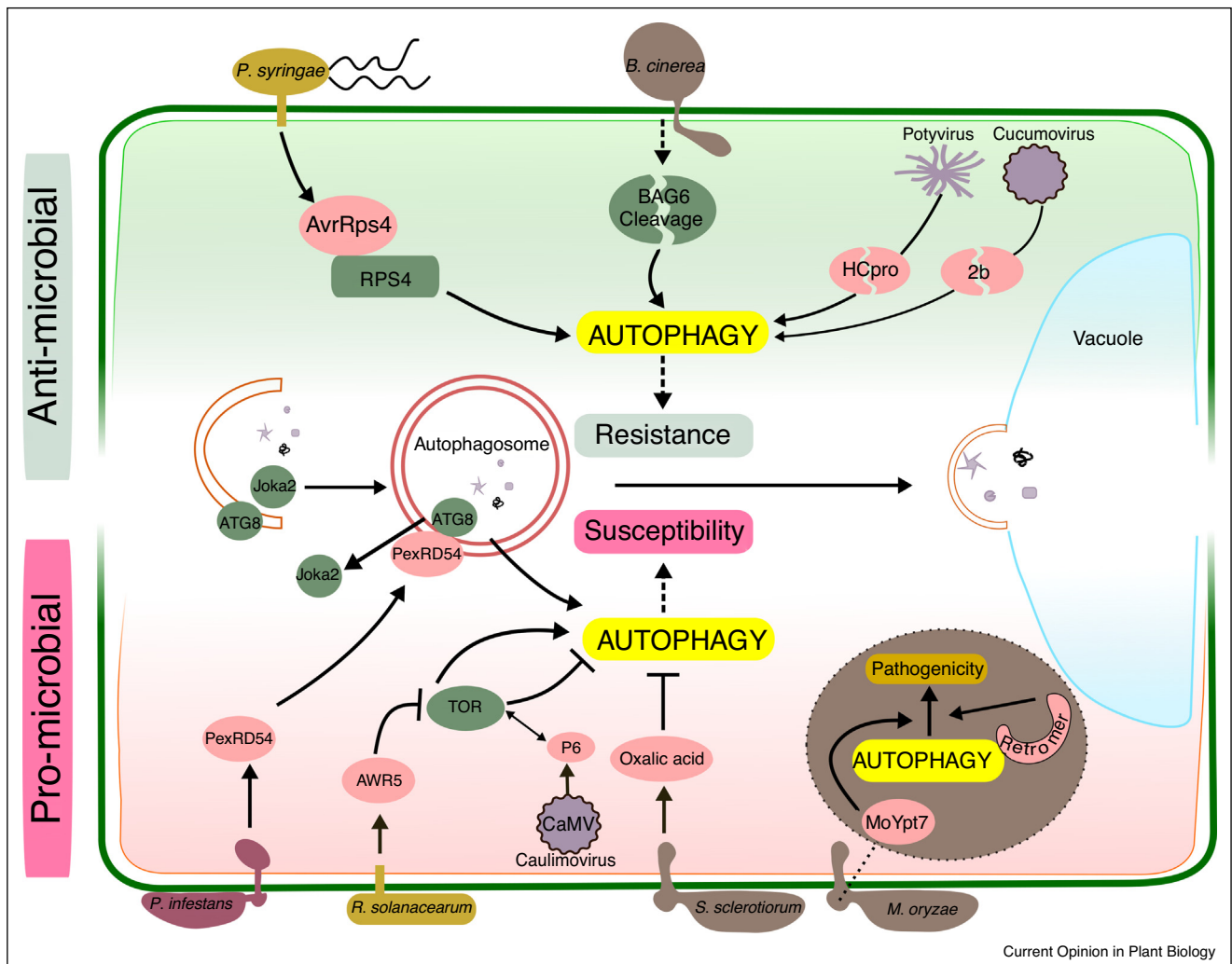


Anti- and pro-microbial roles of autophagy during plant–pathogen interactions.

Autophagy is an integral part of plant immunity. Arabidopsis infection with avirulent *Pseudomonas syringae* pv. *tomato* (*Pst*) DC3000 (*avrRps4*) induces autophagy, which contributes to the hypersensitive response (HR) and disease resistance. Infection of Arabidopsis with the necrotrophic fungus *Botrytis cinerea* triggers cleavage of the BAG6 protein, which results in autophagy activation and reduced disease development. Plant autophagy also participates in antiviral defense by targeted degradation of viral silencing suppressors such as the potyvirus protein HCpro and the cucumovirus protein 2b.

Plant pathogens manipulate the host autophagy machinery to counteract host defense and promote virulence. *Phytophthora infestans* effector PexRD54 binds ATG8 and outcompetes the plant selective autophagy receptor Joka2 from autophagosome association, thereby enhancing disease susceptibility of the host. The AWR5 effector from *Ralstonia solanacearum* inhibits TOR to activate autophagy, which is presumed to be beneficial for nutrient acquisition and successful infection. In contrast, the Cauliflower mosaic virus (CaMV) protein P6 has been proposed to inhibit autophagy by binding and activation of TOR. *Sclerotinia sclerotiorum* secretes the toxin oxalic acid to suppress autophagy and HR-like autophagic cell death as part of the host defense response against necrotrophic infection.

Autophagy in eukaryotic microbial pathogens contributes to pathogenesis. In *Magnaporthe oryzae*, the retromer complex and Rab GTPase MoYpt7 regulate autophagy mechanisms required for appressoria development and function during infection.

In animals, autophagy is a key mechanism in the fight against invading intracellular bacterial and viral pathogens. In contrast, there is surprisingly little knowledge about the contribution of autophagy to basal resistance against viruses, the major intracellular pathogens in plants. Autophagy has been associated with plant antiviral RNA silencing by mediating the targeted degradation of viral silencing suppressors including the cucumovirus protein 2b and potyvirus protein HCpro [43]. Interestingly, potyviral challenge of Arabidopsis lines with reduced expression of the negative autophagy regulator TARGET OF RAPAMYCIN (TOR) revealed strongly decreased levels of Watermelon mosaic virus, whereas Turnip mosaic virus accumulation was only slightly

affected [44•]. Although the significance of these findings has yet to be verified under autophagy-deficient conditions, they imply an antiviral role of autophagy against some potyviruses, and potentially other unrelated viral species. In this context, it remains to be determined whether autophagy can directly eliminate viruses in a process similar to mammalian xenophagy [45].

Finally, the role of autophagy in basal resistance to (hemi) biotrophic pathogens is a matter of ongoing debate. So far, there is no evidence that autophagy is directly involved in the regulation of MTI. In addition, despite some conflicting results, autophagy deficiency seems to rather enhance resistance to the virulent bacterial strain *Pst* DC3000 and some powdery mildew fungal species [9]. These findings could be partly linked to the impact of autophagy on SA levels and signaling, which might be further tested in plant systems with enhanced autophagy levels.

## Pathogen manipulation and pro-microbial role of autophagy

Considering the long-lasting co-evolutionary battle between plants and their pathogens, it is not surprising that successful microbes have evolved sophisticated strategies to modulate autophagy to their benefit (Figure 1).

The necrotroph *S. sclerotiorum* requires the phytotoxin oxalic acid (OA) to trigger unrestricted host cell death and establish successful infection. OA-deficient mutants are non-pathogenic and activate autophagy leading to restrictive HR-like cell death and resistance [13]. Autophagy deficiency restored pathogenicity, indicating that *S. sclerotiorum* secretes OA to suppress antimicrobial autophagy. A similar autophagy-mediated mechanism operates in the non-host *Ustilago maydis*–barley interaction. The biotrophic smut fungus *U. maydis* is recognized by barley, triggering a defense response that neutralizes the pathogen and prevents disease, but results in large necrotic areas and stunted leaf growth. In contrast, *U. maydis* mutants lacking the Pep1 effector show hallmarks of autophagy at the attempted penetration site and remain restricted to the infected area, which might indicate that *Pep1* is an autophagy inhibitor [12]. These findings suggest that autophagy suppression might be a virulence strategy shared by pathogens with completely different lifestyles.

In line with this notion, binding and activation of TOR by the Cauliflower mosaic virus (CaMV) P6 protein has recently been proposed to inhibit autophagy and impact resistance responses to bacterial pathogens [14•]. CaMV infection and transgenic expression of P6 increased the susceptibility to *Pst* DC3000 infection and facilitated growth of the effector-delivery deficient *Pst* mutant *hrc⁻*. This effect appears to be in agreement with P6-induced impairment of MTI responses including oxidative burst and SA accumulation. However, it would be surprising if P6 suppression of autophagy is causally linked to the observed phenotype, as *atg* mutants have been shown to display enhanced rather than reduced SA levels and bacterial resistance [38]. Hence, future efforts need to clarify the involvement of autophagy during CaMV infection and to reveal the potential role of TOR-binding of P6 to modulate this pathway for enhanced pathogenicity.

Other pathogens induce autophagy as part of their infection strategy. For example, the secreted effector AWR5 from the bacterium *Ralstonia solanacearum* inhibits TOR, which results in the activation of autophagy [17•]. Although the mechanistic details of this host–pathogen interaction remain to be elucidated, a tantalizing scenario would be that autophagy induction in the host stimulates plant cell dismissal and metabolic re-routing. This would be beneficial for *R. solanacearum* during its transition to the necrotrophic phase by facilitating nutrient acquisition. Viral pathogens might also promote and hijack autophagy pathways to invade host cells. For instance, the viral silencing suppressor P0 was shown to trigger autophagic degradation of ARGONAUTE1, an essential component of antiviral RNA-induced silencing complexes [16]. Given the frequent connections between viruses and autophagy in animals [46], future research will most likely provide more cases of virus-induced autophagic degradation of antiviral defense components in plants, perhaps even including small RNAs.

Another interesting example for the manipulation of the host autophagy machinery by a plant pathogen comes from the hemibiotrophic oomycete *Phytophthora infestans*. The RXLR effector protein PexRD54 was shown to bind to a specific host ATG8 protein, which prevented interaction of ATG8 with the autophagy cargo receptor Joka2/NBR1 [15••]. Joka2-mediated selective autophagy was further reported to positively influence plant resistance to *P. infestans*; hence, depletion of Joka2 by PexRD54 enhances susceptibility of the host. Interestingly, both Joka2 and PexRD54 trigger the formation of autophagosomes and activate autophagy. This led the authors to speculate that Joka2 facilitates removal of plant or pathogen proteins that negatively impact immunity, whereas PexRD54 might co-opt the autophagy pathway to selectively eliminate defense-related compounds or to recycle and redistribute nutrients in favor of the pathogen.

## Conclusions/future directions

This review highlights the importance of autophagy in the field of plant–pathogen interactions. Autophagy has emerged as a central part of the plant weaponry against invading microbial pathogens. Its significance for plant defense is supported by the evolution of microbial strategies to manipulate the host autophagy machinery for enhanced virulence and disease establishment. In

addition, autophagy in eukaryotic phytopathogens has evolved as an essential process in the development of functional infection structures. However, the examples illustrating the key roles of autophagy in plant–biotic interactions are still limited both in number and mechanistic detail. Current efforts in several laboratories around the world will certainly help to revert this situation in the coming years and further reveal the highly complex and multifaceted integration of autophagy into the plant immune system.

A key direction of future research will be the identification and characterization of selective autophagy receptors that drive plant defense responses and are still hidden in the gray shades of 'bulk' autophagy. In a more refined interaction, we envisage that plants employ and pathogens manipulate particular selective autophagy pathways to benefit defense and disease, respectively. So far, very few autophagy cargo receptors and their substrates have been identified in plants, but the generally very complex outcome of disease in autophagy deficient plants may indicate that selective processes with distinct functions operate in parallel within the full autophagy response. To dissect these mechanisms in greater detail, we need to establish plant lines with increased 'bulk' autophagy to support conclusions from knock-out mutants, and complement these general systems by targeting specifically the different selective autophagy pathways. In addition, due to concomitant, often overlapping roles of autophagy in cellular homeostasis and various developmental and environmental stress responses, it is essential to more precisely inhibit or activate autophagy by inducible and cell type-specific approaches.

Another important area of research relates to the largely unexplored crosstalk between autophagy and other cellular pathways that govern proteostasis, hormone signaling, and programmed cell death in plant–microbe interaction. Notably, the plant ubiquitin-proteasome system was recently found to be degraded by autophagy in response to nutrient starvation or chemical and genetic proteasome inhibition [47]. Whether a similar interplay occurs during immunity and disease is not known; however, recent evidence indicates that the 26S proteasome is central to plant immunity and targeted by multiple pathogen effectors to suppress SA-mediated host defenses [48].

Overall, there are still only very few pathogens identified that directly modulate the plant autophagy machinery to the benefit of infection. Among these, suppression of autophagy seems to be most common strategy, whereas the potential subversion of bulk and selective pathways still remains merely speculative. However, the fundamental role of autophagy in host immunity and microbial pathogenesis anticipates that phytopathogens have evolved sophisticated capacities to evade and exploit autophagy as demonstrated for a multitude of metazoan pathogens, thus adding further complexity to this emerging arena of plant–microbe interactions.

## Note added in proof
Recently, a paper appeared (Hafren et al., 2017 Selective autophagy limits cauliflower mosaic virus infection by NBR1-mediated targeting of viral capsid protein and particles. *Proc. Natl. Acad. Sci. U.S.A.* 114:E2026-E2035) which provides a primary example of virus targeting and elimination via xenophagy in plants. Together with another recent paper (Haxim et al., 2017 Autophagy functions as an antiviral mechanism against geminiviruses in plants. *Elife* 6: e23897), the integration and significance of plant autophagy in antiviral immunity is now evident.

## Acknowledgements

## References and recommended reading
Papers of particular interest, published within the period of review, have been highlighted as:

- • of special interest
- •• of outstanding interest

1. He C, Klionsky DJ: **Regulation mechanisms and signaling pathways of autophagy**. *Annu. Rev. Genet.* 2009, **43**:67-93.

2. Farre JC, Subramani S: **Mechanistic insights into selective autophagy pathways: lessons from yeast**. *Nat. Rev. Mol. Cell Biol.* 2016, **17**:537-552.

3. Boya P, Reggiori F, Codogno P: **Emerging regulation and functions of autophagy**. *Nat. Cell Biol.* 2013, **15**:1017.

4. Anding AL, Baehrecke EH: **Autophagy in cell life and cell death**. *Curr. Top. Dev. Biol.* 2015, **114**:67-91.

5. Yang X, Bassham DC: **New insight into the mechanism and function of autophagy in plant cells**. *Int. Rev. Cell Mol. Biol.* 2015, **320**:1-40.

6. Michaeli S, Galili G, Genschik P, Fernie AR, Avin-Wittenberg T: **Autophagy in plants-what's new on the menu?** *Trends Plant Sci.* 2016, **21**:134-144.

7. Jones JD, Dangl JL: **The plant immune system**. *Nature* 2006, **444**:323-329.

8. Cui H, Tsuda K, Parker JE: **Effector-triggered immunity: from pathogen perception to robust defense**. *Annu. Rev. Plant Biol.* 2015, **66**:487-511.

9. Zhou J, Yu JQ, Chen ZX: **The perplexing role of autophagy in plant innate immune responses**. *Mol. Plant Pathol.* 2014, **15**:637-645.

10. Gomes LC, Dikic I: **Autophagy in antimicrobial immunity**. *Mol. Cell* 2014, **54**:224-233.

11. Winchell CG, Steele S, Kawula T, Voth DE: **Dining in: intracellular bacterial pathogen interplay with autophagy**. *Curr. Opin. Microbiol.* 2016, **29**:9-14.

12. Hof A, Zechmann B, Schwammbach D, Huckelhoven R, Doehlemann G: **Alternative cell death mechanisms determine epidermal resistance in incompatible barley-*Ustilago* interactions**. *Mol. Plant Microbe Interact.* 2014, **27**:403-414.

13. Kabbage M, Williams B, Dickman MB: **Cell death control: the interplay of apoptosis and autophagy in the pathogenicity of *Sclerotinia sclerotiorum***. *PLoS Pathog.* 2013, **9**:e1003287.

14. Zvereva AS, Golyaev V, Turco S, Gubaeva EG, Rajeswaran R,
• Schepetilnikov MV, Srour O, Ryabova LA, Boller T, Pooggin MM: **Viral protein suppresses oxidative burst and salicylic acid-dependent autophagy and facilitates bacterial growth on virus-infected plants**. *New Phytol.* 2016, **211**:1020-1034.
This study proposes that binding and activation of the TOR kinase by the Cauliflower mosaic virus P6 protein prevents SA-mediated induction of autophagy and renders plants more susceptible to virulent bacterial infection.

15. Dagdas YF, Belhaj K, Maqbool A, Chaparro-Garcia A, Pandey P,
•• Petre B, Tabassum N, Cruz-Mireles N, Hughes RK, Sklenar J et al.: **An effector of the Irish potato famine pathogen antagonizes a host autophagy cargo receptor**. *Elife* 2016:5.
This article presents a primary example of how a plant pathogen modulates the autophagy pathway to counteract host defenses and enhance virulence. The *Pytophthora infestans* RXLR effector protein PexRD54 interacts with ATG8 to stimulate autophagosome formation and outcompetes the ATG8-binding cargo receptor Joka2 required for antimicrobial selective autophagy.

16. Derrien B, Baumberger N, Schepetilnikov M, Viotti C, De Cillia J, Ziegler-Graff V, Isono E, Schumacher K, Genschik P: **Degradation of the antiviral component ARGONAUTE1 by the autophagy pathway**. *Proc. Natl. Acad. Sci. U. S. A.* 2012, **109**:15942-15946.

17. Popa C, Li L, Gil S, Tatjer L, Hashii K, Tabuchi M, Coll NS, Arino J,
• Valls M: **The effector AWR5 from the plant pathogen *Ralstonia solanacearum* is an inhibitor of the TOR signalling pathway**. *Sci. Rep.* 2016, **6**:27058.
The authors show that TOR inactivation by the secreted effector AWR5 from *Ralstonia solanacearum* constitutively activates autophagy, which leads to the speculation that autophagy induction might contribute to pathogenicity by facilitating nutrient acquisition during the necrotrophic phase of bacterial infection.

18. Talbot NJ, Kershaw MJ: **The emerging role of autophagy in plant pathogen attack and host defence**. *Curr. Opin. Plant Biol.* 2009, **12**:444-450.

19. Zheng W, Zhou J, He Y, Xie Q, Chen A, Zheng H, Shi L, Zhao X, Zhang C, Huang Q et al.: **Retromer is essential for autophagy-dependent plant infection by the rice blast fungus**. *PLoS Genet.* 2015, **11**:e1005704.

20. Munch D, Teh OK, Malinovsky FG, Liu Q, Vetukuri RR, El Kasmi F, Brodersen P, Hara-Nishimura I, Dangl JL, Petersen M et al.: **Retromer contributes to immunity-associated cell death in Arabidopsis**. *Plant Cell* 2015, **27**:463-479.

21. Liu XH, Chen SM, Gao HM, Ning GA, Shi HB, Wang Y, Dong B, Qi YY, Zhang DM, Lu GD et al.: **The small GTPase MoYpt7 is required for membrane fusion in autophagy and pathogenicity of *Magnaporthe oryzae***. *Environ. Microbiol.* 2015, **17**:4495-4510.

22. Corral-Ramos C, Roca MG, Di Pietro A, Roncero MI, Ruiz-Roldan C: **Autophagy contributes to regulation of nuclear dynamics during vegetative growth and hyphal fusion in *Fusarium oxysporum***. *Autophagy* 2015, **11**:131-144.

23. Ren W, Zhang Z, Shao W, Yang Y, Zhou M, Chen C: **The autophagy-related gene BcATG1 is involved in fungal development and pathogenesis in *Botrytis cinerea***. *Mol. Plant Pathol.* 2017, **18**:238-248.

24. Oku M, Takano Y, Sakai Y: **The emerging role of autophagy in peroxisome dynamics and lipid metabolism of phyllosphere microorganisms**. *Front. Plant Sci.* 2014, **5**:81.

25. Hofius D, Schultz-Larsen T, Joensen J, Tsitsigiannis DI, Petersen NH, Mattsson O, Jorgensen LB, Jones JD, Mundy J, Petersen M: **Autophagic components contribute to hypersensitive cell death in Arabidopsis**. *Cell* 2009, **137**:773-783.

26. Coll NS, Smidler A, Puigvert M, Popa C, Valls M, Dangl JL: **The plant metacaspase AtMC1 in pathogen-triggered**

27. programmed cell death and aging: functional linkage with autophagy. *Cell. Death Differ.* 2014, **21**:1399-1408.

27. Hackenberg T, Juul T, Auzina A, Gwizdz S, Malolepszy A, Van Der Kelen K, Dam S, Bressendorff S, Lorentzen A, Roepstorff P et al.: **Catalase and NO CATALASE ACTIVITY1 promote autophagy-dependent cell death in Arabidopsis**. *Plant Cell* 2013, **25**:4616-4626.

28. Munch D, Rodriguez E, Bressendorff S, Park OK, Hofius D,
• Petersen M: **Autophagy deficiency leads to accumulation of ubiquitinated proteins, ER stress, and cell death in Arabidopsis**. *Autophagy* 2014, **10**:1579-1587.
This study provides evidence that the plant retromer complex is involved in pathogen-triggered HR and plays an important role in the regulation of the autophagic processes, similar to other eukaryotic organisms.

29. Dong J, Chen W: **The role of autophagy in chloroplast degradation and chlorophagy in immune defenses during *Pst* DC3000 (*AvrRps4*) infection**. *PLoS One* 2013, **8**:e73091.

30. Coll NS, Vercammen D, Smidler A, Clover C, Van Breusegem F, Dangl JL, Epple P: **Arabidopsis type I metacaspases control cell death**. *Science* 2010, **330**:1393-1397.

31. Yue J, Sun H, Zhang W, Pei D, He Y, Wang H: **Wheat homologs of yeast ATG6 function in autophagy and are implicated in powdery mildew immunity**. *BMC Plant Biol.* 2015, **15**:95.

32. Han S, Wang Y, Zheng X, Jia Q, Zhao J, Bai F, Hong Y, Liu Y:
•• **Cytoplastic glyceraldehyde-3-phosphate dehydrogenases interact with ATG3 to negatively regulate autophagy and immunity in *Nicotiana benthamiana***. *Plant Cell* 2015, **27**:1316-1331.
This study reveals a direct link between the cytosolic glyceraldehyde-3-phosphate dehydrogenases (GAPC) and the autophagy pathway, and shows that stimulated autophagy activity in GAPC-silenced tobacco leaves promotes HR and disease resistance upon avirulent virus infection.

33. Kwon SI, Cho HJ, Kim SR, Park OK: **The Rab GTPase RabG3b positively regulates autophagy and immunity-associated hypersensitive cell death in Arabidopsis**. *Plant Physiol.* 2013, **161**:1722-1736.

34. Liu Y, Schiff M, Czymmek K, Talloczy Z, Levine B, Dinesh-Kumar SP: **Autophagy regulates programmed cell death during the plant innate immune response**. *Cell* 2005, **121**:567-577.

35. Minina EA, Bozhkov PV, Hofius D: **Autophagy as initiator or executioner of cell death**. *Trends Plant Sci.* 2014, **19**:692-697.

36. Yoshimoto K, Jikumaru Y, Kamiya Y, Kusano M, Consonni C, Panstruga R, Ohsumi Y, Shirasu K: **Autophagy negatively regulates cell death by controlling NPR1-dependent salicylic acid signaling during senescence and the innate immune response in Arabidopsis**. *Plant Cell* 2009, **21**:2914-2927.

37. Fu ZQ, Yan S, Saleh A, Wang W, Ruble J, Oka N, Mohan R, Spoel SH, Tada Y, Zheng N et al.: **NPR3 and NPR4 are receptors for the immune signal salicylic acid in plants**. *Nature* 2012, **486**:228-232.

38. Lenz HD, Haller E, Melzer E, Gust AA, Nurnberger T: **Autophagy controls plant basal immunity in a pathogenic lifestyle-dependent manner**. *Autophagy* 2011, **7**:773-774.

39. Lai Z, Wang F, Zheng Z, Fan B, Chen Z: **A critical role of autophagy in plant resistance to necrotrophic fungal pathogens**. *Plant J.* 2011, **66**:953-968.

40. Katsiarimpa A, Kalinowska K, Anzenberger F, Weis C, Ostertag M, Tsutsumi C, Schwechheimer C, Brunner F, Huckelhoven R, Isono E: **The deubiquitinating enzyme AMSH1 and the ESCRT-III subunit VPS2.1 are required for autophagic degradation in Arabidopsis**. *Plant Cell* 2013, **25**:2236-2252.

41. Li Y, Kabbage M, Liu W, Dickman MB: **Aspartyl protease-
•• mediated cleavage of BAG6 is necessary for autophagy and fungal resistance in plants**. *Plant Cell* 2016, **28**:233-247.
The authors show that infection with *B. cinerea* triggers cleavage of the co-chaperone BAG6 in a caspase-1-like dependent manner and activates autophagy in the host. Autophagy induction results in disease resistance, coupling fungal recognition with defense activation.

42. Minina EA, Filonova LH, Fukada K, Savenkov EI, Gogvadze V, Clapham D, Sanchez-Vera V, Suarez MF, Zhivotovsky B, Daniel G

*et al.*: **Autophagy and metacaspase determine the mode of cell death in plants**. *J. Cell Biol.* 2013, **203**:917-927.

43. Nakahara KS, Masuta C, Yamada S, Shimura H, Kashihara Y, Wada TS, Meguro A, Goto K, Tadamura K, Sueda K *et al.*: **Tobacco calmodulin-like protein provides secondary defense by binding to and directing degradation of virus RNA silencing suppressors**. *Proc. Natl. Acad. Sci. U. S. A.* 2012, **109**:10113-10118.

44. Ouibrahim L, Rubio AG, Moretti A, Montane MH, Menand B,
• Meyer C, Robaglia C, Caranta C: **Potyviruses differ in their requirement for TOR signalling**. *J. Gen. Virol.* 2015, **96**:2898-2903.
This study reports enhanced resistance of TOR-silenced Arabidopsis lines to potyvirus infection, which implies an important role of activated autophagy in antiviral immunity.

45. Paulus GL, Xavier RJ: **Autophagy and checkpoints for intracellular pathogen defense**. *Curr. Opin. Gastroenterol.* 2015, **31**:14-23.

46. Dong X, Levine B: **Autophagy and viruses: adversaries or allies?** *J. Innate Immun.* 2013, **5**:480-493.

47. Marshall RS, Li F, Gemperline DC, Book AJ, Vierstra RD: **Autophagic degradation of the 26S proteasome is mediated by the dual ATG8/ubiquitin receptor RPN10 in Arabidopsis**. *Mol. Cell.* 2015, **58**:1053-1066.

48. Ustun S, Sheikh A, Gimenez-Ibanez S, Jones A, Ntoukakis V, Bornke F: **The proteasome acts as a hub for plant immunity and is targeted by *Pseudomonas* type III effectors**. *Plant Physiol.* 2016, **172**:1941-1958.